GEOLOGICA ULTRAIECTINA

Mededelingen van de
Faculteit Aardwetenschappen der
Rijksuniversiteit te Utrecht

No. 108

Early diagenetic processes and sulphur speciation in pore waters and sediments of the hypersaline Tyro and Bannock Basins, eastern Mediterranean

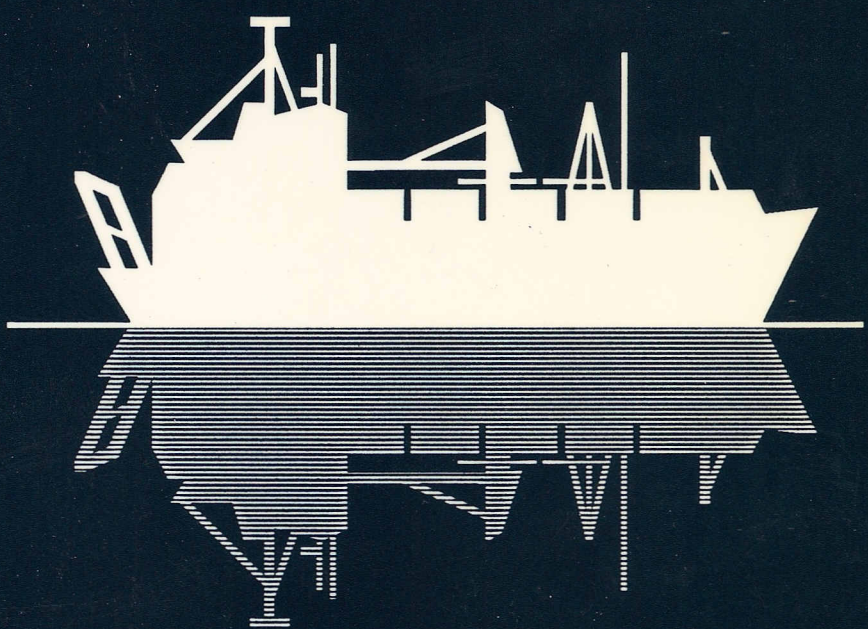

ELSE HENNEKE

GEOLOGICA ULTRAIECTINA

Mededelingen van de
Faculteit Aardwetenschappen der
Rijksuniversiteit te Utrecht

No. 108

Early diagenetic processes and sulphur speciation in pore waters and sediments of the hypersaline Tyro and Bannock Basins, eastern Mediterranean

CIP-DATA KONINKLIJKE BIBLIOTHEEK, DEN HAAG

Henneke, Else

Early diagenetic processes and sulphur speciation in pore waters and sediments of the hypersaline Tyro and Bannock Basins, eastern Mediterranean / Else Henneke. - Utrecht: Faculteit Aardwetenschappen der Rijksuniversiteit Utrecht. - (Geologica Ultraiectina, ISSN 0072-1026 ; no. 108) Thesis Rijksuniversiteit Utrecht. - With ref. - With summary in Dutch.
ISBN 90-71577-63-5
Subject headings: anoxic hypersaline basins / early diagenetic processes / interstitial water chemistry.

Graphic Production: Oosterijssel, Alblasserdam

Early diagenetic processes and sulphur speciation in pore waters and sediments of the hypersaline Tyro and Bannock Basins, eastern Mediterranean

Vroeg diagenetische processen en zwavel speciatie in poriënwaters en sedimenten uit de hypersaliene Tyro en Bannock Bekkens

(met een samenvatting in het nederlands)

PROEFSCHRIFT

TER VERKRIJGING VAN DE GRAAD VAN DOCTOR AAN DE UNIVERSITEIT UTRECHT OP GEZAG VAN DE RECTOR MAGNIFICUS, PROF.DR. J.A. VAN GINKEL, INGEVOLGE HET BESLUIT VAN HET COLLEGE VAN DEKANEN IN HET OPENBAAR TE VERDEDIGEN OP VRIJDAG 10 SEPTEMBER 1993 DES VOORMIDDAGS TE 10.30 UUR

DOOR

ELSE HENNEKE
GEBOREN OP 7 DECEMBER 1962, TE VLAARDINGEN

PROMOTOREN: Prof. Dr. C.H. van der Weijden
Prof. Dr. G.W. Luther III
CO-PROMOTOR: Dr. G.J. de Lange

In herinnering aan oma

VOORWOORD

Het proefschrift zoals dit nu voor U ligt heeft niet kunnen verschijnen zonder de hulp en medewerking van velen. Graag wil ik een ieder voor zijn of haar kleine dan wel grote bijdrage bedanken.

Allereerst wil ik Gert de Lange en Fred Trappenburg bedanken voor het ontwerp van de R.V. Tyro, die de omslag van dit proefschrift siert.

Het grootste gedeelte van het materiaal besproken in dit proefschrift is verzameld gedurende de Anoxic Basin Cruise expeditie met de R.V. Tyro in 1987 o.l.v. Prof. Dr. C.H. van der Weijden. De monsters genomen met de Interface Sampler II zijn verzameld tijdens de EEG Mast expeditie MARFLUX-2, in 1991 met eveneens de R.V. Tyro o.l.v. Dr. G.J. de Lange. Kapitein Blok (1987) en Kapitein de Jong (1991) en hun bemanning, de technici van het NIOZ en alle deelnemers aan deze expedities wil ik graag bedanken voor hun inzet.

Hierbij bedank ik de volgende personen voor hun analytische of technische ondersteuning: Mark van Alphen, Paul Anten, Tilly Bouten, Arnold van Dijk, Bertha Djie-Kwee, Chiel Eussen, Vian Govers, Pieter Kleingeld, Erica Koning, Anita van Leeuwen, Dieneke van de Meent, Jan Meesterburrie, Gijs Nobbe, Guus Peters, Theo van Zessen, de medewerkers van de bibliotheek, de administratie, de reproduktie, de A.V.-dienst, de glasblazerij en de werkplaats, in het bijzonder Hans Bliek en Dirk Steenbeek. Jan Hegeman van het NIOZ bedank ik voor zijn hulp bij de voorbereidingen en het meten van DOC en POC analyses.

Alle collega's van het Instituut voor Aardwetenschappen wil ik bedanken voor de prettige samenwerking en de gezellige tijd. In het bijzonder wil ik Bertil van Os, Jack Middelburg, Peter Pruijsers, Patrick van Santvoort, Marcel Paalman, Guiseppe Frapporti, Hans Eggenkamp, Simon Vriend, Paulien Gaans en Jurian Hoogewerff bedanken. Simon en Paulien wil ook graag bedanken voor hun hulp bij de thermodynamische berekeningen. Bertil bedankt voor de koffie die 's morgens klaar stond en de "trouble shooting" met de computer.

Gert de Lange bedank ik graag voor de aangeboden kans om een promotie-onderzoek te doen aan deze zo unieke anoxische hypersaline bekkens in de oostelijke Middellandse Zee, voor zijn begeleiding als co-promotor en de wetenschappelijke discussies.
Professor van der Weijden bedank ik voor het vertrouwen dat hij in mij stelde als wetenschapper en zijn aanvullende commentaren op de manuscripten voor dit proefschrift.

Het onderzoek beschreven in dit proefschrift is financieel mogelijk gemaakt door de ondersteuning van de stichting Aardwetenschappelijk Onderzoek (AWON 751.355.015) en gedeeltelijk door de Nederlandse Stichting

Onderzoek der Zee (SOZ) en het MARFLUX projekt (EEG MAST programma 0022-C).

Part of this research benefitted from the financial support of the National Science Foundation of the USA (grant OCE-8696121). I like to thank George Luther III for his enthusiasm about sulphur speciation and introducing me to the mysteries of sulphur. I thank Beth and Andrea for feeling me at home in their house in 1988 and Hanzel and Chandra for their hospitality in 1990. Tim Ferdelman, Elizabeth Tsamakis, Joel Kostka, Davis Velenisky, Steven Skarable and Jing Fing Wu are thanked for sharing the lab with me and for all the discussions and their friendship.

Ich danke Frau Reuber und Frau Hinz herzlich fur ihr Hilfe mit die Probe für $\delta^{34}S$. Profesor Dr. J Hoefs danke ich fur seine Mitarbeirtung und Diskussion uber die Schwefel-Isotoop.

Hans, Bep, Gijs, Tom en Mariëlle bedankt voor jullie steun en begrip tijdens het promotie-onderzoek en de uiteindelijke afronding ervan.

SUMMARY

Anoxic hypersaline basins have been found in two different tectonic environments in the eastern Mediterranean. Within the Tyro area (the western Strabo Trench) there are three pull apart basins: the Tyro Basin, presently filled with anoxic hypersaline bottomwater, and the Poseidon and Kretheus Basins, thought to have been anoxic and filled with hypersaline water in the past. The Mediterranean Ridge shows a "cobblestone topography" (Camerlenghi, 1990). The Bannock Basin is the largest depression found within this area and is divided into nine sub-basins. Tectonic deformations of Messinian evaporites are thought to be the major processes involved in the formation of these anoxic hypersaline basins.

The interstitial water chemistry of sediments from these basins have been studied. The fact that the Poseidon and Kretheus Basins have been filled with hypersaline bottomwater is reflected by an increase of the Cl and Na concentration in the pore waters downcore. These brines are thought to have been similar to that of the Tyro Basin. A diffusion-advection model has been applied to the Cl profiles. From time calculations it was possible to estimate the time elapsed since hypersaline conditions in the Poseidon and Kretheus Basins changed into normal saline conditions. A renewal time between 2000 - 3000 years was found.

Organic matter reaching the sediments is decomposed by sulphate reducing bacteria. Despite the high salinity (260 ‰) in the Tyro and Bannock Basins, sulphate reduction rates are higher than in the sediments from the Poseidon and Kretheus Basins. These higher sulphate reduction rates could be related to a better "preservation" of the organic matter in the anoxic brine. The release of inorganic metabolites, such as ammonium, alkalinity, phosphate and sulphide leads to the formation of authigenic minerals in these sediments such as dolomite, gypsum and sulphides.

The sulphur chemistry in the anoxic hypersaline sediments from the Tyro and Bannock Basins have been studied in detail. Despite the difference in major element chemistry of the brines (De Lange et al., 1990a) their sulphur chemistry in the sediments is very similar. The following sulphur species have been determined and quantified: elemental sulphur, Acid Volatile Sulphur (AVS), organic polysulphides, humic sulphur (0.5 M NaOH extractable) and pyritic sulphur. Pyritic sulphur was found to be the main phase of the inorganic reduced sulphur (50 - 80% of the total sulphur pool) and was at the same level (250 μmoles per gram dry weight) in both cores. Remarkably, humic sulphur was found to account for 17 to 28% of the total sulphur pool

in the Tyro Basin and for 10 - 43 % in the Bannock Basin. Sulphur isotope data show negative $\delta^{34}S$ values for both pyritic sulphur (-16 to -40 ‰) and humic sulphur (-16 to -30 ‰). Pyritic and humic sulphur are thought to be mainly formed at the interface of oxic seawater and anoxic hypersaline bottom water. At this interface material is captured due to the large density difference. Higher amounts of particulate and dissolved organic carbon have been observed at these interfaces as well as sulphate reduction and sulphide oxidation processes. Turbiditic deposition transports pyritic and humic sulphur compounds to the sediments in the Tyro and Bannock Basins.

SAMENVATTING

Anoxische hypersaliene bekkens zijn enkele jaren geleden in het oostelijke gedeelte van de Middellandse Zee aangetroffen. In het westelijke gedeelte van de Strabo Trog liggen de Tyro, Poseidon en Kretheus Bekkens. Het Tyro Bekken bevat op dit moment anoxisch hypersalien bodemwater op een waterdiepte van meer dan 3400 m. Van de Poseidon en Kretheus Bekkens wordt gedacht dat er in het verleden anoxische hypersaliene condities zijn geweest. Het Bannock Bekken ligt in een gebied dat wordt gekenmerkt door een "cobblestone topografie" (Camerlenghi, 1990). Dit bekken bestaat uit negen sub-bekkens. Voor alle bekkens geldt dat deze gevormd zijn door een combinatie van het oplossen van Messiniën evaporieten en tectonische bewegingen.

De poriënwater chemie van sedimenten uit deze bekkens is nader bestudeerd. Het feit dat de Poseidon en Kretheus Bekkens in het verleden gevuld waren met anoxisch hypersalien water is nog waar te nemen door de toename van Cl en Na met de diepte in deze poriënwaters. Aangenomen wordt dat de samenstelling van deze pekels identiek was aan die van de huidige pekel in het Tyro Bekken. De Cl-profielen zijn gemodelleerd met behulp van een diffusie-advectie model. Aan de hand van dit model kan er bepaald worden hoe lang geleden de Poseidon en Kretheus Bekken anoxisch hypersalien waren. Voor beide bekkens is dit ongeveer 2000 - 3000 jaar.

Het organisch materiaal wat deze sedimenten bereikt wordt afgebroken door sulfaat reducerende bacteriën. Ondanks de hoge saliniteit (260 ‰) in de Tyro en Bannock Bekkens is de sulfaat reductie snelheid hier hoger dan in de Poseidon en Kretheus Bekkens. Dit is waarschijnlijk gerelateerd aan een betere "preservatie" van het organisch materiaal in de anoxische pekel. De afbraakprodukten (ammonium, alkaliteit en fosfaat) en het gevormde sulfide leiden tot de vorming van authigene mineralen in deze sedimenten, zoals dolomiet, gips en sulfiden.

De zwavelchemie in de anoxische hypersaliene sedimenten uit de Tyro en Bannock Bekkens is bestudeerd in wat meer detail. Ondanks het verschil in de chemie van de hoofdelementen in de twee pekels (De Lange et al., 1990a) is de zwavelchemie grotendeels gelijk. De volgende zwavelspecies zijn waargenomen: elementair zwavel, monosulfides, organische polysulfides, zwavelhoudende humus (0.5 M NaOH extraheerbaar) en pyritische zwavel. Het pyritische zwavel is de belangrijkste fase van het anorganische zwavel (50 - 80% van de totale hoeveelheid zwavel) en is in beide bekkens ongeveer 250 μmoles per gram droog gewicht. Uniek is het hoge percentage aan zwavelhoudende humus in deze sedimenten. In het Tyro Bekken is dit

17 tot 28% van het totale gehalte aan zwavel, terwijl in het Bannock Bekken dit zo'n 10 tot 43% is. Het pyritische zwavel en het zwavel in de humus hebben een negatieve $\delta^{34}S$; -16 tot -40 ‰ en -16 tot -30‰, respectievelijk. Van beide zwavelprodukten wordt gedacht dat deze op de interface tussen het normale zeewater en de anoxische pekel worden gevormd. Op deze interface wordt materiaal ingevangen ten gevolge van het dichtheidsverschil. Een hoger gehalte aan opgelost en particulair organisch koolstof is op beide interfaces waargenomen, evenals sulfaat reductie en sulfide oxidatie processen. Turbidieten zorgen ervoor dat het pyritische en de zwavelhoudende humus in de sedimenten van de Tyro en Bannock Bekkens terecht komen.

CONTENTS

Chapter 1: Introduction

The occurrence of anoxic hypersaline basins in the deep-sea environment has been reported for only a few locations: the Red Sea (Swallow and Crease, 1965), the Orca Basin in the Gulf of Mexico (Shokes et al., 1977) and the Tyro (De Lange and Ten Haven, 1983; Jongsma et al., 1983) and Bannock (Scientific Staff of Cruise Bannock 1984-1,1985) Basins in the eastern Mediterranean.

Tectonic deformations of the sediment and dissolution of the underlying Messinian evaporites are thought to be the major processes involved in the formation of the anoxic hypersaline basins in the eastern Mediterranean (Camerlenghi, 1990). The Tyro and Bannock Basins both contain anoxic hypersaline bottom water. The chemical composition of the Tyro brine is related to dissolution of a halite evaporite, whereas the Bannock brine displays more the composition of a late stage evaporite including K,Mg-chlorides and Mg-sulphates (De Lange et al., 1990a).

Since their discovery, the Tyro and Bannock Basins (Fig. 1.1) have received much attention (special issues edited by Van Hinte et al., 1987; Van der Weijden et al., 1990; Cita et al., 1991). The major scope of these studies has been on the geochemical composition of these brines, and on the sedimentology. Less attention has been paid on the interstitial water and sediment chemistry. De Lange and Ten Haven (1983) and Ten Haven et al. (1987a) were the first who pointed out the interesting geochemical features of the anoxic hypersaline sediments from these basins.

In 1987 a scientific expedition with the R.V. Tyro was held to the anoxic basins in the eastern Mediterranean. This Anoxic Basin Chemistry (ABC) cruise had three major objectives: 1) to determine in as much detail as possible the chemistry of the brines; 2) to characterize and analyze the sediments in these anoxic hypersaline basins and relate this with the sedimentary and diagenetic history of the basin sediments; and 3) to collect cores containing as many sapropel layers as possible for a sedimentological, micropaleontological and geochemical study. The first objective has been intensively

discussed in a special issue of *Marine Chemistry* (Van der Weijden et al., 1990). For the third objective the reader is referred to Van Os et al. (1991; 1993) and Pruysers et al. (1991). This thesis will be dealing with the second objective of the ABC expedition, i.e. sediments from the Tyro and Bannock area have been studied for their interstitial water and sediment chemistry.

Within the Tyro area three basins are found. At present, the Tyro Basin is filled with anoxic hypersaline bottom water, whereas the Poseidon and Kretheus Basins are thought to be filled with oxygenated seawater. Using the salinity gradients in pore waters, it will be shown that these basins have been hypersaline in the past (chapter 2). A transient diffusion-advection model is presented to describe the chlorinity profiles.

Material reaching the sediments is subjected to early diagenetic processes. The interstitial water chemistry has been demonstrated to be a sensitive tool to study such processes. Early diagenetic processes in anoxic hypersaline sediments from the Tyro and Bannock areas are discussed in chapters 3, 4 and 5. These chapters focus on the decomposition of organic matter and authigenic mineral formation. Such processes may lead to mobilization of barite in anoxic hypersaline sediments (chapter 6).

Due to the large density difference at the interface between oxic seawater and brine, material is captured at this interface. Accumulation of all kinds of material is observed as will be shown in chapter 7 for dissolved and particulate organic carbon in the Tyro and Bannock Basins.

The Tyro and Bannock Basins are amongst the most sulphidic bodies of water in the world (Luther et al., 1990). The H_2S content is 2 to 3 $mmol.l^{-1}$ (De Lange et al., 1990a; Luther et al., 1990). Therefore, these basins form an excellent opportunity to study the sulphur cycle in the anoxic brine and sediments. The methods used to identify and quantify the various sulphur species are reported in chapter 8, while the distribution of the sulphur species are presented and discussed in chapter 9.

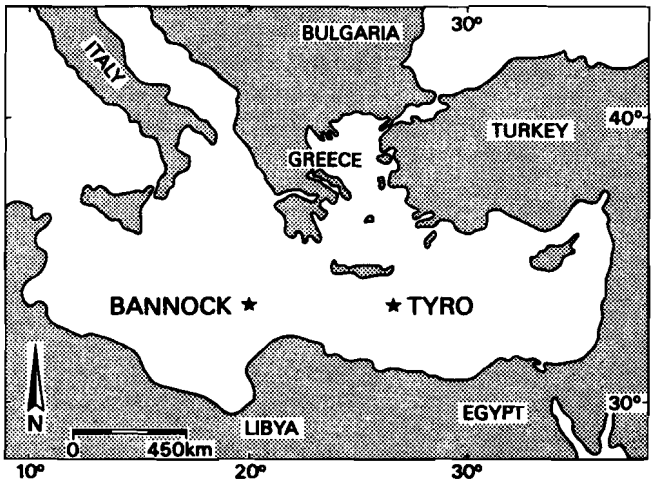

Figure 1.1: Location of the Tyro and Bannock Basins in the eastern Mediterranean.

Chapter 2: Anoxic hypersaline sediments from the Tyro area -salinity gradients-

Abstract

Within the Tyro area there are three basins: the Tyro Basin, presently filled with anoxic hypersaline water, and the Poseidon and Kretheus Basins, thought to have been anoxic and filled with hypersaline water in the past. The interstitial water chemistry of the "salinity" elements Na, Cl and K in the sediment-waters from these basins has been studied.

The concentrations of Cl, Na and K in the pore waters of sediments from the Tyro Basin (ABC15) are constant with depth. In contrast, in the sediments from the Poseidon (ABC17) and Kretheus (ABC23) Basins the Cl concentration in the pore waters increases with depth. This increase is accompanied by a similar increase in the Na concentration. The concentration profiles of Cl and Na in these sediments are due to diffusion along the concentration gradient between normal seawater and brine. The brine composition is thought to have been similar to that of the Tyro brine. The distribution of K is influenced by diagenetic reactions.

A diffusion-advection model has been used to describe the Cl profiles. Changes in time parameter appears to cause significant differences between the Cl profiles, while the model appears to be hardly sensitive to diffusion coefficients and sediment accumulation rates.

From time calculations it has been possible to estimate the time elapsed since hypersaline conditions changed into normal saline conditions in the Poseidon and Kretheus Basins. For core ABC17 a renewal time between 2000-3000 years is found. A similar time is found in core ABC23 applied for depth below 150 cm. The top of this core is probably influenced by turbiditic deposition from within the last 500 years.

2.1 Introduction

Tectonic deformation of sediments and dissolution of the underlying Messinian evaporites are thought to be the major processes involved in the formation of the anoxic hypersaline basins in the eastern Mediterranean (Camerlenghi, 1990). The Tyro, Poseidon and Kretheus Basins are pull-apart basins within the Strabo Trench (Fig. 2.1). These depressions are characterized areas of strike-slip motion (Camerlenghi, 1990). At present, the Tyro Basin contains anoxic hypersaline bottom water. The Poseidon Basin has been hypersaline and is thought to be normal saline at this moment. However, as no data are available from the deepest part of the basin, there is some uncertainty in this statement. The Kretheus Basin is now filled with oxygenated seawater, but has previously been anoxic hypersaline.

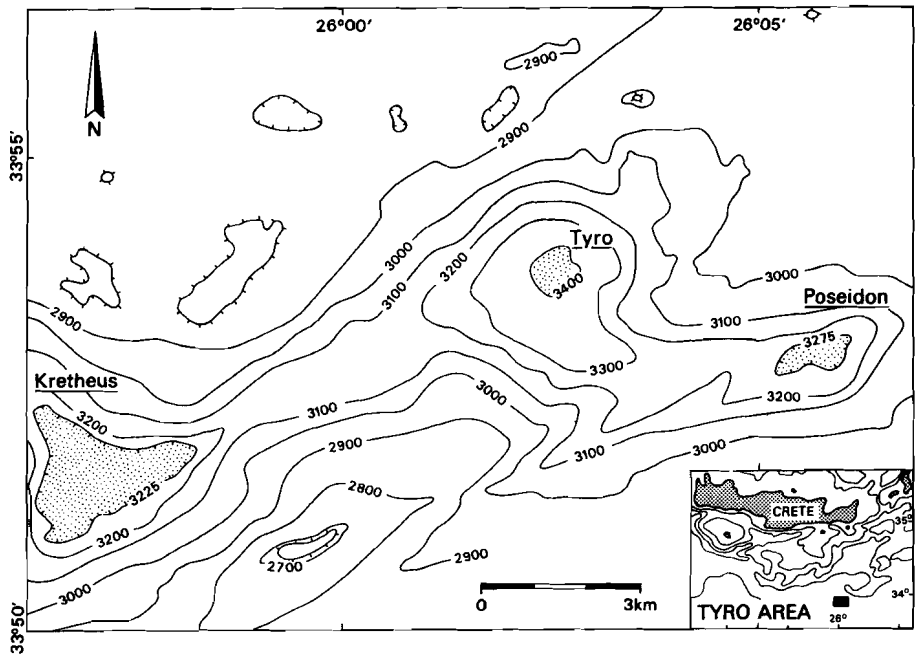

Figure 2.1: Location of the basins in the Tyro area, Strabo Trench. At present only the Tyro Basin is filled with anoxic hypersaline water (below 3330 dbar)

Pore water profiles are sensitive indicators for changes occurring in the sediments. Changes in the concentration of elements provide information on diagenetic processes such as decomposition of organic matter, dissolution of minerals, and adsorption and desorption reactions. Pore waters may also provide information on the composition of the burial water and the history of the sedimentary basin. Middelburg and De Lange (1989) have shown that pore water chlorinity (Cl) profiles in Kau Bay (Indonesia) give direct evidence for salinity changes during the Quaternary Era.

This chapter will focus on the pore water concentration of the "salinity" elements Na, Cl and K in order to assess their relation to hypersaline or normal marine conditions. Applying a transient diffusion-

advection model to the pore water Cl profile of the Poseidon and Kretheus Basins, an estimate can be made of the time elapsed since hypersaline conditions changed into normal saline.

2.2 Material and methods

Three different gravity cores were selected for detailed investigation (Table 2.1). These cores were collected during the Spring of 1987 with the Dutch R.V. Tyro. The sediments are of Late Pleistocene to Holocene age (*Emiliania huxleyi* Acme zone, i.e. younger than 70,000 yr B.P.) (Erba, 1991).

Core ABC15 was taken from the anoxic brine in the Tyro Basin. Sediments from this core are completely anoxic with many turbiditic intervals. The sequence is characterized by alternations of green gelatinous mud and grey reduced ooze (Erba, 1991). The top 60 cm consists of a homogeneous carbonate ooze, followed by approximately two meters of structureless gelatinous mud. Till maximum depth of recovery (564 cm) repetitive turbidites are observed with some organic rich units.

Core ABC17 was recovered from the slope of the Poseidon Basin. Sediments from this core are anoxic muds (Erba, 1991). A striking feature in this core is a thick layer of gelatinous pellicles starting at approximately two meters depth till the maximum depth of recovery (546 cm.). The top consists of faintly laminated gelatinous mud and a pteropod-rich layer at 70 cm. Between these layers organic rich gelatinous mud with carbonate ooze was observed.

Core ABC23 was recovered from the Kretheus Basin, a previous anoxic basin, located SW from the Tyro Basin. In core ABC23 the pre-anoxic/anoxic boundary as well as the restoration of the oxygenated conditions is recorded. The anoxic sediments are characterized by laminated gelatinous mud and carbonate ooze. The pre-anoxic sediments (from 475 cm till maximum depth 535 cm) contain carbonate ooze and silty or sandy bioclastic layers. A few oxidized layers have been observed at 500 cm depth (Erba, pers. comm.). The top of the core (upper 150 cm) consists of an alternation of carbonate ooze

and organic rich green layers. The organic rich green layers show turbiditic graded bedding. Only the top centimetre shows evidence of oxidized mud.

In all the cores no sapropel(lic) (sensu stricto) layers were observed. The lithology of the cores is presented in figure 2.2.

Table 2.1: Location and recovery of the sediment cores from the Strabo Trench

Core	Basin	Depth m	Recovery Depth cm	Remarks
ABC15	Tyro	3370	564	anoxic
ABC17	Poseidon	3170	546	anoxic
ABC23	Kretheus	3250	535	oxic/anoxic/oxic

The shipboard procedure for sample processing has been described in detail by De Lange (1992). Sediment samples were squeezed with modified Reeburgh-type squeezers in a glove box flushed with high-purity nitrogen and held at a constant bottom water temperature of 13°C. Interstitial water was collected in acid cleaned bottles. Na and K were measured by Inductively Coupled Plasma Emission Spectrometry (ICPES, ARL 34.000) after 10 to 100 times dilution, obtaining a concentration for Na equal to one-tenth of that of normal seawater. Analytical precision was determined by replicate analyses of Atlantic seawater (Madeira Abyssal Plain). Usually a precision of 1% and 2% for Na and K, respectively, was obtained. Chloride was analyzed by potentiometric titration using 0.06 M $AgNO_3$ solution (De Lange, 1986) usually with a precision of better than 1%.

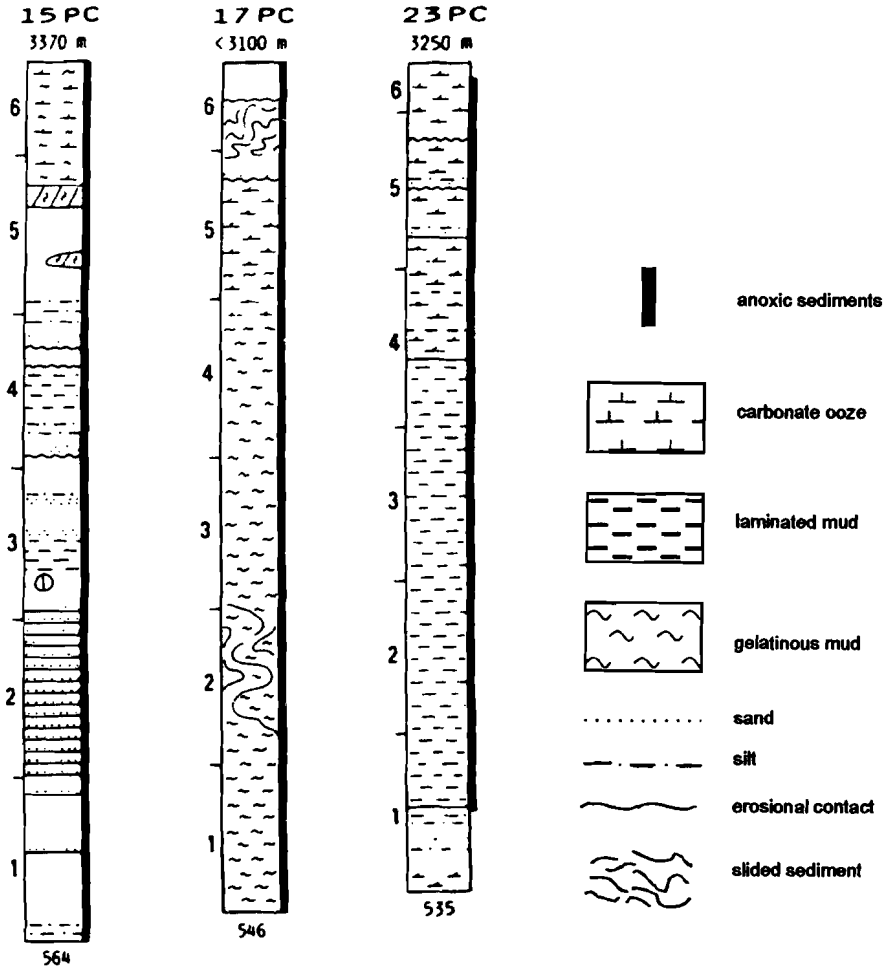

Figure 2.2: Lithology of cores ABC15 (Tyro Basin), ABC17 (Poseidon Basin) and ABC23 (Kretheus Basin) after Erba (1991)

2.3 Results and Discussion

The pore waters from core ABC15 show constant profiles of Cl, Na and K concentrations with depth (Fig. 2.3). Their concentrations are similar to those in the Tyro brine (De Lange et al., 1990a; Fig. 2.3). The results for cores ABC17 and ABC23 are shown in figure 2.4 and 2.5, respectively.

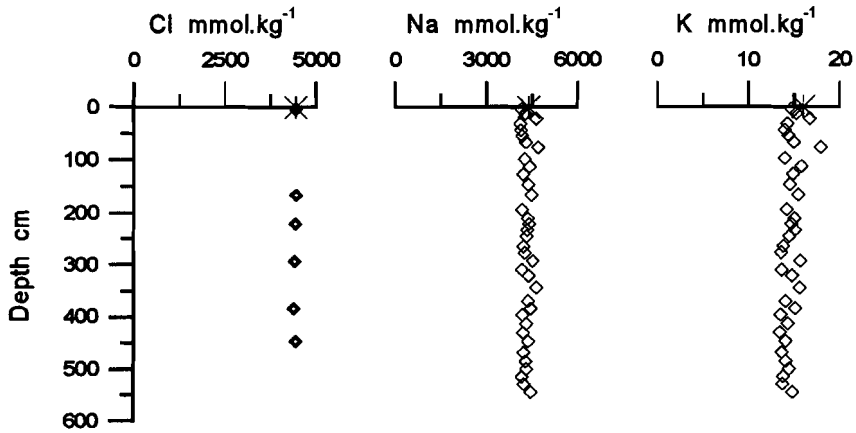

Figure 2.3: Cl, Na and K concentration versus depth in pore waters from core ABC15, Tyro Basin. The asterix symbol represents the average concentration in the Tyro brine.

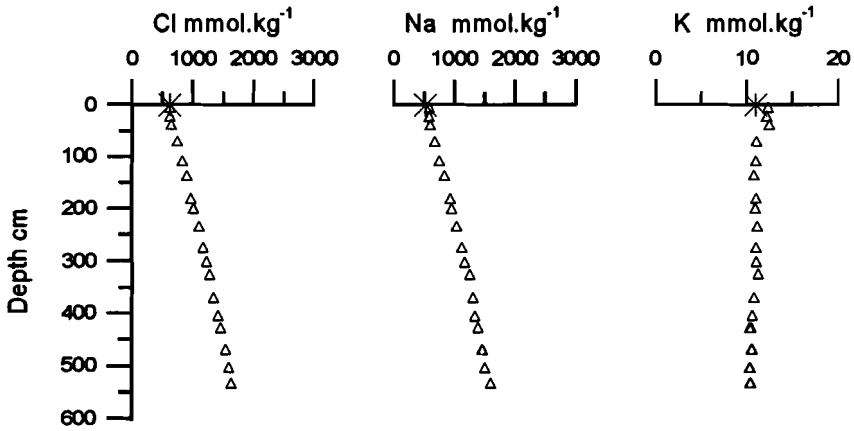

Figure 2.4: Cl, Na and K concentration versus depth in pore waters from core ABC17, Poseidon Basin. The asterix symbol represents the average concentration in eastern Mediterranean seawater.

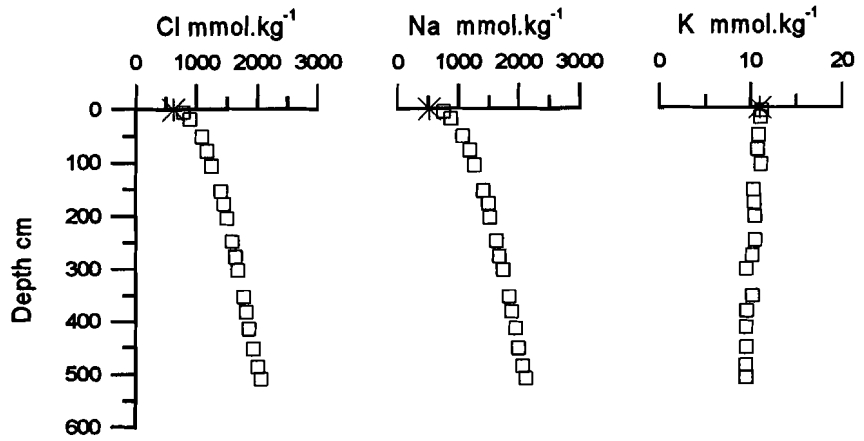

Figure 2.5: Cl, Na and K concentration versus depth in pore waters from core ABC23, Kretheus Basin. The asterix symbol represents the average concentration in eastern Mediterranean seawater.

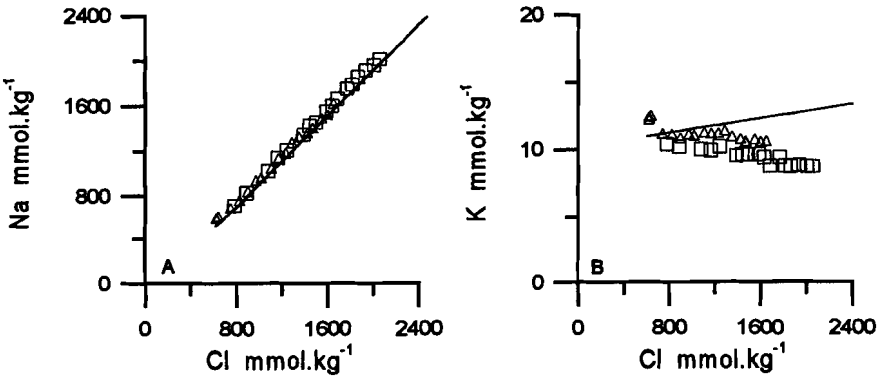

Figure 2.6: A) Na versus Cl in pore waters of core ABC17 (triangle) and ABC23 (square). The solid line represents the seawater-brine conservative mixing curve. B) K versus Cl in pore waters of core ABC17 (triangle) and ABC23 (square). The solid line represents the seawater-brine conservative mixing curve.

Core ABC17 and core ABC23 show a linear increase in Cl concentration with depth (correlationcoefficients of 0.999 and 0.981, respectively). The increase in Cl concentration is accompanied by an identical increase in Na concentration (Fig. 2.6A). The K concentration in the top

of core ABC17 is slightly higher than the value found in normal seawater. These higher values cannot be explained satisfactorily. From 50 cm depth on the concentration of K remains almost constant with depth in this core. However, in core ABC23 a small decrease in the K concentration with depth is observed. The pore waters of core ABC17 and ABC23 are depleted in K with respect to the seawater-brine conservative mixing curve (Fig. 2.6B). The distribution of K is thought to be influenced by diagenetic reactions, such as ion-exchange, adsorption-desorption and silicate precipitation (Kastner et al,. 1990). Similar observations are common for normal marine sedimentary settings (Gieskes, 1975; De Lange, 1986).

The concentration profiles of Cl and Na in cores ABC17 and ABC23 are due to diffusion along the concentration gradient between normal seawater and brine.

2.4 Modelling Cl profiles

It has been reported that the Tyro brine is formed by the dissolution of Messinian salt from the sides of the basin (De Lange and Ten Haven, 1983; Jongsma et al., 1983). The brines of the Poseidon and Kretheus Basins may originate from an "overflow" of the Tyro brine or may have been formed by the dissolution of the same evaporitic depositions, that constitute the source for the Tyro brine. A relative uplift of the sills between the Tyro and the Poseidon Basin and the Tyro and the Kretheus Basin might have stopped this "overflow" or reduced the formation of a brine in the Poseidon and Kretheus Basins.

The pore waters of core ABC17 and ABC23 have Na/Cl ratios that are consistent with a diffusive mixing of normal eastern Mediterranean seawater and Tyro brine. Therefore, it is proposed that the Poseidon and Kretheus Basins have contained anoxic hypersaline bottom water with a composition similar to that of the Tyro brine (Fig. 2.6A).

From the pore water chlorinity profiles it is possible to estimate at which time in the past conditions in the Poseidon and the Kretheus Basins have changed from hypersaline to normal salinity. For convenience, and in absence of data, it is assumed that this change

has occurred instantly.

The concentration of a solute in the interstitial pore waters changes as a function of time and depth according to the differential equation (Middelburg and De Lange, 1989):

$$R\frac{\delta C}{\delta t} = \frac{\delta (D[\delta C/\delta x]}{\delta x} - \frac{\delta (vC)}{\delta x} + \Sigma R_i \qquad [2.1]$$

R = retardation-factor
C = concentration solute
D = diffusion coefficient
v = rate of flow relative to sediment-water interface
ΣR_i = chemical reactions involved
x = depth
t = time

For Cl there are no chemical reactions involved ($\Sigma R_i = 0$) and there are no equilibrium sorption processes ($R = 1$) (Middelburg and De Lange, 1989).

The following assumptions have been made:

1) constant porosity with depth, so D is independent of depth.
2) there is no advective flow; i.e. v is equal to sediment accumulation rate ω

Using these assumptions equation 2.1 can be rewritten as:

$$\frac{\delta C}{\delta t} = D\frac{\delta^2 C}{\delta x^2} - \omega\frac{\delta C}{\delta x} \qquad [2.2]$$

For the pore water chlorinity profiles in cores ABC17 and ABC23 there are the following boundary conditions: at t=0; the concentration of Cl in the brine at time of isolation C_i is 4425 mmol.kg^{-1} (the concentration found in the Tyro brine), and at t>0 and x=0 the concentration Cl is equal to the present-day concentration, C_0. Because of the lack of bottom water data, the average concentration observed in the trip core ABC17 is chosen for C_0 in case of core ABC17, whereas for core ABC23 the value in the top is taken. C_0 is 625 and 775 mmol.kg^{-1} for ABC17 and ABC23, respectively.

Assuming, that below the depth where the Cl concentration is equal to that of the brine no further changes in the chlorinity occur, a semi-infinite model can be chosen; x -> ∞

$$\frac{\delta C}{\delta x} = 0 \qquad [2.3]$$

Then the solution to equation 2.2 becomes:

$$C = C_i + (C_o - C_i)\, A(x,t) \qquad [2.4]$$

where

$$A(x,t) = 0.5\ erfc[(x-t\omega)/2\sqrt{Dt}] + 0.5\ \exp(\omega x/D)\ erfc[(x+t\omega)/2\sqrt{Dt}]$$

erfc = error function complement, this error function complement can be approximated with a Taylor serie of ten.

The diffusion coefficient for Cl is calculated according to Li and Gregory (1974). Detailed information on the calculation of the diffusion coefficients can be found in appendix A.

Modelling calculations show that equation 2.4 is rather insensitive to changes in the diffusion coefficient of Cl (Fig. 2.7A). Therefore, the cross-coupling terms (calculated according to McDuff and Ellis, 1979; see also appendix A) have not been taken into account in the calculation of the diffusion coefficient. In addition, the sediment accumulation rate appears to have little influence on the pore water chlorinity profile (Fig. 2.7B). Model curves are most sensitive to time (Fig. 2.7C). Hence, pore water chlorinity versus depth profiles and equation 2.4 can be used together to obtain estimates for time since re-establishing of normal saline conditions in the Poseidon and Kretheus Basins.

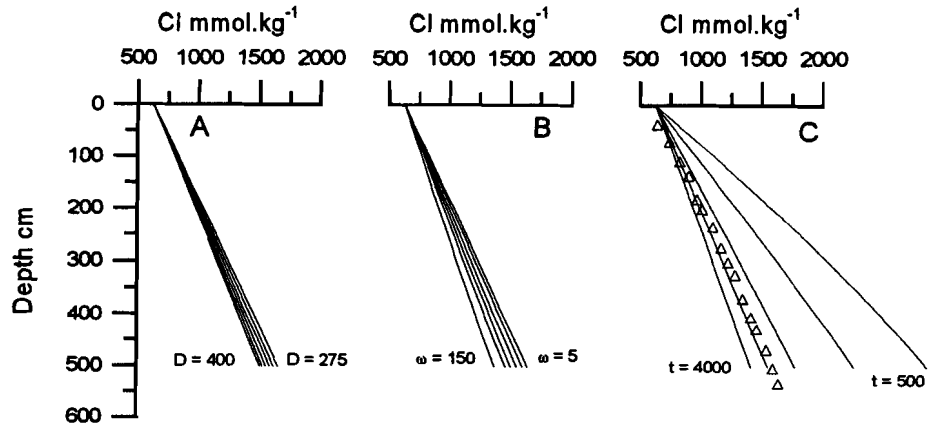

Figure 2.7: Calculated Cl versus depth profiles using the model after Middelburg and de Lange (1989), see text; A) for various diffusion coefficients, D_d is 275, 300, 325, 350, 375 and 400 $cm^2.yr^{-1}$, respectively. B) for various sedimentation rates: ω is 5, 25, 50, 75, 100 and 150 $cm.kyr^{-1}$, respectively; C) for various times: t is 500, 1000, 2000, 3000 and 4000 yr, respectively. Open diamond symbols represent Cl profile observed in core ABC17. C_i = 4425 $mmol.kg^{-1}$ and C_0 = 625 $mmol.kg^{-1}$ for all curves, the other parameters are shown in the figures.

2.5 Estimates for time past since hypersaline conditions changed into normal saline conditions in the Poseidon and Kretheus Basins

For the Poseidon and the Kretheus Basins model calculations have been made, using the parameters shown in Table 2.2. For the Poseidon Basin a best fit was obtained for time values between 2000 - 3000 years. The pore water profile of Cl in the Kretheus Basin is consistent with a more recent time value between 1000 and 2000 years (Fig. 2.8).

Table 2.2: Parameters used for modelling the Cl profile and estimating turnover time for the Poseidon and Kretheus Basin

	Poseidon (ABC17)	Kretheus (ABC23)
D $cm^2.yr^{-1}$ [a]	350	287
ω $cm.kyr^{-1}$ [b]	50	50
C_i $mmol.kg^{-1}$	4425	4425
C_0 $mmol.kg^{-1}$ [c]	625	775
t yr	2000 - 3000	1000 - 2000

[a] differences in D results from different porosities (see Appendix A)

[b] best estimate for sedimentation rate (see also chapter 3)

[c] C_0 in ABC17 is the average concentration found in the tripcore; for ABC23 the top value has been used.

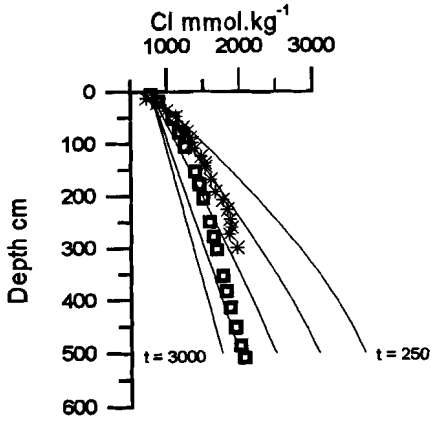

Figure 2.8: Calculated Cl versus depth profiles for various times: t is 250, 500, 1000, 2000 and 3000 yr, respectively. C_i = 4425 and C_0 = 775 $mmol.kg^{-1}$; ω = 50 $cm.kyr^{-1}$ and D_{Cl} = 287 $cm^2.yr^{-1}$. Semi-closed squares represent Cl profile of ABC23. Asterix symbols show Cl data from T83-45 (Ten Haven et al., 1987a).

The Cl profile of core T83-45 from Ten Haven et al. (1987a) corresponds closely with that of core ABC23 (Fig. 2.8). Using the same parameters and method as used for the Kretheus Basin the renewal time for core T83-45 is calculated to be between 500 and 1000 years. (Fig. 2.8). The estimated renewal time for the Kretheus Basin is in the same range as that calculated by Ten Haven et al. (1987a). These authors calculated a renewal time ranging from 250 to 4000 years.

In the top of cores ABC23 and T83-45, the pore water Cl concentration is higher than can be accounted for by the presently used diffusion-advection model (Fig. 2.8). In case of core ABC23, it might have been influenced by turbiditic hypersaline anoxic layers in the upper 150 cm. The lithology of this core displays an alternation of anoxic and oxic layers. Applying the diffusion-advection model to the upper 150 cm alone results in a turnover time of about 500 years. For the deeper part (below 150 cm) the best fit gives a time of 2000-3000 years (Fig 2.9). This value is in the same range as the time observed in the Poseidon Basin. The discrepancy between the upper and lower part in core ABC23 may have been influenced by the recent deposition of turbidites, containing anoxic more saline layers.

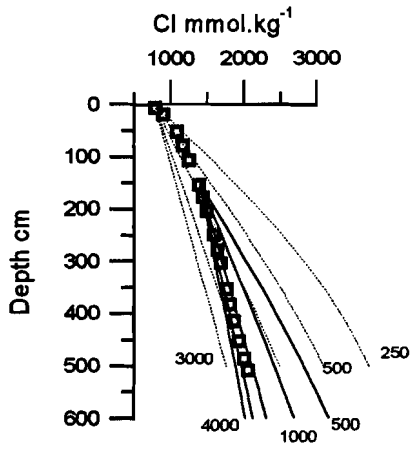

Figure 2.9: Calculated Cl versus depth profiles for various times in core ABC23 (semi-closed squares). A distinction has been made between the upper 150 cm and the depths below this depth (see text). Time, t, is 250, 500, 1000, 2000, 3000 and 4000 yr, respectively. C_i = 4425 and C_0 = 775 mmol.kg^{-1}; ω = 50 cm.kyr^{-1} and D_{Cl} = 287 cm^2.yr^{-1}.

From the data set presented here the shutdown of brine inflow or brine formation is calculated to have occurred some 2000-3000 years ago. A relative uplift of the sills at the Tyro Basin or a slowdown of the formation rate of Tyro brine can be mentioned as possible causes for the Poseidon and Kretheus Basins becoming normal saline. The presented data set does not allow to make firm conclusions whether these possibilities are linked to the Minoan Santorini eruption (3500 yr B.P.) as have been suggested by De Lange and Ten Haven (1983).

In addition, it must be noted that the calculated time is dependent on a-priori assumptions. First, it is assumed that the "overflow" from the Tyro Basin suddenly stopped. In fact, it is more likely that the Poseidon and Kretheus Basins will gradually become less saline due to the mixing with normal seawater. Therefore, the calculated time will be a lower limit for the renewal time. Secondly, the changes are thought to have occurred instantly and simultaneously at all depths in the basins. This will result in calculated shutdown times that are much shorter for cores taken from the deeper part of the basins relative to cores from the boundaries. Therefore, for these cores the estimated time will always be less than the actual time of shutdown of brine inflow.

2.6 Summary and conclusions

Pore water profiles from core ABC17 (Poseidon Basin) and core ABC23 (Kretheus Basin) show an increase in Cl with depth. This increase in Cl concords with the idea that the Poseidon and the Kretheus Basins have been hypersaline. The brine composition of these basins is likely to have been similar to that of the Tyro brine, regarding the similarity of their origin of the dissolving evaporites.

A diffusion-advection model has been used to describe the Cl profiles. This model appears to be hardly sensitive to the diffusion coefficients and sediment accumulation rates. Changes in the parameter time appears to cause significant differences between the Cl profiles. Calculations have been made to estimate the renewal time from hypersaline to normal marine conditions. A renewal time between 2000-3000 years is found for core ABC17. A similar time is found in

the Kretheus Basin for core ABC23 applied for depths below 150 cm. The top of this core is probably influenced by turbiditic deposition from within the last 500 years.

Chapter 3: Organic matter decomposition in the Tyro area.

Abstract

Changes in pore water concentrations of sulphate, ammonium and phosphate, and stoichiometric modelling are used to estimate the average composition of the decomposing organic matter and to estimate sulphate reduction rates in anoxic hypersaline sediments from the Tyro area. The average composition of the decomposing organic matter can be represented by: $(CH_2O)_{106}(NH_4)_{17}(H_3PO_4)_{0.03}$. The relatively high N/P ratio of about 600 compared to the Redfield ratio of 16 could be due to phosphate limitation for the primary production in the water column and to selective removal of phosphate in the pore waters by adsorption on calcium-carbonates. In the Tyro Basin sulphate reduction takes place in the sediments despite the high salinity (260 ‰). The sulphate reduction rates are found to be higher in these sediments, than in the sediments from the Poseidon and Kretheus Basins. The latter basins have been anoxic hypersaline and are thought to contain oxygenated normal saline seawater at present time. The higher sulphate reduction rate observed in the Tyro Basin could be related to a better "preservation" of the organic matter in the anoxic brine.

Dissolved organic carbon (DOC) is an important intermediate in the decomposition of organic matter by sulphate reducing bacteria. Pore waters from the Tyro and Poseidon Basins show an increase of DOC with depth. This increase correlates with the decrease in sulphate and the increases of alkalinity, ammonium and phosphate with depth in the sediments.

3.1 Introduction

Organic matter is one of the most reactive compounds in the marine environment. The breakdown of organic matter is the driving force behind early diagenesis in marine sediments (Berner, 1980). In anoxic marine sediments the major process involved in the decomposition of organic matter is sulphate reduction (Goldhaber et al., 1977; Elderfield et al., 1981; Jørgensen, 1982; Westrich and Berner, 1984; Middelburg, 1991; and others). Decomposition of organic matter by sulphate reducing bacteria will increase the concentration of the metabolites (HCO_3^-, NH_4^+, PO_4^{3-} and H_2S) in the pore waters (e.g. Berner, 1980; Gaillard, 1988). Accumulation of metabolites such as alkalinity and ammonium has been reported for many locations: coastal sediments (e.g. Nissenbaum et al., 1972a; Goldhaber et al., 1977; Jørgensen, 1978; Elderfield et al., 1981), organic-rich sediments in the coastal upwelling zone of Peru (Rowe and Howarth, 1985), anoxic

sediments from Kau Bay (Middelburg, 1990) and the Black Sea (e.g. Manheim and Chan, 1974).

Dissolved organic carbon (DOC) is an important intermediate in the decomposition of organic matter in anoxic marine sediments (Nissenbaum and Kaplan, 1972; Krom and Sholkoviz, 1977; Krom and Westrich, 1980; Orem et al., 1986). It may further be decomposed by sulphate reducing bacteria to inorganic metabolites. Part of the DOC may also be involved in polymerisation reactions and thus act as intermediates in the formation of sedimentary humic material and kerogen (Nissenbaum and Kaplan, 1972; Krom and Sholkovitz; 1977).

Hypersaline environments may play an important role in the formation of petroleum and its precursors (Lyons et al., 1982). The anoxic hypersaline sediments from the Tyro area form an excellent opportunity to study the preservation and mineralization of organic matter under such conditions. The Tyro area consists of three basins: the anoxic hypersaline Tyro Basin, and the Poseidon and Kretheus Basins. The latter two basins have been anoxic hypersaline in the past but are thought to be overlain by oxygenated seawater at present (see chapter 2). Sediments from these three basins of the Tyro area have been studied for their interstitial water chemistry.

In the first part of this chapter the changes in concentration of the dissolved inorganic metabolites and stoichiometric modelling are used to estimate the average composition of the decomposing organic matter and to estimate the sulphate reduction rates in these anoxic hypersaline sediments. The second part of this chapter will focus on the distribution of DOC and its relation to the diagenetic processes.

3.2 Material and methods

Sediment cores from the Tyro, Poseidon and Kretheus Basins have been studied for their interstitial water and their bulk sediment chemistry. Core ABC15 is taken from the anoxic hypersaline Tyro Basin, whereas core ABC17 and core ABC23 are taken from the Poseidon and Kretheus Basins, respectively. The sediments from the Tyro and the Poseidon Basins are completely anoxic. Core ABC23 from

the Kretheus Basin displays oxic and anoxic sediment deposition. A description of the cores and the basins has been given in chapter 2.

On board ship, sediment samples were squeezed with modified Reeburgh-type squeezers in a glove box flushed with high-purity nitrogen and held at a constant bottom water temperature of 13°C as described by De Lange (1992). Interstitial water was collected in acid-cleaned bottles.

The nutrients (NH_4^+ and PO_4^{3-}) and alkalinity were analyzed on board ship usually within 24 hours after collection. Phosphate and ammonium were done by routine auto analyzer methods using a TRAACS-800 system. Total alkalinity was measured by an automatic potentiometric titration system using 0.05 M HCl.

DOC was analyzed by measuring the carbon dioxide resulting from wet oxidation of organic matter (Wilson, 1961; Menzel and Vaccaro, 1964). For DOC measurements, an aliquot of 2 to 5 ml pore water was put into a glass ampoule, to which 250 μl of 6% phosphoric acid and 200 mg $K_2S_2O_8$ were added. The ampoules were purged for 6 min to remove inorganic carbon and then sealed. Four months after recovery all the ampoules were analyzed for CO_2 with an IR carbon analyzer (Oceanographic International, model 0524B). Prior to the analyses the ampoules were heated for 3½ hours at 130°C for total oxidation of the organic matter. Most DOC values are single measurements. A few duplicates were analyzed, from which an error of precision of 3.5% was derived.

Sulphate was measured as total S using ICPES (ARL 34.000) after a 10 to 100 times dilution, obtaining a concentration for Na equal to one-tenth of that of normal seawater. Samples for the SO_4-S isotopes in the pore waters were measured with a Finnigan MAT 271/45 mass spectrometer. The $\delta^{34}S$ values are reported relative to the Canyon Diablo standard. The sulphur isotope ratio is expressed as:

$$\delta^{34}S = \left(\frac{(^{34}S/^{32}S)_{sample}}{(^{34}S/^{32}S)_{standard}} - 1\right) * 1000‰$$

Prior to the analyses of $\delta^{13}C$ of the organic carbon, carbonate carbon was removed with 1 M HCl. Organic carbon was oxidized with CuO at 900°C in a closed circulation system. The released CO_2 was separated from the other gases and measured for the isotopic composition. The $\delta^{13}C_{org.}$ was measured with a VG SIRA 24 mass spectrometer. The isotopic data are reported relative to the PeeDee Belemnite standard.

3.3 Organic matter decomposition

Results of Ten Haven et al. (1987b) indicate that the organic matter in the Tyro Basin is characterized by matter produced in the photic zone, terrigenous material and organic living at the seawater-brine interface. The authors found that the terrigenous compound was of minor importance. The $\delta^{13}C$ of the organic matter in the sediments cores from the Tyro, Poseidon and Kretheus Basins, studied here, ranges from -22‰ to -25‰ (majority between -22‰ and -23.5‰). The lighter isotopic composition of the organic matter in these sediments in relation to marine material ($\delta^{13}C$ is -18‰ to -23‰; Gaskell et al., 1975) might be related to the organic matter living at the interface between seawater and brine. These bacterial mats, gelatinous pellicles, have been observed in all three sediment cores.

Decomposition of organic matter is investigated by studying the down-core distribution of the inorganic chemical species. The ammonium, phosphate, total alkalinity and sulphate data of the pore waters from the Tyro Basin (ABC15), Poseidon Basin (ABC17) and the Kretheus Basin (ABC23) are shown in figures 3.1, 3.2 and 3.3, respectively.

The decrease in sulphate concentration with depth and the accompanying increase of ammonium, phosphate and total alkalinity in core ABC15 indicate decomposition of organic matter by sulphate reducing bacteria. This is strongly supported by the increase of the $\delta^{34}S$ of the sulphate in the pore waters (Fig. 3.1). Sulphate reducing bacteria fractionate the sulphur atoms producing sulphide which is enriched in ^{32}S. Consequently, the sulphate that remains will be more enriched in ^{34}S. In core ABC15 the $\delta^{34}S$ increases from 30.5‰ in the top to 44.7‰

at a depth of 222 cm (Fig. 3.1). In cores ABC17 and ABC23, an increase in ammonium, phosphate and total alkalinity is also observed, while the decrease in sulphate is less pronounced at these locations.

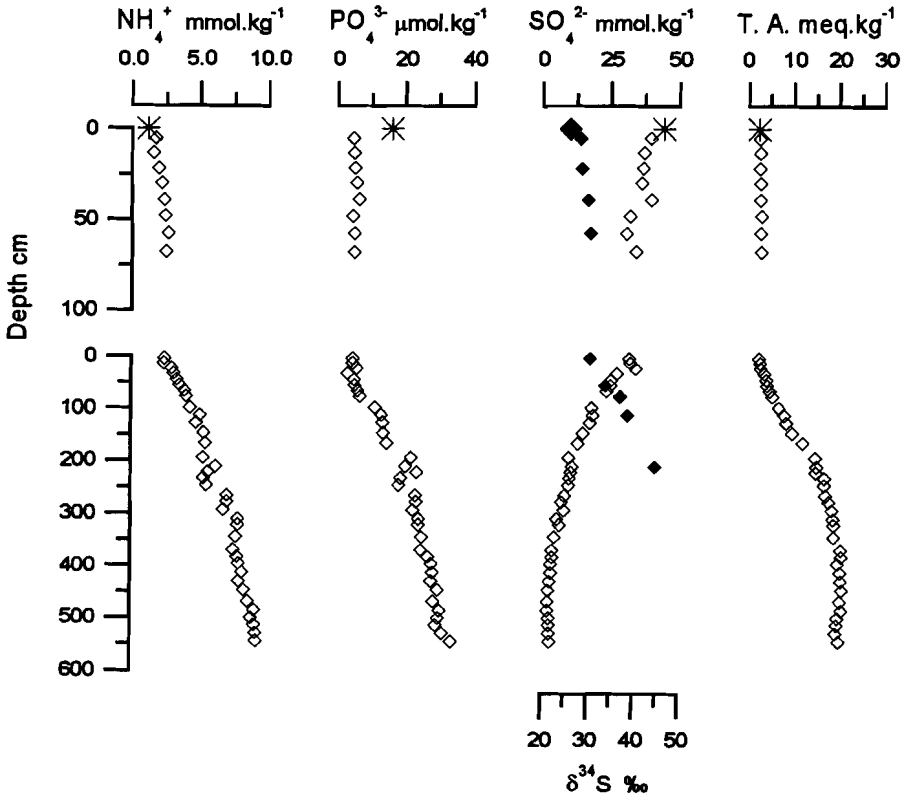

Figure 3.1: Pore water profiles versus depth of ammonium, phosphate, sulphate and total alkalinity (T.A.) in core ABC15. Closed diamond symbols represent the $\delta^{34}S$ of the sulphate pore water; large diamond is $\delta^{34}S$ of the sulphate in the Tyro brine. The asterix symbol represents the concentration in the Tyro brine. The upper graphs are data from the tripcore ABC15

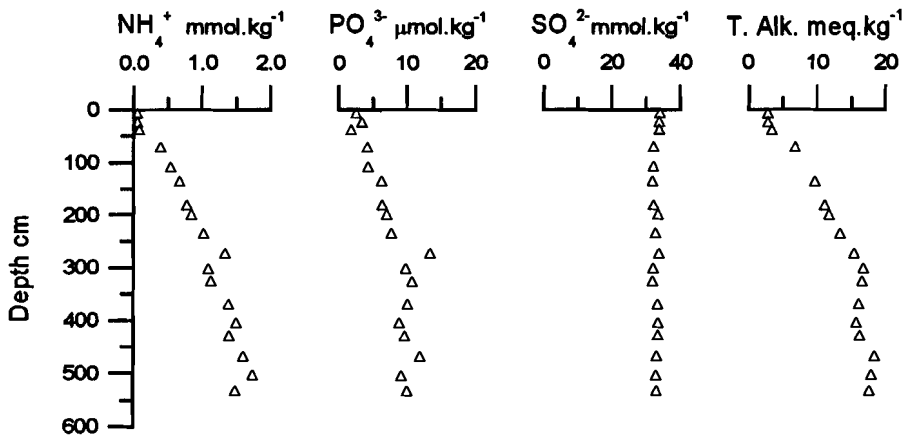

Figure 3.2: Pore water profiles versus depth of ammonium, phosphate, sulphate and total alkalinity (T.A.) in core ABC17.

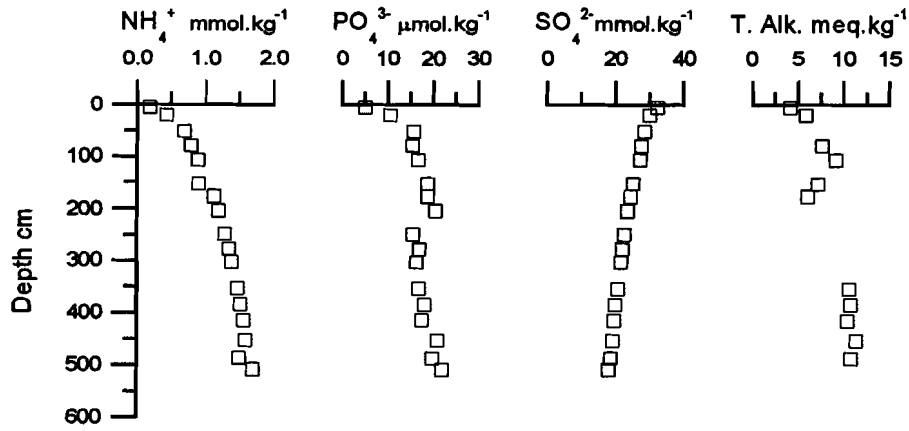

Figure 3.3: Pore water profiles versus depth of ammonium, phosphate, sulphate and total alkalinity (T.A.) in core ABC23.

3.3.1 Sulphate reduction

The organic matter decomposition by sulphate reducing bacteria is generally described as:

$$(CH_2O)_x(NH_3)_y(H_3PO_4)_z + 0.5xSO_4^{2-} \rightarrow xHCO_3^- + yNH_4^+ + zHPO_4^{2-} + 0.5xH_2S$$

x,y and z are the stoichiometric coefficients depending on the composition of the organic matter involved. The organic matter decomposition by sulphate reducing bacteria will, amongst others, increase the ammonium concentration in the pore waters. At steady state the distribution of dissolved ammonium can be described using (Berner, 1980):

$$D_n \frac{\partial^2 C}{\partial x^2} - v(1+K)\frac{\partial C}{\partial x} + Fk_nN = 0 \qquad [3.2]$$

where C is the concentration of dissolved ammonium, D_n is the diffusion coefficient of ammonium, K linear adsorption constant, F is a concentration conversion factor, N is the concentration of non-diffusible metabolizable organic nitrogen and k_n is the first-order rate constant for organic nitrogen decomposition. The following assumptions have been made:

1. steady state diagenesis is present
2. diffusion occurs via molecular processes only
3. there are no porosity gradients with depth
4. equilibrium adsorption is present and follows a simple linear isotherm K
5. the advection rate v is equal to the sediment accumulation rate ω
6. precipitation of ammonium in authigenic minerals does not occur
7. decomposition of nitrogen-bearing organic matter occurs via first-order kinetics, k_n.

Applying appropriate boundary conditions for equation 3.2:

$x = 0; N = N_0; C = C_0$

and

$x \rightarrow \infty ; N \rightarrow 0$ and $C \rightarrow C_\infty$

where C_0 is the concentration of ammonium at the sediment-water interface. For this concentration the value observed in the top of the sediment core was chosen. This value may deviate from the bottom water concentration because of core top loss. N_0 is the initial amount metabolizable organic N and C_∞ the asymptotic concentration of ammonium. The solution for these boundary conditions is:

$$C = C_0 + \frac{(\omega^2 F N_0)}{(D_n k + (1+K)\omega^2} [1 - \exp(-\frac{k_n}{\omega} z)]$$

or

$$C = C_0 + (C_\infty - C_0) [1 - \exp(-\frac{k_n}{\omega} z)] \qquad [3.3]$$

The measured profiles of dissolved ammonium were fitted to equation 3.3. Results of the modelling efforts are shown in figure 3.4 and tabulated in table 3.1.

Table 3.1: Parameters used to describe ammonium profiles

	ABC15	ABC17	ABC23
C_0 mmol.kg^{-1}	2.35	0	0.4
C_∞ mmol.kg^{-1}	12.4	2.0	2.0
k/ω[a] cm^{-1}	2E-3	2.7E-3	3E-3
k_n *10^{-3}.yr^{-1}	0.30[b]	0.14[c]	0.15[c]
ω cm.kyr^{-1}	150[b]	50[c]	50[c]

[a]) obtained by curve fitting

[b]) ω is obtained from the sulphate profile and k is calculated from the k/ω ratio

[c]) ω is estimated from a 35 m long core in the Kretheus Basin (Van Santvoort and De Lange, pers. comm.) and k is calculated from the k/ω ratio.

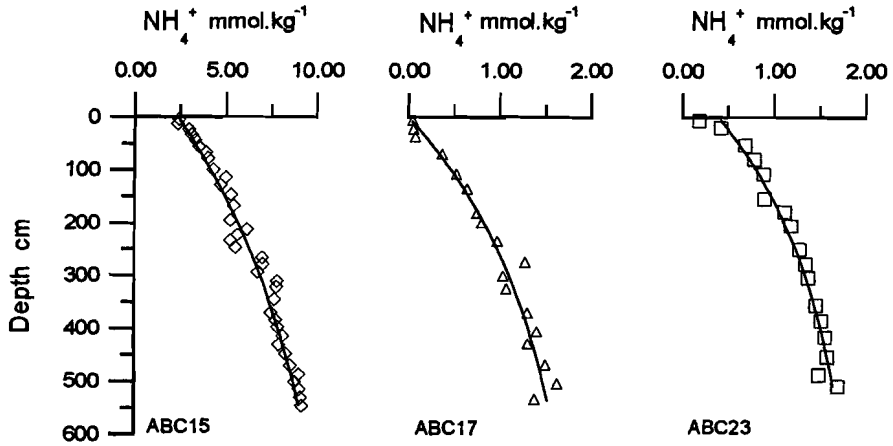

Figure 3.4: Ammonium versus depth in core ABC15, ABC17 and ABC23. Solid lines represent model fits (see table 3.1 for the parameters used).

Similarly, it is possible to model the sulphate concentration. In anoxic sediments, where organic carbon is limiting for sulphate reduction and sulphate remains present in the pore waters, the sulphate profile can be described by (Martens and Klump, 1984; Middelburg, 1990):

$$C = C_\infty + (C_0 - C_\infty) \exp\left(-\frac{k_s}{\omega} z\right) \qquad [3.5]$$

In which C_∞ is the concentration at some depth below which no further concentration change in sulphate concentration occurs and C_0 is the sulphate concentration at the top of the sediment core. The sulphate profile of core ABC15 from the Tyro Basin has been modelled using the equation 3.5. Due to core top loss the C_0 value is much lower than the brine concentration (44 mmol.kg^{-1}). Modelling efforts substituting the brine concentration for C_0 gave k/ω values that were not significantly different. The k_s is the first-order rate constant for organic matter decomposition obtained from curve fitting of the sulphate profile. In

figure 3.5 the best fit for the sulphate profile in core ABC15 is shown. Parameters used for modelling can be found in table 3.2.

Table 3.2: Parameters used to describe sulphate profile in core ABC15

	ABC15
C_o mmol.kg^{-1}	32
C_∞ mmol.kg^{-1}	1
k/ω cm^{-1}	6E-3
k_s *10^{-3}.yr^{-1}	0.9[a)]
ω cm.yr^{-1}	150[a)]

[a)]estimated from k/ω and $k = A\omega^2$, in which A is an empirical constant 0.04cm^{-2}.yr (Berner, 1978).

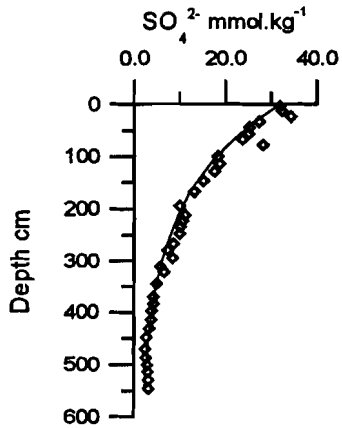

Figure 3.5: Sulphate versus depth in core ABC15. Solid line represents the best fit (see table 3.2 for the parameters used).

Toth and Lerman (1977) showed that over a large range of sedimentation rates the rate constant for sulphate reduction k_s is directly proportial to the sediment accumulation rate ω. They proposed:

$$k = A\,\omega^2 \qquad [3.4]$$

in which A is an empirical constant. For concave-down profiles of sulphate versus depth the average value for A is found to be 0.04 $yr.cm^{-2}$ (Berner, 1978). Using equation 3.4 and the k/ω ratio found for the sulphate profile of core ABC15 it is possible to estimate the sediment accumulation rate ω and the rate constant for sulphate reduction k_s. For core ABC15 ω is estimated to be 150 $cm.kyr^{-1}$, and k_s to be $0.9*10^{-3}$ yr^{-1}. The reactivity constant for organic nitrogen is obtained by applying the estimated ω value to the k/ω ratio found for the ammonium profile. A k_n value of $0.3*10^{-3}$ yr^{-1} is found for core ABC15. The relationship between k_n and ω, $k_n = 0.013\omega^2$, corresponds closely to the value of A found by Toth and Lerman (1977), being $k_n = 0.01\ \omega^2$.

The first-order rate constant for organic matter breakdown obtained from the sulphate profile, k_s, is higher than that estimated from the ammonium release, k_n. This could be due to several factors. First of all, one has to bear in mind that modelling is always subject to a-priori assumptions such as asymptotic values, constant sedimentation rates and no coretop loss. Secondly, k_n is estimated from modelling of an organic nitrogen compound and k_s from modelling of organic carbon. It is known that the organic nitrogen compounds are relatively reactive compounds. Before reaching the sediments these compounds most likely have been partly mineralized within the water column. Within the Tyro brine decomposition of organic matter takes place (De Lange et al, 1990a; Henneke and De Lange, 1990). A value of 1 $mmol.kg^{-1}$ NH_4^+ is observed in the brine, indicating the decomposition of nitrogen bearing organic matter. The organic matter that reaches the sediment surface contains less reactive organic nitrogen compounds, therefore a lower k_n can be observed.

Additionally, sulphate reduction by anoxic methane oxidation may have occurred in these sediments. There is no direct evidence for methanogensis in the sediments from core ABC15. However, in figure 3.6 the ammonium and the phosphate concentrations still increase while the sulphate concentration remains constant. This may indicate organic matter decomposition by methanogenesis. Consumption of sulphate by upward diffusion of methane has been reported for several anoxic marine environments (Devol and Ahmed, 1981; Middelburg, 1990). The consumption of sulphate by methane in core ABC15 is most likely to occur at the bottom of this core (> 500 cm). This has hardly any effect on the estimated k_s value obtained from curve fitting. Therefore the difference between k_s and k_n in core ABC15 is attributed to the variation of the organic matter decomposed in these sediments.

Using the relationship for k_n and ω found in core ABC15 for the cores ABC17 and ABC23 a sediment accumulation rate of 200 and 225 cm.kyr^{-1}, respectively, is found. This sedimentation rate is much higher than that found in a recently recovered 35 m long core taken from the Kretheus Basin. This sediment core shows the *Emiliana huxleyi* Acme zone (younger than 70.000 yr. B.P.) till a depth of 35 meter (Van Santvoort and De Lange, pers. comm.). Assuming that the average sedimentation rate in the Kretheus Basin is comparable for all sites in the basin and the average sedimentation rate in the Poseidon Basin is equal to that in the Kretheus Basin a sedimentation rate ω of about 50 cm.kyr^{-1} would be a better estimate for the cores ABC17 and ABC23. Additionally, sediments from the Tyro Basins display a more turbiditic pattern (Erba, 1991), indicating a higher sedimentation rate than in the Poseidon and Kretheus Basins.

Applying a sedimentation rate of 50 cm.kyr^{-1} the reactivity constant for organic nitrogen is found to be $0.14*10^{-3}$ and $0.15*10^{-3}$ yr^{-1} for ABC17 and ABC23, respectively. Consequently, the empirical relationship between k_n and ω in these cores must be approximately $k_n = 0.06\omega^2$.

The discrepancy between the k_n and ω relationship in the Tyro Basin and this relationship in the Poseidon and Kretheus Basins could be due to the different depositional environments. Aller and Mackin (1984) showed that the relationship between k and ω (equation 3.4) is

determined by various factors such as supply of electron acceptors, initial flux of organic matter and environment of sediment deposition.

The difference observed here can be attributed to the presence of an anoxic brine in the Tyro Basin, whereas the Poseidon and Kretheus Basins are thought to be oxygenated normal saline. The presence of an anoxic brine in the Tyro Basin may have a preservative effect on the organic matter reaching the sediment, whereas in the oxygenated water columns of the Poseidon and Kretheus Basins the most reactive organic matter may have been decomposed, before being burried in the sediment. Also, it is known that in the upper cm of a sediment core the most effective decomposition of organic matter by oxygen and iron- and manganese-oxides occurs (e.g. Froelich et al., 1979; De Lange, 1986). Therefore, in the top centimetres of the cores ABC17 and ABC23 most of the reactive organic matter might be decomposed before reaching the sulphate reduction zone. This would lead to a lower reactivity constant for the organic nitrogen in such cores and therefore an other relationship would be found than for sediments overlain by anoxic seawater.

The sulphate profiles in the pore waters from cores ABC17 and ABC23 are not only controlled by sulphate reduction but also by diffusive mixing of normal seawater with brine water. In both cores an increase of ammonium and total alkalinity with depth is observed (Figs. 3.2 and 3.3). Also sulphide has been measured, in core ABC17 up to a concentration of 2 mmol.kg^{-1} and in core ABC23 about 0.2 mmol.kg^{-1} (unpublished results, Catalano). The sulphate profile in ABC17 is constant with depth, whereas in core ABC23 a small decrease in sulphate is observed. The complexity of the simultaneous occurrence of sulphate reduction and diffusive mixing, perturbates the modelling of the sulphate profiles in these cores.

The sulphate reduction rate can be calculated from either SO_4^{2-} or NH_4^+ profiles. Bender and Heggie (1984) stated that the depth-integrated sulphate reduction rate (F_{SO4}) is equal to the SO_4^{2-} flux at $z=0$ or equal to the production rate of ammonium. At steady state the rate of sulphate reduction will be balanced by sulphate inputs of

molecular diffusion or advection (Canfield, 1991). Equation 3.6 gives the sulphate reduction rate at steady state. In equation 3.7, the sulphate reduction rate is estimated from the production rate of ammonium. The 0.5x/y is the ratio of sulphate consumption to ammonium production. For the Tyro Basin this ratio is 0.5*106/17 according to the calculated C/N ratio from equation 3.10, where D_s and D_n are the diffusion coefficients of sulphate and ammonium and ϕ the porosity (see appendix A).

$$F_{SO_4} = D_s\left(\frac{dSO_4}{dz}\right)_{z=0} * \phi - \phi\omega C_0 + \phi\omega C_\infty \qquad [3.6]$$

$$F_{SO_4} = \left(\frac{0.5x}{y}\right) D_n\left(\frac{dNH_4}{dz}\right)_{z=0} * \phi \qquad [3.7]$$

For the Tyro Basin a sulphate reduction rate of 15 μmol.cm^{-2}.yr^{-1} is found using equation 3.6. Based upon the ammonium profile (equation 3.7) and the C/N ratio the sulphate reduction rate is estimate to be 12 μmol.cm^{-2}.yr^{-1}. It seems that the high salinity (260 ‰) in the Tyro brine and sediments does not inhibit organic matter decomposition by sulphate reducing bacteria. Similar observations have been found in the Orca Basin (Sheu, 1990).

In case of the Poseidon and the Kretheus Basins the sulphate reduction rates are estimated from the ammonium production alone. The organic matter composition, reaching the sediment, is assumed to be similar to that in the Tyro Basin. For cores ABC17 and ABC23 sulphate reduction rates of 5 and 3 μmol.cm^{-2}.yr^{-1} are calculated, respectively.

The sulphate reduction rates observed in the anoxic sediments from the eastern Mediterranean are in the range of values observed in continental margins and marginal seas (Canfield, 1991). Sulphate reduction rates in the Poseidon and the Kretheus Basins are significantly lower than the sulphate reduction rate observed in the

Tyro Basin. This corresponds with a lower reactivity constant for organic nitrogen and lower sedimentation rates in these cores. Additionally, at the interface of the Tyro brine organic material is formed (DeDomenico and DeDomenico, 1989;Henneke et al., 1990; Erba, 1991). This newly formed organic matter will also reach the sediments and may contribute to the higher rate of sulphate reduction in the Tyro Basin.

It can be concluded that in anoxic hypersaline sediments from the eastern Mediterranean sulphate reduction takes place, even in the highly saline sediments from the Tyro Basin. Sulphate reduction rates are high in those sediments overlain by an anoxic brine, due to "preservation" of the reactive organic matter. When the anoxic brine is replaced by normal marine oxygenated seawater the sulphate reduction rates become lower.

3.3.2 Composition of the decomposing organic matter

A best estimate of the average chemical composition of the decomposing organic matter can be made from the stoichiometric relation between the changes in concentration of sulphate, ammonium and phosphate. In figure 3.6 the dissolved sulphate, ammonium and phosphate concentrations from the Tyro Basin (ABC15) are plotted against each other. The slopes of the straight lines between sulphate depletion, ammonium and phosphate enrichments can be used to estimate the C:N:P stoichiometry, provided that corrections are made for differential diffusion and adsorption (Berner, 1977). The appropriate equations of C/N and N/P ratios are:

$$\frac{C}{N} = \frac{2\Delta SO_4 \ (\omega^2 + kD_s)}{\Delta NH_4 \ (\omega^2(1+K_n) + kD_n)} \qquad [3.8]$$

$$\frac{N}{P} = \frac{\Delta NH_4 \ (\omega^2(1+K_n) + kD_n)}{\Delta PO_4 \ (\omega^2(1+K_p) + kD_p)} \qquad [3.9]$$

Where ΔSO_4 is the sulphate depletion, ΔNH_4 and ΔPO_4 are the ammonium and phosphate enrichments; K_n and K_p are the linear sorption coefficients of ammonium and phosphate, with values og 1.4 and 1.8 respectively. Rosenfeld (1979) found a value of 1.3 for K_n in marine sediments. For the anoxic hypersaline sediments from core ABC15 a value of 1.4 was found for K_n, based upon the relation between exchangeable ammonium and the dissolved ammonium concentration (unpublished data). Krom and Berner (1980) published a value for K_p of 1.8. For the sediments investigated in this study, the contribution of the term ω^2 in equations 3.8 and 3.9 is very small in comparison with the kD term and can therefore be neglected. This leads to the following simplifications of the above equations (3.8 and 3.9):

$$\frac{C}{N} = \frac{2\Delta SO_4 * D_s}{\Delta NH_4 * D_n} \quad , \quad \frac{N}{P} = \frac{\Delta NH_4 * D_n}{\Delta PO_4 * D_p} \qquad [3.10]$$

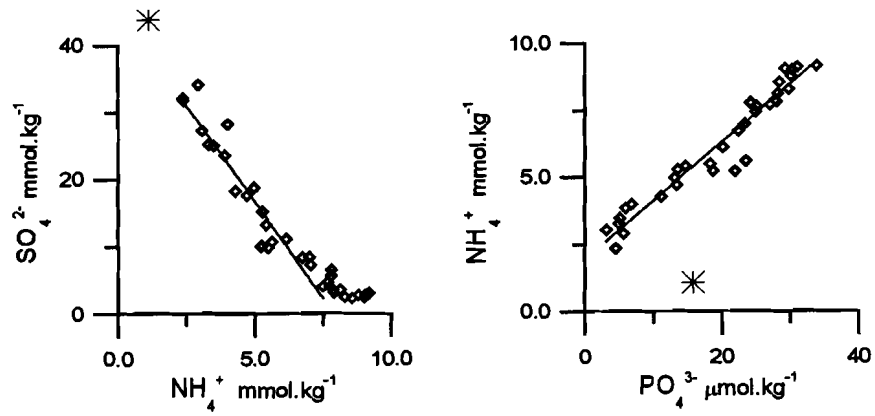

Figure 3.6: Sulphate versus ammonium and ammonium versus phosphate in pore waters from ABC15. The asterix symbol represents the concentration in the Tyro brine.

The slope of the solid lines in figures 3.6A and 3.6B are used to estimate the C/N and N/P ratio, respectively. The C/N molar ratio of decomposing organic matter in the sediments of the Tyro Basin is calculated to be 6.1, whereas the N/P ratio range is 597. Accordingly, the composition of organic matter reaching the sediment-water interface in the Tyro Basin can be represented by:

$$(CH_2O)_{106}(NH_4)_{17}(H_3PO_4)_{0.03}$$

The high N/P ratio indicates that the pore waters of the anoxic hypersaline sediments in the Tyro Basin contain more ammonium than phosphate in comparison to the Redfield ratio (N/P = 16). This could mean that the N/P ratio has been overestimated because of the preferential removal of phosphate. Phosphate can be removed by authigenic P-bearing mineral formation (Martens et al., 1978), such as apatite and struvite, or by adsorption on calcium-carbonates (Froelich et al., 1982). Alternatively, if phosphate is limiting for the primary production, higher N/P ratios in the organic matter can be expected. Krom et al. (1991) reported on phosphate limitation in the eastern Mediterranean. These authors found higher N/P ratios, on the average around 28, in the water column than the Redfield ratio.

It is unlikely that the high N/P ratio of the decomposing organic matter can be explained by the higher N/P ratios found in the water column (Krom et al., 1991) and Tyro brine (N/P is 68, marked as * in Fig. 3.1; De Lange et al., 1990a). Pore waters from the tripcore and the top of core ABC15 are depleted in phosphate with respect to the concentration in the Tyro brine (Fig. 3.1). Consequently, the depletion in P in the pore waters is due to selective removal of dissolved phosphate. Within the sediments of the tripcore and the top of core ABC15 calcium-carbonate precipitation has been shown to occur (see chapter 4). Adsorption of phosphate on calcium-carbonates could explain the removal of phosphate from the pore waters.

3.4 Dissolved organic carbon

The distributions of DOC in the pore waters of anoxic hypersaline sediments (cores ABC15 and ABC17) are shown in figure 3.7. The concentration of DOC in the pore waters of these sediments are in the range of the values reported for other anoxic marine sediments (Table 3.3).

Table 3.3: The range of DOC in pore waters found in different anoxic marine sediments

Location	Range of DOC, mmol.l^{-1}	Reference
Black Sea	1.3 - 1.7	Starikova, 1970
Sea of Azov	1.2 - 5.0	Starikova, 1970
Loch Duich, Scotland	0.7 - 5.5	Krom and Sholkovitz, 1977
Great Bay, N.H.	0.2 - 11	Lyons et al., 1979
Orca Basin	5.3 - 19	Ishizuka et al.,
Mangrove Lake	0.3 - 3.3	Orem et al., 1986
Tyro Basin	1.1 - 11	this study
Poseidon Basin	0.8 - 7.7	this study

The DOC concentration in the pore waters from the cores ABC15 and ABC17 increases with depth (Figs. 3.7). This increase correlates very closely ($r > 0.95$) with the decrease in sulphate concentration in core ABC15 and the increase of ammonium, phosphate and total alkalinity (Fig. 3.8) in both cores. Similar results have been obtained by studies of Starikova (1970), Krom and Sholkovitz (1977) and Krom and Westrich (1980).

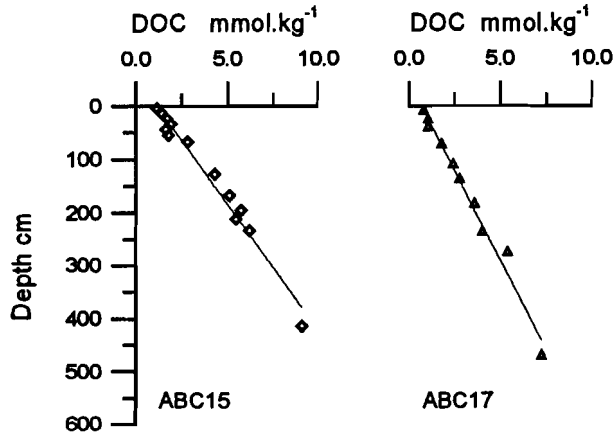

Figure 3.7: The DOC concentration in core ABC15 (diamond) and core ABC17 (triangle) versus depth.

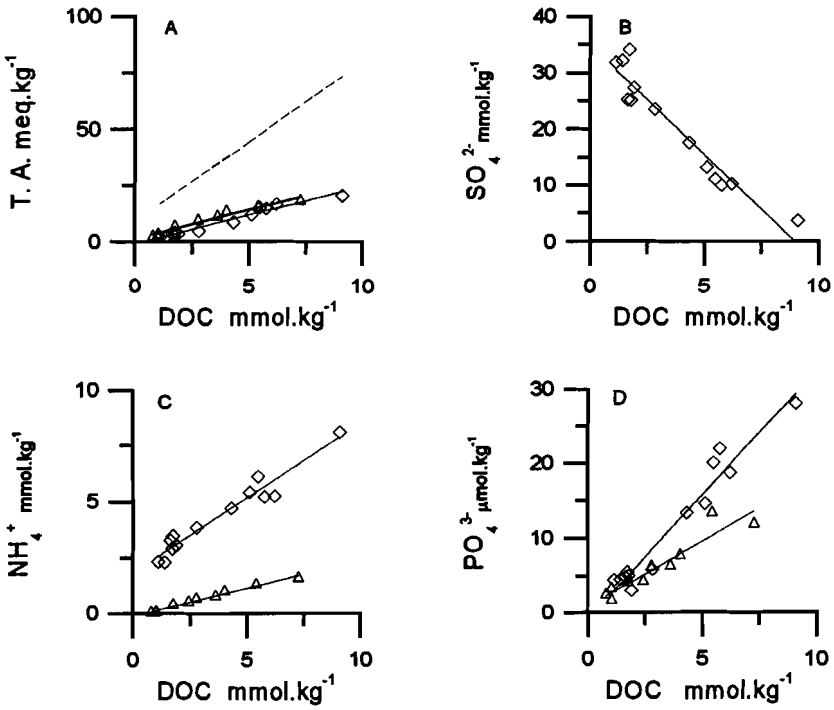

Figure 3.8: A) Total alkalinity versus DOC; diamond symbols are ABC15 and triangle symbols are ABC17. The dashed line represents the best fit for alkalinity values calculated from ammonium for core ABC15 (see text) versus the DOC. B) Sulphate versus DOC for core ABC15. C) Ammonium versus DOC. D) Phosphate versus DOC. The best linear fits are shown.

In figure 3.8 total alkalinity versus DOC is shown. It can be noticed that there is a similar slope between total alkalinity and DOC for the pore waters from both basins. However, in core ABC15 the total alkalinity profile is strongly influenced by carbonate precipitation (see chapter 4). This is less the case in core ABC17. When the potential alkalinity is calculated from the ammonium or sulphate profile (see equation 4.1, chapter 4) in core ABC15, the slope is much higher. Also the slopes for phosphate versus DOC and for ammonium versus DOC are much higher in the Tyro Basin than in the Poseidon Basin (Fig. 3.8).

DOC is known to be an important intermediate in the decomposition of organic matter by sulphate reducing bacteria (e.g. Nissenbaum et al., 1972b; Krom and Westrich, 1980; Capone and Kiene, 1988). The observed correlations between DOC and sulphate in core ABC15 and DOC and the metabolites in both cores confirm the involvement of DOC in the sulphate reduction process in these anoxic hypersaline sediments.

The general pathway of mineralization of organic matter by sulphate reducing bacteria can be described briefly as follows (e.g. Nissenbaum et al., 1972b; Krom and Westrich, 1980; Capone and Kiene, 1988; Alperin, 1989): labile organic matter is broken down microbially to polymers (High Molecular Weight DOC) and subsequently to monomers. This latter process is called fermentation. Sulphate reducing bacteria utilize only monomers, such as acetate and lactate, forming inorganic metabolites (e.g. Barcelona, 1980). An outline of this model is shown in figure 3.9.

In both cores DOC is accumulating till the same level of 10 mmoles.kg^{-1} (Fig. 3.7). In core ABC15 per one mmol DOC 7 meq alkalinity, 0.66 mmol ammonium and 331 μmol phosphate is present (Fig. 3.8). However, in core ABC17 per mmol DOC 2.5 meq alkalinity, 0.25 mmol ammonium and 174 μmol phosphate is observed (Fig. 3.8). This means that in the sediments of the Poseidon Basin the amount of metabolites formed per mol DOC is only one third of that formed in the sediments of the Tyro Basin.

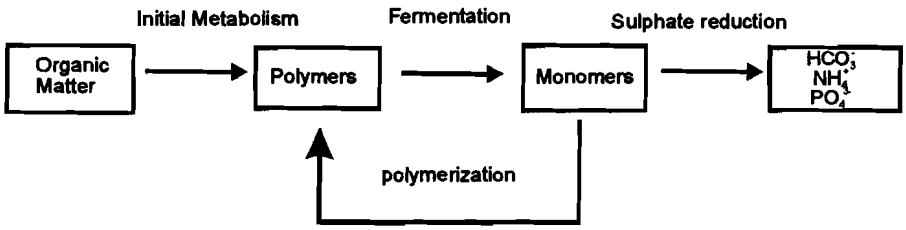

Figure 3.9: General pathway of mineralization of organic matter by sulphate reducing bacteria (e.g. Nissebaum et al., 1972b; Krom and Westrich, 1980; Capone and Kiene, 1988; Alperin, 1989).

The sulphate reduction rate in the sediments from the Tyro Basin is about three times higher than the rate observed in the sediments from the Poseidon Basin. A higher sulphate reduction rate implies more monomer formation according to the model in figure 3.9. Krom and Westrich observed that 90% of the DOC consists of HMW DOC in anoxic marine pore waters, and stated that the amount of monomers in the pore waters is due to an equilibrium between the production of these monomers and the formation of HMW DOC by polymerization or consumption by sulphate reducing bacteria. Assuming a similar rate of monomers formation in the sediments of the Tyro and Poseidon Basins a higher amount of DOC is expected to be present in the sediments of the Tyro Basin. However, the amount of DOC in the pore waters of both cores is comparable. Therefore, it is suggested that it rather is the turnover rate of HMW DOC to monomers than the decomposition of organic matter to DOC that determines the sulphate reduction rate in these anoxic hypersaline sediments

3.5 Summary and conclusions

The pore water data from the anoxic sediments from the Tyro, Poseidon and Kretheus Basins indicate that organic matter is decomposed by sulphate reducing bacteria. This is shown by a decrease in sulphate concentrations and increase in products as ammonium, alkalinity and phosphate. It seems that despite the high salinity content in the Tyro brine, sulphate reduction in not inhibited. The sulphate reduction rate in the Tyro Basin is much higher than the rates observed in the Poseidon and Kretheus Basins. This due to 1) the anoxic brine in the Tyro Basin, which has an preservative effect on the organic matter reaching the sediment and, 2) in the top of the cores ABC17 and ABC23 most reactive material would have been decomposed by manganese and iron-oxides before reaching the sulphate reduction zone.

Incomplete mineralization of the organic matter causes an increase in DOC in the pore waters from the Tyro and Poseidon Basins. In both basins accumulation of DOC occurs till about 10 $mmol.kg^{-1}$. The accumulation of DOC correlates with the decrease of sulphate in core ABC15 and the increase of alkalinity, ammonium and phosphate in cores ABC15 and ABC17. The amount of metabolites formed per mol DOC in the sediments of the Poseidon Basin is only one third of that formed in the sediments from the Tyro Basin. It is proposed that the turn over rate of polymers to monomers determines the sulphate reduction rates in the anoxic hypersaline sediments from the eastern Mediterranean.

Chapter 4: Carbonate diagenesis in anoxic hypersaline sediments from the Tyro area.

Abstract

Pore water chemistry is used to identify authigenic carbonate formation in anoxic hypersaline sediments from the Tyro, Poseidon and Kretheus Basins. The distribution of alkalinity, Ca, Mg and Sr in the pore waters indicate the formation of Ca,Mg-carbonates in these sediments. A model program PHRQPITZ (Plummer et al., 1988) has been applied in order to determine which carbonates are formed. All pore waters are supersaturated with respect to dolomite. Cores ABC15 from the Tyro Basin and ABC23 from the Kretheus Basin also show a loss in alkalinity, whereas this is not the case in core ABC17 from the Poseidon Basin.

Organogenic dolomite and high Mg-calcite formation is likely to have taken place in the anoxic hypersaline sediments from the Tyro Basin. The loss in alkalinity estimated from the potential and the measured alkalinity is linearly related to the decrease in Ca and Mg. This stoichiometric relation implies that dolomite has been formed by direct precipitation. In contrast dolomite formation in the Poseidon and Kretheus Basins is more likely to have occurred by replacement of calcite and aragonite. In core ABC17 the incorporation of Mg in opal-CT could have been an other sink for Mg in these pore waters.

4.1 Introduction

The release of inorganic metabolites, due to the decomposition of organic matter by sulphate reducing bacteria, may result in the formation of authigenic minerals when their concentrations exceed the solubilities of these minerals (Suess, 1979; Middelburg et al., 1990; Morse and Mackenzie, 1990). The formation of sulphide, phosphate and carbonate minerals in organic-rich anoxic marine sediments has been a subject of research for many scientists (e.g. Martens et al., 1978; Suess, 1979; Berner, 1984; Middelburg et al., 1990). The occurrence and formation of sulphides will be discussed in chapter 9.

Decomposition of organic matter will not only lead to authigenic carbonate formation, but may also lead to dissolution or recrystallization of biogenic carbonates (Morse and Mackenzie, 1990). Calcite and aragonite may dissolve or be replaced by other carbonates, such as high Mg-calcite and dolomite (see for a review Morrow, 1982; Morse and Mackenzie, 1990).

In hypersaline environments authigenic dolomite and other minerals are often related to evaporitic processes, such as in the Persian Gulf sabkhas (Morrow, 1982). However, in deep-sea environments dolomite formation is related to the decomposition of organic matter (Compton, 1988; Suess et al., 1988). The decomposition of organic matter by sulphate-reducing bacteria promotes the formation of dolomite by simultaneously increasing the alkalinity and decreasing the sulphate concentration to near zero (Compton, 1988; Middelburg et al., 1990). This so-called organogenic dolomite is often found in trace amounts in organic-rich anoxic sediments (Morrow, 1982; Baker and Burns, 1985; Compton, 1988).

In this study pore water chemistry is used to identify authigenic carbonate mineral formation in anoxic hypersaline sediments from the eastern Mediterranean.

4.2 Material and methods

Sediment cores from the Tyro, Poseidon and Kretheus Basins have been studied for their interstitial water chemistry. Core ABC15 is taken from the anoxic hypersaline Tyro Basin, whereas core ABC17 and core ABC23 are taken from the Poseidon and Kretheus Basins, respectively.

Shipboard procedure for sample processing has been described in detail by De Lange (1992). The sediment samples were squeezed with modified Reeburgh-type squeezers in a glove box flushed with high-purity nitrogen and in a room held at a constant bottom water temperature of 13°C. Interstitial water was collected in acid-cleaned bottles.

Total alkalinity was measured on board ship, usually within 24 hours after collection, by an automatic potentiometric titration system using 0.05 M HCl. Major cations were measured by ICPES (ARL 34.000) after 10 to 100 times dilution, obtaining a concentration for Na equal to one-tenth of that of normal seawater. Analytical presicion was determined by replicate analyses of Atlantic seawater (Madeira Abyssal Plain). Usually a precision of 3% was obtained for Ca, Mg and Sr.

The pH in the sediments was determined by punch-in pH measurements using a glass-carbon electrode (Ingold) with an internal reference electrode.

4.3 Alkalinity

Total alkalinity and punch-in pH data from cores ABC15, ABC17 and ABC23 are shown in figures 4.1, 4.2A and 4.2B, respectively.

The total or titration alkalinity refers to the acid neutralizing capacity of the pore waters (Stumm and Morgan, 1981; Morse and Mackenzie, 1990). The contribution of carbonate to the total alkalinity is called carbonate alkalinity and is defined as:

$$Alk_{carb.} = [HCO_3^-] + 2[CO_3^{2-}].$$

At the pH of the anoxic hypersaline sediments, the following species may contribute significantly to the total alkalinity: HCO_3^-, CO_3^{2-}, OH^-, H^+, $B(OH)_4^-$, HS^-, HPO_4^{2-} and $H_3SiO_4^-$. To obtain the carbonate alkalinity one has to correct the total alkalinity for the contribution of borate, sulphide, phosphate and silicate. Because of their relative low concentrations the contributions of phosphate and silicate have been neglected. In figure 4.1 the alkalinity corrected for borate and sulphide is shown. This correction is rather small (< 10%). Therefore, the measured total alkalinity is assumed to be equal to the carbonate alkalinity.

The carbonate alkalinity in pore waters in anoxic marine sediments is determined by the following reactions, amongst others (Berner et al, 1970; Froelich et al., 1979; Devol et al., 1984; Middelburg, 1990):

I. organic matter decomposition by bacterial sulphate reduction

$$(CH_2O)_{106}(NH_3)_{16}(H_3PO_4) + 53SO_4^{2-} \rightarrow$$
$$106HCO_3^- + 16NH_4^+ + HPO_4^{2-} + 53H_2S$$

II. methanogenesis

$$(CH_2O)_{106}(NH_3)_{16}(H_3PO_4) \rightarrow 16NH_3 + 53CH_4 + 53CO_2 + HPO_4^{2-}$$
$$NH_3 + CO_2 + H_2O \rightarrow NH_4^+ + HCO_3^-$$

III. anoxic methane-oxidation

$CH_4 + SO_4^{2-} \rightarrow HCO_3^- + HS^- + H_2O$

IV. precipitation and dissolution of carbonates

$CO_2 + H_2O + CaCO_3 \rightleftharpoons Ca^{2+} + 2HCO_3^-$

V. authigenic silicate formation

$3Al_2Si_2O_5(OH)_4 + 2K^+$ (or with Na^+ and Mg^{2+}) $+ 2HCO_3^- \rightleftharpoons$

$2KAl_3Si_3O_{10}(OH)_2 + 2CO_2 + 5H_2O$

Additionally, sulphide precipitation effects the pH and can even buffer the pH at a near constant level (Boudreau and Canfield, 1993). The precipitation of iron-sulphides may therefore influence the carbonate precipitation/dissolution.

The carbonate alkalinity expected from the decomposition of organic matter by sulphate reduction (reaction I) can be calculated either from the ammonium concentrations or from the decrease in the sulphate concentrations in the pore waters.

Assuming stoichiometric decomposition of the organic matter decomposing in the Tyro area (C:N:P = 106:17:0.03; see chapter 3) an estimate of the produced alkalinity (HCO_3^-) can then be made using the following equation:

$$[HCO_3^-] = \frac{106\ D_n\ [NH_4^+]}{17\ D_{alk}} \qquad [4.1A]$$

or

$$[HCO_3^-] = \frac{D_s\ [SO_4^{2-}]}{0.5 D_n} \qquad [4.1B]$$

In which $[HCO_3^-]$, $[NH_4^+]$ and $[SO_4^{2-}]$ are the potential alkalinity, the increase in the ammonium concentration and the decrease in sulphate concentration, respectively. The diffusion coefficients D_n, D_s and D_{alk} have been calculated according to Li and Gregory (1974) and can be found in appendix A.

For core ABC15 the potential alkalinity, based upon the ammonium and the sulphate concentrations, is much higher than the alkalinity actually observed in the pore waters (Fig. 4.1). A similar discrepancy is found for core ABC23, in which the potential alkalinity is calculated from the ammonium data (Fig. 4.2B). For core ABC17 the alkalinity estimated from ammonium is similar to the measured alkalinity (Fig. 4.2A).

The loss of alkalinity in the pore waters of core ABC15 and core ABC23 may be related to reactions such as IV and V, and will be discussed in more detail in section 4.5.

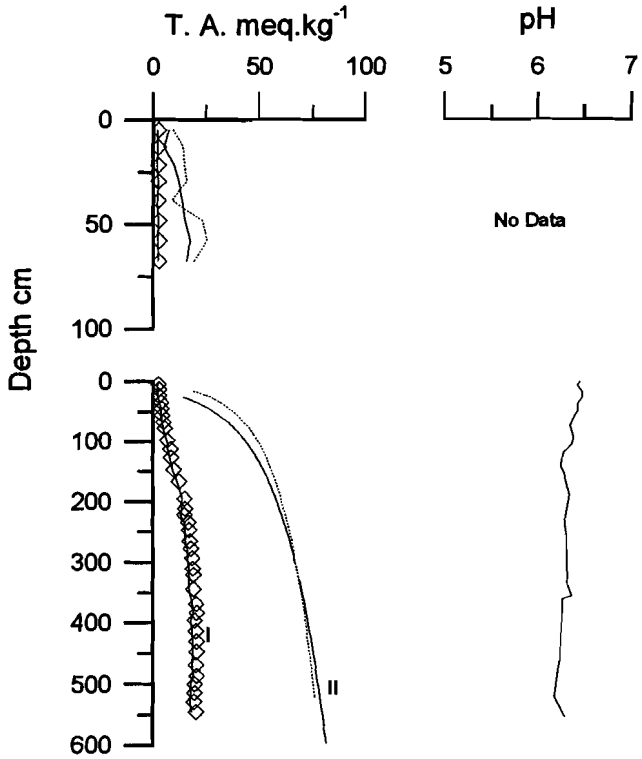

Figure 4.1: Alkalinity and pH versus depth profiles in core ABC15. Diamond symbols represent total alkalinity values measured in the pore waters. Solid line I is the alkalinity profile corrected for borate and sulphide. Solid line II is the alkalinity profile calculated from ammonium measurements and the dashed line the profile calculated from the sulphate data according to equation 4.1. Upper graph show data from tripcore of ABC15.

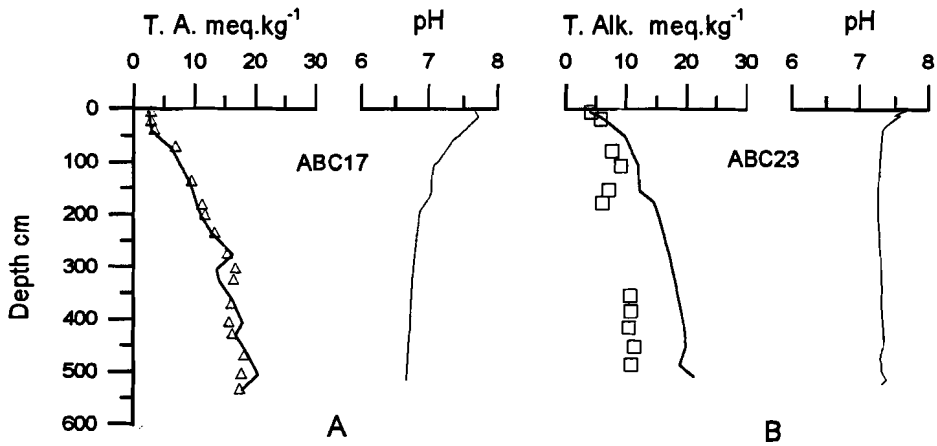

Figure 4.2: Alkalinity and pH versus depth profiles in core ABC17 (A) and core ABC23 (B). Symbols represent the measured total alkalinity data and the solid line the alkalinity profile calculated from the ammonium data (equation 4.1A).

4.4 The major ions: Ca, Mg and Sr

The pore waters from core ABC15 are strongly depleted in Ca and Mg compared to the concentration of the elements observed in the Tyro brine (Fig. 4.3). The concentrations of both Ca and Mg decrease with depth, whereas the alkalinity first increases and finally remains constant at a concentration of approximately 20 meq.kg^{-1} (Fig. 4.1). - The difference between the Ca and Mg concentration in pore water and brine correlates nicely with the difference in the potential alkalinity and the observed alkalinity (Fig. 4.4). This strongly suggests the precipitation of Ca, Mg-carbonates in the sediments of the Tyro Basin. The Sr concentration in this core is almost constant with depth, a slight increase is observed at the bottom of this core (> 500 cm) (Fig. 4.3). During carbonate diagenesis Sr can be mobilized because of the recrystallization of the carbonates (Walls et al., 1977; Baker et al., 1982).

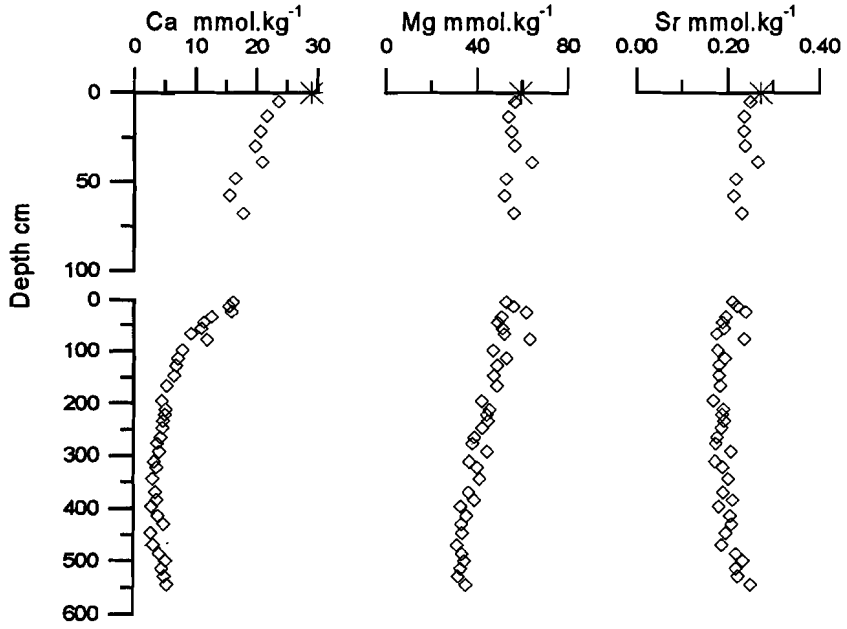

Figure 4.3: Pore water profiles versus depth of Ca, Mg and Sr in core ABC15. Asterix symbol represent values observed in the Tyro brine. Upper graphs show data from tripcore ABC15.

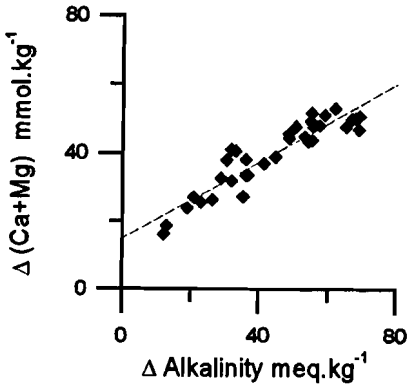

Figure 4.4: The difference in Ca and Mg concentration between the pore waters of ABC15 and the Tyro brine versus the difference between calculated alkalinity and observed alkalinity. Dashed line represents the best fit.

In core ABC17 Mg decreases with depth, whereas Ca and Sr slightly increase with depth (Fig. 4.5). Also in core ABC23 the Mg concentration decreases with depth (Fig. 4.6). In this core Ca shows a slight decrease and the Sr concen-tration remains almost constant (Fig. 4.6).

In chapter 2 it has been shown that the pore water composition of cores ABC17 and ABC23 is influenced by diffusive mixing of normal seawater and brine. Based on the Na/Cl ratio it was proposed that this brine had a similar composition to that of the Tyro brine. Assuming that the brines in the Poseidon and Kretheus Basins had a similar composition for the other elements to that of the Tyro brine the contribution of diffusive mixing to the pore waters can be estimated. However, it was shown that the composition of the elements such as Mg, Ca, SO_4^{2-} and Sr varies between the basins in the Bannock area, although their Na/Cl ratio is similar (De Lange et al., 1990a). Such differences may be present between the Tyro, Poseidon and Kretheus brines as well. Therefore the interpretation of diffusive mixing should be done with care.

Profiles of diffusive mixing between normal seawater and brine for Ca, Mg and Sr are calculated with the model discussed for the Cl-profiles (see chapter 2). The concentration at time of isolation C_i is equal to that of the Tyro brine, whereas the present-day concentration C_0 is the average concentration of eastern Mediterranean seawater. Values used for modelling are shown in table 4.1. All diffusive-mixing profiles are calculated for a sedimentation rate of 50 cm.kyr^{-1} and a time of 2000 and 3000 years. The diffusion coefficients can be found in appendix A.

Table 4.1: C_i is the brine concentration and C_0 the present day concentration of average eastern Mediterranean seawater.

	C_i Tyro brine	C_0 eastern Med.
Ca mmol.kg^{-1}	29	12
Mg mmol.kg^{-1}	59	57
Sr μmol.kg^{-1}	272	96

The Sr data in cores ABC17 and ABC23 seem to be related to a diffusive mixing profile when cross-coupling terms are taken into account (Figs. 4.5 and 4.6). In appendix A, the calculation of cross-coupling terms according to McDuff and Ellis (1979) is reported. Especially the diffusion coefficient of Sr is influenced by cross-coupling terms. A similar observation was found by Ten Haven et al. (1987) in another core taken from the Kretheus Basin.

The concentration of Mg in the Tyro brine is almost equal to that of average eastern Mediterranean seawater. A contribution of diffusive mixing to the Mg profile can be neglected. The decrease of Mg with depth in the pore waters of cores ABC17 and ABC23 is related to diagenetic processes (Figs. 4.5 and 4.6).

For Ca the picture is more complicated. In core ABC17 the slight increase of Ca in the top 200 cm corresponds with the diffusive mixing profile (Fig. 4.5). Below this depth the Ca concentration is lower than expected from the diffusive mixing profile and remains nearly constant with depth (Fig. 4.5). This could either mean that Ca is removed from the pore waters by diagenetic processes or that the Ca concentration in

the Poseidon brine might have been lower than in the Tyro brine. In core ABC23 the Ca concentration is significantly lower than expected from the diffusive mixing profile (Fig. 4.6). Together with the observation of a decrease in Mg concentration in the pore waters and the observed loss in alkalinity, formation of Ca, Mg-carbonates are proposed to act as sinks for Ca, Mg and alkalinity in core ABC23. This is not that straightforward in core ABC17.

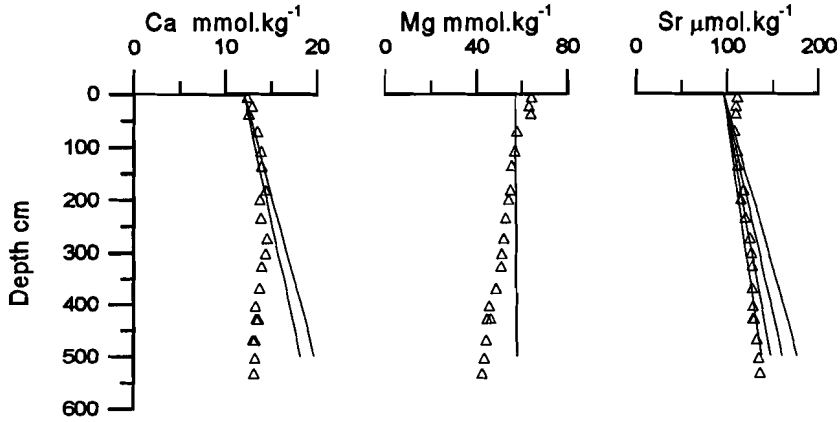

Figure 4.5: Pore water profiles versus depth of Ca, Mg and Sr in core ABC17. Solid lines show diffusive-mixing profiles between normal seawater and brine.

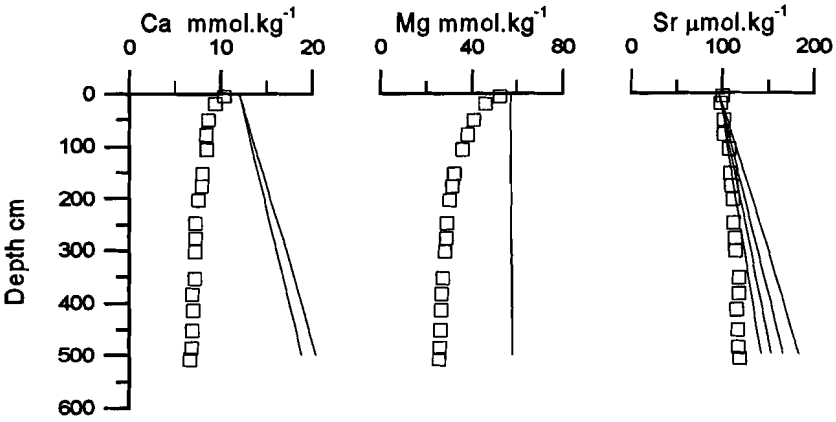

Figure 4.6: Pore water profiles versus depth of Ca, Mg and Sr in core ABC23. Solid lines show diffusive-mixing profiles between normal seawater and brine.

In order to determine which carbonates may be formed the ion-activity product has been calculated using the model program PHRQPITZ (Plummer et al., 1988). An outline of this program is given in appendix B

4.5 Dolomitization

The pore waters from core ABC15 appear to be supersaturated with respect to the mineral dolomite, pK_{dol} is 16.79 (Fig. 4.7). The pore water composition seems to reach an apparent equilibrium with respect to protodolomite (pK = 15.5).

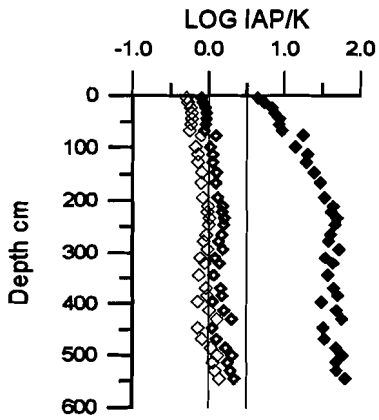

Figure 4.7: Calculated saturation index (Log IAP/K) for aragonite (open diamond; pK = 8.15), calcite (semi-closed diamond; pK = 8.35) and dolomite (closed diamond; pK = 16.79) in core ABC15. Solid lines mark area of thermodynamic solubility (see text for detail).

Dolomitization in sediments can occur by the following stoichiometric relations (Morrow, 1982; Baker and Burns, 1985).

I Aragonite or calcite replacement

$$2CaCO_3 + Mg^{2+} \Rightarrow CaMg(CO_3)_2 + Ca^{2+}$$

II Direct precipitation from pore water solution

$$Ca^{2+} + Mg^{2+} + 4HCO_3^- \Rightarrow CaMg(CO_3)_2 + 2CO_2 + 2H_2O$$

III An intermediate stoichiometry, for example

$$CaCO_3 + Mg^{2+} + 2HCO_3^- \Rightarrow CaMg(CO_3)_2 + CO_2 + H_2O$$

In order to determine which of these reactions occurs in anoxic hypersaline sediments the following assumptions have been made: (1) dolomite is forming and (2) the pore water chemistry shown here represents steady state and reflects the chemistry at the time of dolomitization.

The decrease of Ca in the pore waters of core ABC15 and the accompanying decrease of Mg rules out dolomitization according to the first reaction. In figure 4.4 it has been shown that the decrease in Ca and Mg correlates with the loss in alkalinity. The stoichiometric relation is near 0.5, implying direct precipitation of dolomite according to reaction II. However, the pore waters show a decrease in the Ca concentration only till 150 cm depth, while the Mg concentration still decreases. In these sediments, dolomitization seems not to be limited by the availability of Mg and carbonate alkalinity but most likely by Ca. Therefore, the dissolution of calcium-carbonates below a depth of 150 cm may lead to dolomite formation according to reaction III. According to the thermodynamic calculations, the pore waters are undersaturated with respect to calcite (pK_{cal} = 8.35) and aragonite (pK = 8.15). So, dissolution of these minerals may occur.

The offset Δ(Ca+Mg) in figure 4.4 is related to the large difference between Ca in the brine and in the pore waters of the top of core ABC15. In the trip core of core ABC15 the Ca concentration decrease from about 23 to 15 mmol.kg^{-1}, whereas the Mg concentration and alkalinity are constant (Figs. 4.1 and 4.3). From the ammonium profile the loss of alkalinity in the trip core can be estimated (see above), which is about 10 meq.kg^{-1}. Ca-carbonate formation is likely to occur at the top of this sediment core. The lithological description of this core

describes the occurrence of homogeneous carbonate ooze at the top meter of core ABC15 and within the trip core.

The pore waters from the Poseidon Basin and the Kretheus Basin are supersaturated with respect to dolomite too (Fig. 4.8). However, the pore water profiles display hardly any loss in alkalinity (Fig. 4.2). The removal of Mg from these pore waters can be due to the replacement of calcite or aragonite (reaction I). Both pore water profiles are undersatured with respect to those minerals. Additional removal of Mg in core ABC17 may occur be incorporation of Mg in opal-CT. Core ABC17 differs in lithology from the cores ABC15 and ABC23 because of the presence of a thick layer of gelatinous pellicles from two meter depth till maximum depth of recovery (546 cm). In the sediments of this core diatoms and siliceous microfossils are the dominant components, whereas in core ABC15 calcareous plankton is more abundant (Erba, 1991). During early diagenesis siliceous ooze (opal-A) has been reported to be transformed into opal-CT in deep-sea sediments and Mg is incorporated (Kastner et al., 1977; Baker and Kastner, 1981). The transformation of opal-A to opal-CT is greatly enhanced by solutions high in Mg and alkalinity and in the absence of reactive clay minerals (Kastner et al., 1977). Conditions in ABC17 seem to favour such removal mechanism for Mg.

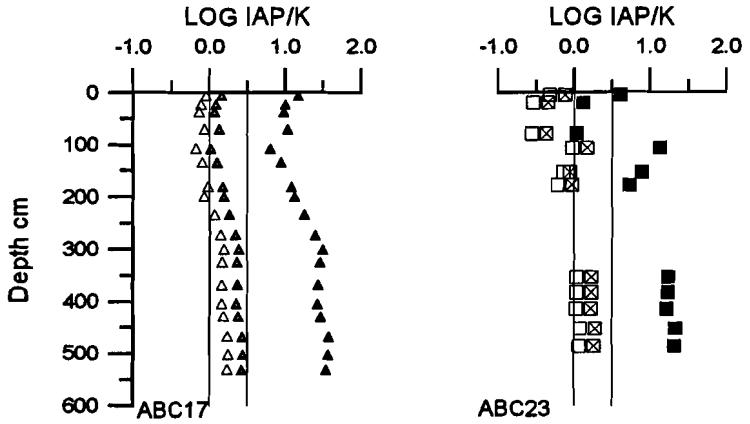

Figure 4.8: Calculated saturation index (Log IAP/K) for aragonite (open triangle; pK = 8.15), calcite (semi-closed triangle; pK = 8.35) and dolomite (closed triangle; pK = 16.79) in core ABC17. For core ABC23 Log IAP/K of aragonite (open square), calcite and dolomite (closed square). Solid lines mark area of thermodynamic solubility (see text for detail).

4.6 Summary and conclusions

Using stoichiometric organic matter decomposition and the measured ammonium data the potential increase in alkalinity was determined. The pore waters from cores ABC15 (Tyro Basin) and ABC23 (Kretheus Basin) show a loss in potential alkalinity, whereas this is not the case in core ABC17. This removal of alkalinity can be explained by authigenic carbonate mineral formation.

Organogenic dolomite and high Mg-calcite formation is likely to have taken place in the anoxic hypersaline sediments of core ABC15. Due to the decomposition of organic matter by sulphate reducing bacteria the alkalinity increases strongly. The loss in alkalinity estimated from the potential alkalinity and the measured alkalinity is linearly related to the decrease in Ca and Mg. The stoichiometric relation implies that dolomite is formed by direct precipitation. In contrast the removal of Mg from the pore waters of cores ABC17 and ABC23 is related to the replacement of calcite or aragonite. Formation of high Mg-calcite or dolomite is these sediments seems not to be inhibited by the presence of sulphate as was proposed by Baker and Kastner (1981). Additional information from thermodynamic equilibrium calculations showed that the pore waters in all cores are close to saturation with respect to dolomite.

In the pore waters of core ABC17 a decrease in the Mg concentration is observed, while there is no loss in alkalinity. The sediments from this core contain high amounts of siliceous oozes. Incorporation of Mg during diagenesis of these siliceous oozes to opal-CT is thought to be the sink for Mg in this core.

Chapter 5: Interstitial water chemistry in an anoxic hypersaline sediment core from the Bannock Basin

Abstract

The interstitial water chemistry of core ABC45 from the Bannock Basin has been studied. Pore water from this core show a decrease in the sulphate concentration with depth, while there is no significant increase in ammonium, phosphate and alkalinity concentration down-core. The decrease in sulphate is due to bacterial sulphate reduction in the top of the core and gypsum formation deeper in the core. The sulphate reduction rate is estimated to be 9.5 μmoles.cm^{-2}yr^{-1}.

Thermodynamic calculations with PHRQPITZ (Plummer et al., 1988) indicate that the pore waters are saturated with respect to gypsum and supersaturated with respect to dolomite. This is in agreement with observations in the Bannock Basin, which show dolomite and gypsum formation (De Lange, 1990b). Dolomite is though to be formed by replacement of aragonite or calcite. The release of Ca is partly removed from the pore waters by the formation of gypsum.

5.1 Introduction

Anoxic hypersaline basins have been observed in two different tectonic environments within the eastern Mediterranean. The basins in the western Strabo Trench - the Tyro area - have been discussed in the previous chapters.

The Mediterranean Ridge, an accretionary prism forming as a response to the convergence between the African and European plates, shows a "cobblestone topography" (Camerlenghi, 1990). The Bannock Basin is the largest depression found within this area (Fig. 5.1) and is divided into nine sub-basins. Data will be presented from the Borea Basin. At present, this basin has anoxic hypersaline bottom water with a salinity of ten times seawater. In this chapter the interstitial water chemistry of an anoxic hypersaline core from the Bannock Basin will be discussed.

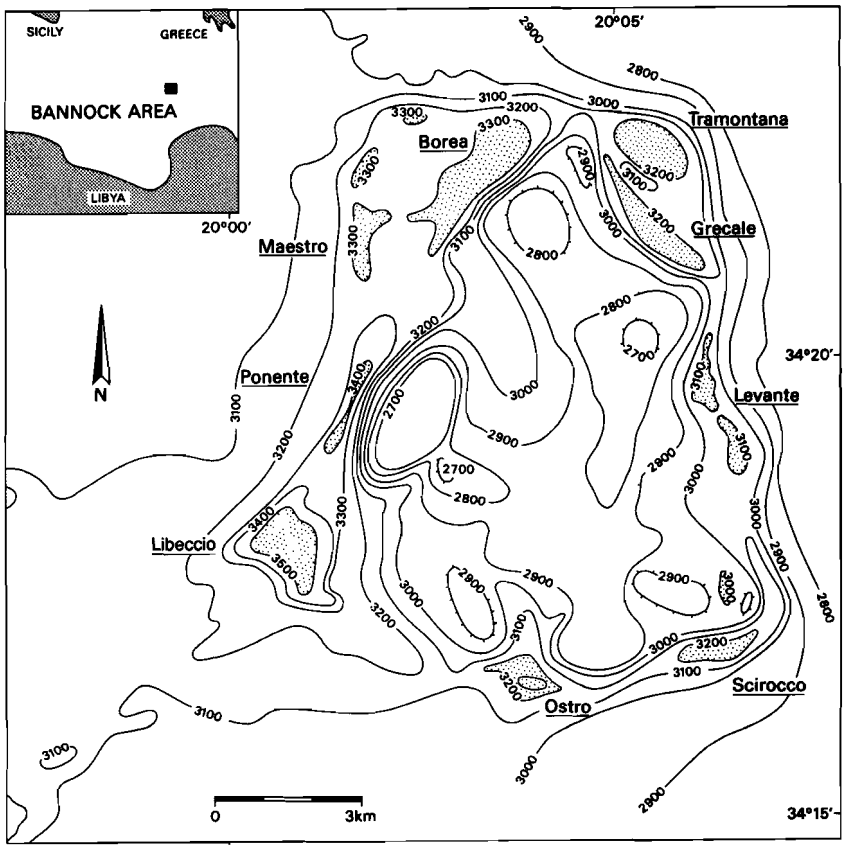

Figure 5.1: Location of the Bannock Basin in the eastern Mediterranean

5.2 Material and Methods

Core ABC45 is taken from the sub-basin Borea at a depth of 3350 m. The anoxic sediments in this core show thin laminated green gelatinous mud and grey oozes, which display a turbiditic pattern (Erba, 1991). The lithology of this core is presented in figure 5.2.

Shipboard procedure and analytical methods have been described briefly in chapters 2, 3 and 4 for nutrients, alkalinity, sulphate and sulphate isotopes, and the major cations.

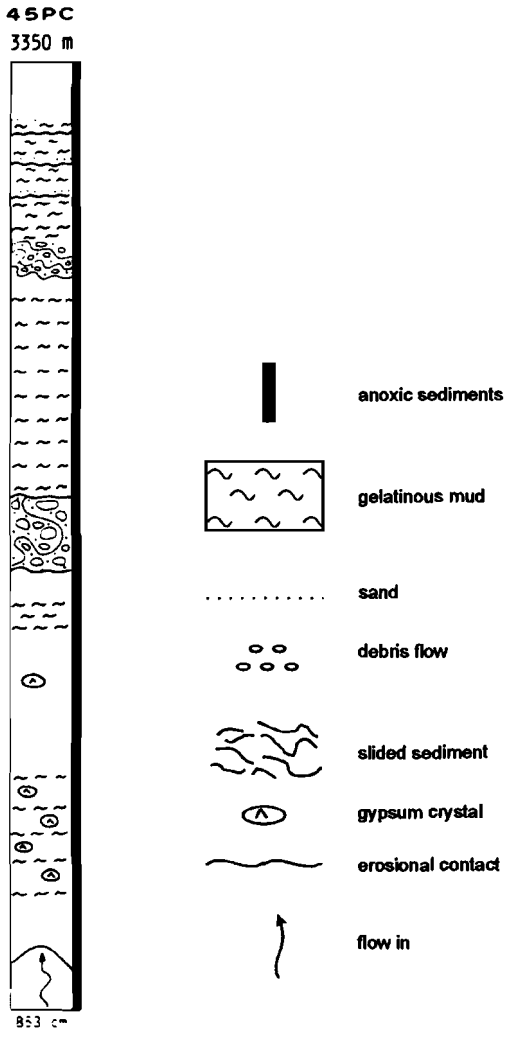

Figure 5.2: Lithological description of core ABC45 after Erba (1991).

5.3 Results and discussion

5.3.1 Sulphate, ammonium, phosphate and alkalinity

Except for the top 100 cm the pore waters from the Bannock Basin (ABC45) do not show an increase in the concentrations of ammonium, phosphate and total alkalinity with depth (Fig. 5.3). However, the decrease in sulphate concentration and in particular the increase of $\delta^{34}S$ of sulphate from 23 to 28 (Fig. 5.3) in the pore waters down-core indicate that organic matter decomposition takes place by sulphate reduction.

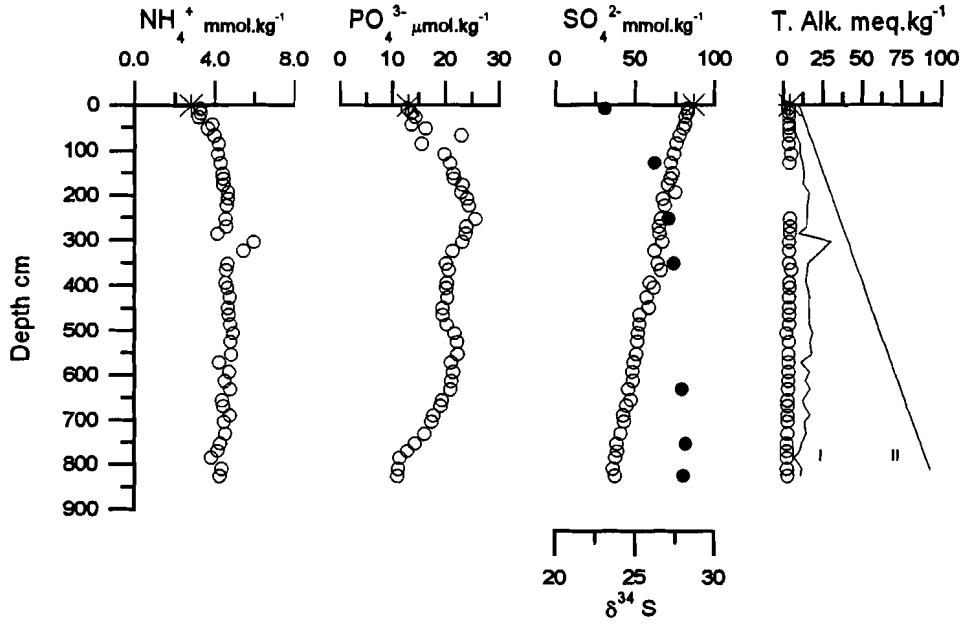

Figure 5.3: Pore water profiles in core ABC45 of A) ammonium, B) phosphate, C) sulphate (open circles) and sulphate-$\delta^{34}S$ (closed circles) and D) alkalinity (open circles) and calculated alkalinity with the ammonium(solid line I) and sulphate (solid line II) profiles versus depth.
Asterix symbol represents the concentration observed in the Bannock brine I.

The titration alkalinity in the pore waters of core ABC45 is almost equal to the carbonate alkalinity as corrections for other ions such as borate and sulphide are relatively minor (see chapter 4). At the pH of the sediments (pH $\approx$ 6) the carbonate alkalinity is represented almost entirely by HCO_3^-. Assuming stoichiometric decomposition of the organic matter in the sediments from core ABC45 the potential alkalinity can be estimated from the sulphate or ammonium profiles (see also chapter 4). In figure 5.3 the results of these calculations are shown. The alkalinity calculated from the decrease in sulphate is much larger than the actual measured alkalinity and the potential alkalinity calculated from ammonium. The discrepancy between the potential alkalinity calculated from the ammonium and sulphate profiles could be related to either the removal of ammonium from the pore waters or to the removal of sulphate by other processes than bacterial sulphate reduction.

Ammonium may have been removed from anoxic marine pore waters by ion-exchange processes or authigenic mineral formation (Martens et al., 1978; Middelburg, 1990). Ion-exchange reactions of ammonium are not important in these anoxic hypersaline sediments. Concentrations of cations (Na, K, Ca and Mg) are 10 to 1000 fold higher than the ammonium expected from organic matter decomposition. Therefore, the competition of ammonium for ion-exchange reactions can be neglected.

Ammonium-rich pore waters have been reported to be in equilibrium with struvite (Martens et al., 1978; Elderfield et al., 1981). Indirect evidence for struvite formation can be obtained by calculation of the saturation index. The ion activity product of struvite ($MgPO_4NH_4.6H_2O$) is calculated by:

$$IAP = \gamma_{Mg} * \gamma_{PO4} * \gamma_{NH4} * m_{Mg} * m_{PO4} * m_{NH4} * a^6_{H2O}$$

in which γ is the total ion activity coefficient, m is the concentration and a_{H2O} is the activity of H_2O. The total ion activity coefficients and the activity of H_2O have been obtained from the geochemical modelling program PHRQPITZ (Plummer et al., 1988) and from CHARON (N.M. de Rooy, Delft Hydraulics Laboratory). Both programs calculated similar total ion activity coefficients for the major ions. The following total ion

activity coefficients and activity for H_2O have been used:

$\gamma_{Mg} = 2$, $\gamma_{PO4} = 1.3*10^{-5}$, $\gamma_{NH4} = 0.57$ and $a_{H2O} = 0.75$.

The solubility product of struvite is reported to be pK = 13.2 (Martens et al., 1978). In figure 5.4 the Log (IAP) for struvite calculated for the pore waters of core ABC45 is shown. Pore waters from core ABC45 are in equilibrium with struvite. However, it is unlikely that struvite formation has occurred in these pore waters. Stoichiometric precipitation of struvite would remove an equal amount of phosphate and ammonium from the pore waters. This would imply a N/P ratio of the decomposing organic matter ranging between 1 and 2, which would be very unrealistic. Additional removal of phosphate from these pore waters can be neglected. Therefore an underestimation of ammonium due to the removal of ammonium from the pore waters is thought to be of no importance.

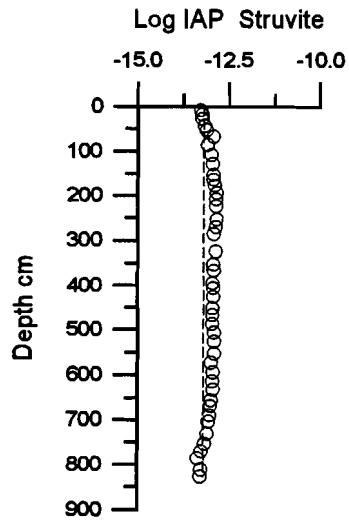

Figure 5.4: Log(IAP) of struvite in the pore waters of core ABC45 versus depth. Dashed line shows the logarithm of the solubility product.

The decrease in the sulphate concentrations with depth could be related to bacterial sulphate reduction and to gypsum formation. Assuming a closed system the bacterial isotope fractionation factor α can be obtained from a Raleigh plot (see chapter 9). This fractionation factor is very small for core ABC45, α is 1.005, which could indicate that the decrease in sulphate is not only due to bacterial sulphate reduction. The largest increase in $\delta^{34}S$ is observed in the top 150 cm. In this part bacterial sulphate reduction might be the major process. The depth integrated sulphate reduction in this part is estimated to be about 9.5 μmoles.cm^{-2}.yr^{-1}, using the following equation:

$$F_{SO_4} = D_s \left(\frac{dSO_4}{dz}\right)_{z=0} * \phi \qquad [5.1]$$

In which D_s is the diffusion coefficient for sulphate calculated according to Li and Gregory (1974) (see appendix A) and ϕ is the porosity. The sulphate reduction rate in the sediments of the Bannock Basin is comparable with the rate observed in the sediments of the Tyro Basin (see chapter 3).

Below a depth of about 200 cm sulphate removal by gypsum precipitation may have been more important than bacterial sulphate reduction since the $\delta^{34}S$ remains almost constant with depth. In addition, the ammonium and phosphate concentrations are almost constant in this depth interval, which does not support a continuing sulphate reduction with depth in this core.

5.3.2 Major elements

The pore water concentrations of Na, Cl and K are constant with depth in core ABC45 and almost identical to those in the Bannock brine I (Fig 5.5). In contrast, the concentrations of Ca and Sr increase with depth, whereas that of Mg slowly decreases (Fig. 5.6). In the next paragraphs the early diagenetic processes involved in the distribution of these major elements will be closer viewed.

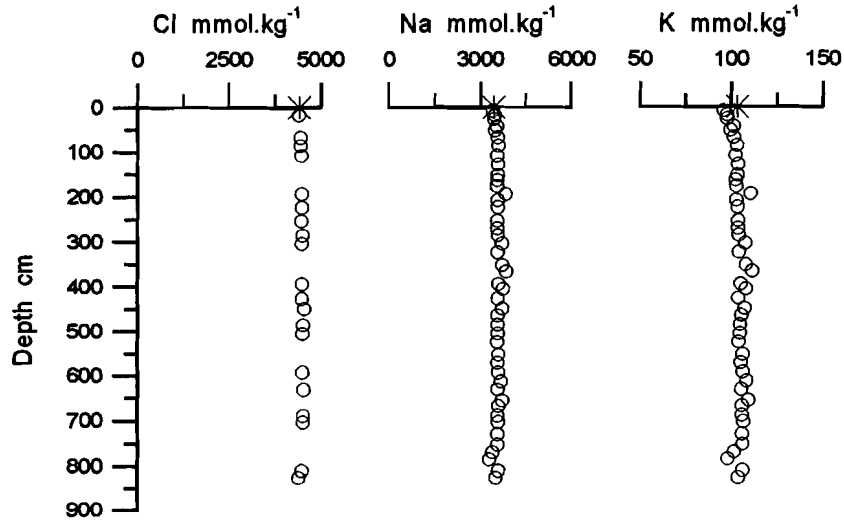

Figure 5.5: Cl, Na and K concentration in the pore waters of core ABC45 versus depth. Asterix symbol represents the concentration observed in the Bannock brine I.

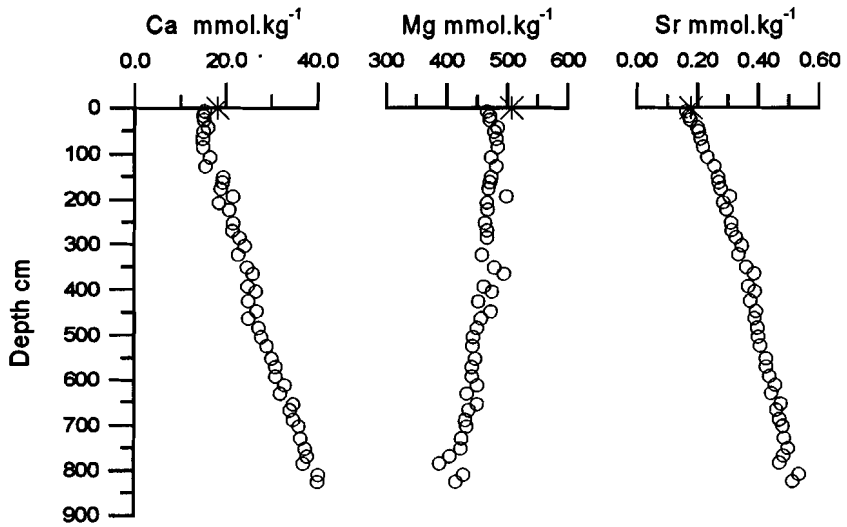

Figure 5.6: Ca, Mg, and Sr concentration in pore waters of core ABC45 versus depth. Asterix symbol represents the concentration observed in the Bannock brine I.

5.4 Dolomitization and gypsum precipitation

The saturation indices for carbonate and sulphate minerals have been calculated for the pore waters from core ABC45 by the modelling program PHRQPITZ (Plummer et al.,1988; see appendix B). This program is based on the Pitzer equations and can therefore be applied to solutions with high ionic strength. Major ions and alkalinity concentrations of the pore waters and the punch-in pH measurements are used to calculate the ion activity product of Ca-sulphates, Ca,Mg-carbonates and halite.

The pore waters of core ABC45 are in apparent equilibrium with respect to gypsum (pK = 5.12). This is in agreement with the observations by De Lange et al. (1990b) for the Bannock Brine, where the brine composition is reported to be in equilibrium with gypsum.

Calcite and aragonite are undersaturated in these pore waters (Fig. 5.7). The increase of Ca and Sr with depth can therefore be explained

by the dissolution of these carbonates. The pore waters appear to be supersaturated with respect to dolomite. Dolomite formation has been reported to occur in the Bannock Basin (De Lange et al., 1990b).

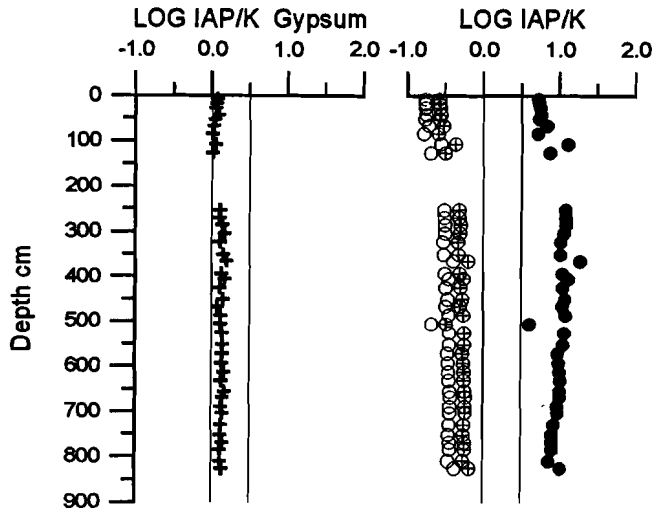

Figure 5.7: Saturation indices, LOG (IAP/K), of gypsum, aragonite (open circle), calcite (open circle with cross) and dolomite (closed circle) versus depth in core ABC45. The area between the solid lines shows the error in saturation area due to two different scaling possibilities in the program PHRQPITZ (see for detailed discussion appendix B).

The process of dolomitization and gypsum formation could have occurred according to the following reactions:

replacement of aragonite or calcite

I. $2CaCO_3 + Mg^{2+} \rightarrow CaMg(CO_3)_2 + Ca^{2+}$

and gypsum formation

II. $Ca^{2+} + SO_4^{2-} \rightarrow CaSO_4$

Replacement of aragonite or calcite with dolomite will increase the Ca concentration with approximately 60 $mmol.kg^{-1}$, since a decrease of about 60 $mmol.kg^{-1}$ in Mg is observed in the pore waters of core ABC45. This Ca may subsequently react with SO_4^{2-} and form gypsum.

A removal of 35 mmol.kg^{-1} of SO_4^{2-} balances the increase of 25 mmol.kg^{-1} of Ca in these pore waters. The potential alkalinity in the top of this core may have been removed by upward diffusion to the sediment-water interface. There is a large difference between the concentration of Mg in the top of core ABC45 and the concentration observed in the brine (Fig. 5.6). Dolomite formation at the sediment water interface could in part explain the loss in alkalinity and Mg in the top of this core.

Based upon the pore water profiles, stoichiometric relations and the thermodynamic calculations it can be concluded that dolomite or high Mg-carbonates are formed in the sediments of the Bannock Basin. This observation is consistent with the findings of high-Mg calcite and dolomite in hardgrounds from this area (Aghib et al, 1991).

In contrast to Baker and Kastner (1981) high concentrations of sulphate (>35 mmol.kg^{-1}) in the pore waters apparently do not inhibit dolomite formation in these sediments. The Mg/SO_4^{2-} ratio in the pore waters of core ABC45 ranges from 5.5 to 10.5. These ratios are much higher than the ratio found in normal seawater (Mg/SO_4^{2-} = 1.8). The mechanism of the inhibiting effect of sulphate for dolomite formation in normal seawater is still unknown (Baker and Kastner, 1981). The formation of Mg-SO_4^{2-} ion pairs has been suggested to be such a mechanism. Pore water data from core ABC45 indicate that if the Mg concentrations are much higher than the sulphate concentrations, dolomite can be formed. So there will be Mg available even if all sulphate ions will form Mg-SO_4^{2-} ion pairs.

The pore water profiles and the presence of gypsum crystals at large depth in core ABC45 favour a mechanism of dolomite and subsequently gypsum formation in these sediments.

5.5 Summary and conclusions

The anoxic hypersaline sediments of core ABC45 from the Bannock Basin were studied for their pore water chemistry. Pore water profiles of the metabolites and the major ions are determined by early diagenetic processes. Decomposition of organic matter occurs by sulphate reducing bacteria. The sulphate reduction rate is estimated to be 9.5 μmol.cm^{-2}.yr^{-1}. Sulphate reduction is only important in the top 150 cm of core ABC45. The decrease of sulphate concentration below this depth is ascribed to gypsum formation.

The formation of organogenic dolomite or high Mg-carbonates is the major sink for the alkalinity in the top of core ABC45 and for Mg throughout this core. In contrast to other reports dolomitization seems not to be inhibited by the presence of sulphate ions in the pore waters. Dolomite is formed by the replacement of Ca by Mg in aragonite or calcite.

Chapter 6: The mobility of barium in anoxic hypersaline sediments from the Tyro and Bannock Basins, eastern Mediterranean.

Abstract

Dissolved barium and sulphate has been measured in the pore waters of anoxic hypersaline sediments from the Tyro (ABC15) and Bannock (ABC45) Basins. Additionally the barium and organic carbon content in the sediments have been determined.

The concentrations of dissolved barium are higher than the value observed in the overlying brine. In both cores an increase of dissolved barium is observed at depth. For the Tyro Basin this increase is very sharp and large, values up to 190 μmol.kg^{-1} are measured. In the Bannock Basin the barium concentration goes up to 500 nmol.kg^{-1}. Barium is mobilized by both sulphate reduction and lowering of the activity coefficient of SO_4^{2-} in brines. The pore water concentrations of barium and sulphate are close to saturation to pure barite. The apparent solubility product of barite in these pore waters is estimated to be : pK $\approx$ 10.25.

The barium content in these sediments are comparable with those of normal marine sediments from the Mediterranean. At most depths the enrichments in barium correspond with a high organic carbon content. Upward diffusion of dissolved barium and subsequent precipitation of barium may have lead to enrichments of barium above high organic carbon contents in the sediments.

6.1 Introduction

In the water column barite ($BaSO_4$) precipitates in association with biological particulate matter (Bishop, 1988). Therefore, barium (Ba) is often associated with organic matter (Dymond et al., 1992). Sedimentary barite concentrations have been suggested to be an indicator for paleoproductivity. However, preservation of sedimentary Ba and the distribution of dissolved Ba in sediments are primarily controlled by the formation and regeneration of barite (Michard et al., 1974; Van Os et al., 1991). Application of Ba as a paleoproductivity indicator causes problems in suboxic and anoxic sediment (Brumsack and Gieskes, 1983; Von Breymann et al., 1990; Dymond et al., 1992). In anoxic sediments, where sulphate reduction takes place, dissolution of barite is likely to occur (Brumsack and Gieskes, 1983; Van Os et al., 1991; Dymond et al., 1992).

The Tyro and Bannock Basins, in the eastern Mediterranean, contain anoxic hypersaline bottom water (De Lange and Ten Haven, 1983; Jongsma et al., 1983; Scientific Staff of Cruise Bannock 1984-12, 1985).

The Ba concentration in the brines is much higher than in normal seawater, 490 nM and 130 nM Ba in the Tyro and Bannock brine respectively. Barite has been reported to be close to saturation in both brines (De Lange et al., 1990b). The sulphate concentration in the brines seems to determine the dissolved barium concentration (De Lange et al., 1990b).

Both basins have a high sulphate content, 44 $mmol.kg^{-1}$ and 86 $mmol.kg^{-1}$ for the Tyro and Bannock-I brine respectively (De Lange et al.,1990a). To determine the equilibrium of barite with the dissolved barium concentration in the anoxic hypersaline sediments from the Tyro and Bannock Basins a high resolution pore water and sediment study has been performed.

6.2 Material and methods

Gravity cores ABC15 and ABC45 are recovered from the anoxic hypersaline Tyro and Bannock Basins, respectively. The sediments in these cores are completely anoxic and extend over a period of Late Pleistocene to Holocene. Core ABC15 is strongly turbiditic. The sequence is characterized by thin laminations consisting of alternating green gelatinous mud and grey, reduced oozes. The lithology of core ABC45 is comparable. In neither core any sapropelic (sensu stricto) layers have been observed.

Sample processing has been described in detail by De Lange (1992). Briefly, sediment samples were squeezed with modified Reeburgh-type squeezers in a glove box flushed with high-purity nitrogen and held at a constant bottom water temperature of 13°C. Interstitial water was collected in acid-cleaned bottles. The squeezed sediment was subsampled for the further analyses.

Pore waters: Sulphate was measured as total S by ICPES (ARL 34.000) after 100 times dilution. Analytical precision was obtained by replicate analyses of seawater (Madeira Abyssal Plain). The precision obtained for S was about 5%. Ba was measured with a VGPQ1 ICP mass spectrometer (ICPMS) at MIT (Cambridge, USA), a standard deviation of less than 5% was found.

Sediment: After complete dissolution of the sediment with an acid

mixture of $HF/HNO_3/HClO_4$ the Ba content was measured by ICPES. Analytical precision was obtained by replicate analyses of an international standard SO-1 and an in-house standard. Organic carbon was determined by burning the organic carbon in an oxygen atmosphere at 900°C and measuring the CO_2 volumetrically. Prior to the analyses carbonate carbon was removed by reaction with 1M HCl. Based on duplicate analyses the standard deviation of the organic carbon measurements is 3.5%.

6.3 Results and discussion

The results of Ba, sulphate and organic carbon are shown in figures 6.1 and 6.2 for cores ABC15 and ABC45, respectively. The dissolved Ba concentrations are higher than the values observed in the overlying brine (490 nM and 130 nM Ba in the Tyro and Bannock brine, respectively; Klinkhammer and Lambert, 1989; De Lange et al., 1990b). A steady increase in dissolved Ba is observed at depths greater than 350 cm for core ABC15. The Ba concentration reaches values up to 190 $\mu mol.kg^{-1}$. In core ABC45 the dissolved Ba increases up to 500 $nmol.kg^{-1}$ at depth greater than 600 cm. The increase in Ba corresponds with a decrease in the sulphate concentration in both cores.

The downward increase of dissolved Ba in both cores suggests that the dissolved Ba concentration is controlled by barite dissolution. Similar pore waters profiles of Ba and sulphate have been found by others (Brumsack, 1986; Michard et al., 1974; Von Breymann et al., 1990). Dissolution of barite in the lower part of core ABC15 can be expected since sulphate decreases to near zero due to sulphate reduction. Although sulphate concentrations are high in core ABC45, an increase of dissolved Ba in the pore waters is observed.

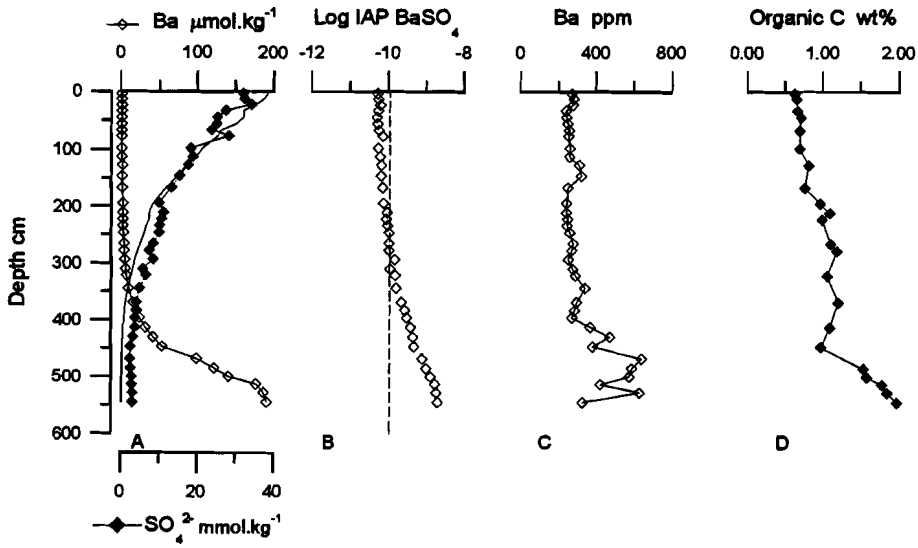

Figure 6.1: A)Dissolved Ba and sulphate profile versus depth in core ABC15. Solid line shows sulphate data calculated from the apparent solubility product (Log IAP = -10.25) and the activity of dissolved barium; B)The Log(IAP) of barite, dashed line is - pK (-9.96) of barite; C) Sedimentary Ba in ppm; D) Organic carbon content in wt%

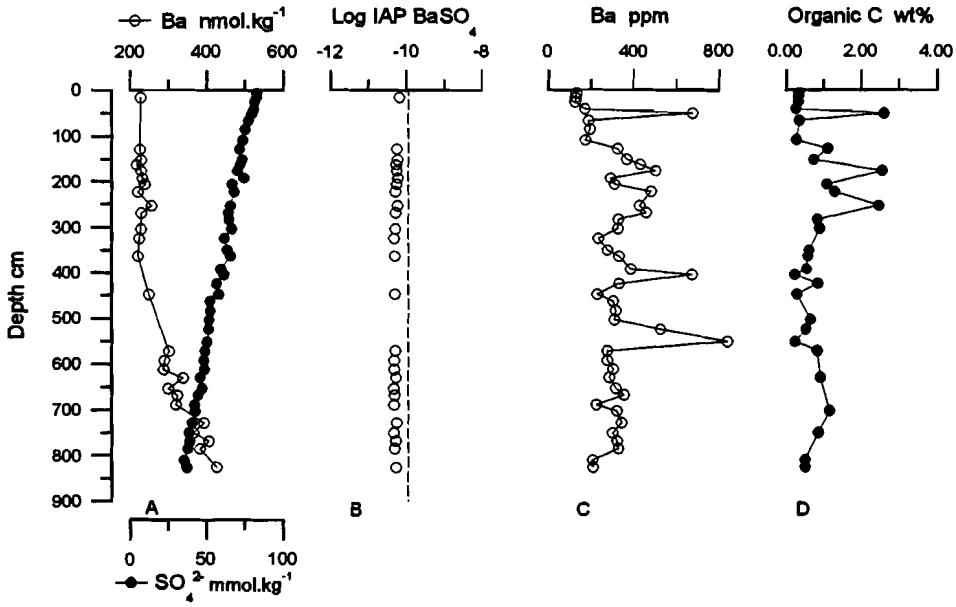

Figure 6.2: A) Dissolved Ba and sulphate profile versus depth in core ABC45; B) The Log(IAP) of barite, dashed line is - pK (-9.96) of barite; C) Sedimentary Ba in ppm; D) Organic carbon content in wt%

Brine-induced changes in the activity coefficients of Ba and sulphate may be an important factor for the solubility barite in a hypersaline environment.The ion activity product of barite has been determined using the activity coefficients of Ba^{2+} and SO_4^{2-} calculated with the modelling program PHRQPITZ (Plummer, 1988). More information on this program can be found in appendix B. The ion activity product is calculated as follows:

$$IAP = \gamma^T_{Ba}.m_{Ba} * \gamma^T_{SO4}.m_{SO4}$$

In which γ^T_{Ba} and γ^T_{SO4} are the total ion activity coefficients for Ba^{2+} (γ = 0.20) and for SO_4^{2-} (γ = 0.017), respectively. The activity coefficient for Ba^{2+} is in the range of values for Ba in normal seawater (Church and Wolgemuth, 1972), whereas the activity coefficient of SO_4^{2-} is about three times lower than values found in seawater (Church and Wolgemuth, 1972). Dissolution of barite in core ABC45, where concentrations of sulphate are high in the pore waters, might be related to this lower activity coefficient for SO_4^{2-} in brines. The pK of barite ranges from 9.77 to 10.05 (review, Falkner et al., 1993). Correction for temperature and pressure have not been applied. Church and Wolgemuth (1972) showed that the decrease in temperature from 25°C to 1° reduces the solubility product with a factor of two, while an increase in pressure from 1 atm to 500 atm increases the K value about three times. For sediments of the Tyro and Bannock Basins temperature is 13°C and waterdepth is about 3400 m (350 atm). The combined effect of temperature and pressure is therefore balanced and masked by the range of pK values reported in the literature.

Pore waters of core ABC15 are close to saturation relative to pure barite till a depth of 350 cm (Fig. 6.1). Below this depth the pore waters become supersaturated because of the strong increase in dissolved Ba. In core ABC45 the pore waters are near saturation until maximum depth of recovery (Fig. 6.2). Despite the differences in the dissolved Ba and sulphate concentrations between cores ABC15 and ABC45 the ion activity product in the pore waters are similar; Log IAP is about -10.25. The offset in core ABC15 below a depth of 350 cm might be due to an overestimation of the sulphate concentration. Pore water samples were

measured for their total sulphur content, samples could have been enhanced by the oxidation of sulphide. This contamination would be significant at depths where the sulphate concentration decreases to zero. An estimation of this contamination can be calculated from the apparent solubility product (Log IAP = -10.25) and the activity of dissolved barium. The sulphate concentration, which is in equilibrium with the apparent solubility product, is shown in figure 6.1. Below 350 cm this concentration approaches zero. This indicate that the measured sulphate concentration at the bottom of this core can be attributed to oxidized sulphide.

The concentrations of sedimentary Ba in these anoxic hypersaline sediments are comparable with those of normal marine sediments from the Mediterranean (Calvert, 1983; Van Os et al, 1991; Pruysers et al, 1991). DeHairs et al. (1987) reported that 96% of the barium is biological related in western Mediterranean sediments. Van Os (1993) found similar values for the eastern Mediterranean sediments. In both basins the enrichments of Ba correspond with higher organic carbon contents (Figs. 6.1 and 6.2). This is in agreement with the association of Ba and organic matter often found (Dymond et al., 1992; Pruysers et al., 1991; Van Os et al., 1991). Deeper in core ABC45 diagenetic remobilization of Ba may occur. This is indicated by the increase of dissolved Ba and the suspicious Ba enrichment at 550 cm depth (Fig. 6.2). The onset of this increase is not matched with a higher amount of organic carbon.

6.4 Conclusions

Pore waters of anoxic hypersaline sediments from cores ABC15 and ABC45 are saturated with respect to barite. The apparent solubility product of barite in these pore waters is estimated to be: $pK \approx 10.25$. From the pore water data it is shown that barite can be mobilized by both sulphate reduction and lowering the activity coefficient of SO_4^{2-} in brines. Upward diffusion of Ba may lead to barium enrichments above high organic carbon contents as observed in core ABC45.

Chapter 7: The distribution of DOC and POC in the water column and brines of the Tyro and Bannock Basins[1]

Abstract

DOC (dissolved organic carbon) and POC (particulate organic carbon) have been measured in the Tyro and the Bannock basins in the eastern Mediterranean Sea. These basins contain an anoxic, hypersaline brine with the interface at 3383 dbar and 3330 dbar respectively.

In the oxic water-column DOC is at its maximum at 70 - 100 m depth (~2.5 mg $C.l^{-1}$). Below this layer the DOC value is constant around 1.5 mg $C.l^{-1}$ down to the depth at which the seawater/brine interface occurs. In the oxic water-column POC values gradually decrease from 20 μg $C.l^{-1}$ to 5 μg $C.l^{-1}$ with increasing depth. POC and DOC show a sharp increase at the seawater/brine interface, where values of 150 μg $C.l^{-1}$ and ~4.0 mg $C.l^{-1}$ respectively have been observed. Within the brine the POC values are about 10 times higher (~50 μg $C.l^{-1}$) than in the oxic overlying seawater. The DOC content in the brine is about 2 - 2.5 times higher (4-4.5 mg $C.l^{-1}$) than in the oxic seawater.

The accumulation of POC at the interface and the presence of a high POC and DOC concentration in the brine favor bacterial activity at the interface.

7.1 Introduction

During recent decades several authors have pointed out that organic matter is of extreme importance in biogeochemical cycles in the marine environment (Duursma, 1961; Krom and Sholkovitz, 1977; Elderfield, 1981; Heggie et al., 1987; Berger et al., 1989). Although organic matter is only a minor component of seawater, it plays a major role in biological (productivity), geological (sedimentation and early diagenesis) and chemical processes (metal complexation, flocculation, adsorption phenomena) (Cauwet, 1984).

Little is known about the characteristics of dissolved organic matter; so far only 10-20% of this pool of organic matter has been characterized (Ehrhardt, 1977). The pool of dissolved organic carbon (DOC) in the ocean is sixteen times the annual production of organic material (Fredericks and Sackett, 1970). This estimate is obtained by taking 120 g $C.m^{-2}$ as the average annual productivity, 3800 meters as the mean depth of the ocean, and 0.5 mg $C.l^{-1}$ as the global mean concentration of DOC. Thus

[1] Henneke and De Lange, 1990. Mar. Chem., 31: 113-122

a knowledge of the distribution of DOC and coexisting particulate organic carbon (POC) is essential for a complete understanding of the carbon cycle in the ocean (Fredericks and Sackett, 1970). Berger et al. (1989) pointed out that the removal of organic carbon from the photic zone in the form of POC and as DOC acts as a "biological pump" which lowers the partial pressure of CO_2 in the surface waters. The DOC profiles given by Sugimura and Suzuki (1988) suggest that the ocean's DOC pool is at least twice as big as the atmospheric CO_2 reservoir (Toggweiler, 1989).

DOC in the deep ocean has a long residence time. The residence time of DOC in the Pacific Ocean at 2000 m has been estimated to be ~3400 yr. (Williams et al., 1969). Assuming a steady-state situation Williams et al. (1969) calculated that this age means that 0.51 per cent of the fixed carbon enters the deep sea. The utilization of DOC and the production of POC by free-living bacteria have been reported by Cho & Azam (1988) and Pett (1990).

The first data on dissolved organic matter in the Mediterranean were reported more than ninety years ago. In 1892 Natterer found 2 $mg.l^{-1}$ of dissolved organic matter in the surface water in the open sea, and 10-20 $mg.l^{-1}$ in water taken from near the coast of Greece (Duursma, 1965). Williams (1975) reported dissolved organic carbon values ranging from 0.8 to 1.3 mg $C.l^{-1}$ for the western Mediterranean. To the best of our knowledge, the present paper is the first to report on the distribution of DOC and POC in the eastern Mediterranean. we report here not only on the DOC and POC content of seawater, but also on that of the brine-filled depressions in two areas, namely the Tyro and the Bannock areas (De Lange and ten Haven, 1983; Jongsma et al., 1983; Scientific staff of cruise Bannock 1984-12, 1985).

7.2 Sampling and methods

Samples were collected from the Tyro and the Bannock Basins on the ABC87 cruise with the Dutch R.V. Tyro in June 1987. Sea water samples for DOC and POC were collected with Niskin bottles.

DOC and POC were analyzed by measuring the carbon dioxide resulting from wet oxidation of organic matter (Wilson, 1961; Menzel and Vaccaro,

1964). The procedure for the sample preparation will be outlined briefly below. All the glass ampoules had been pre-heated at 500°C for four hours to remove any organic contamination. All the other preparations were done on board ship; the actual measurements were done in a shore-based lab. For DOC 5 ml of filtered seawater, filtered through a Whatman GF/F glass fibre filter, were put into a glass ampoule. To this ampoule 250 μl of 6% phosphoric acid and 200 mg $K_2S_2O_8$ were added. The ampoules were purged for 6 minutes to remove inorganic carbon. then the ampoules were sealed and heated for three and a half hours at 130°C for total oxidation of the organic matter. For POC, 500 or 1000 ml seawater were filtered through a Whatman GF/F glass fibre filter. The filter was put into an ampoule, to which 5 ml of Q-dest and 250 μl of 6% phosphoric acid and 200 mg $K_2S_2O_8$ were added. The ampoules were prepared in the same way as for DOC. In the autumn of 1987 all the ampoules were analyzed, with a CO_2 infrared carbon analyzer (Oceanographic International, model 0524B).

All DOC values are the mean of two different sub-samples. The precision of these data is estimated to be better than 10%. POC data are all single measurements. A standard curve was constructed from carbonate solutions of varying concentration. The reported DOC and POC values of the samples have been calculated from this standard curve. A glucose standard curve (20 -100 μg $C.l^{-1}$) was prepared, similar as those of the samples. Extrapolation through zero concentration gave a blank value of 0.5 $mg.l^{-1}$. All DOC data have been corrected for this blank.

7.3 Results

A detailed study has been made of DOC and POC content of seawater and brines in two basins in the eastern Mediterranean. Figures 7.1A and 7.2A show the DOC profiles for the Tyro and Bannock Basins respectively. In the oxic water column there is a maximum of DOC at 70 - 100 m. The DOC values in the oxic water column range in the Tyro and Bannock Basins from 1.4 to 2.5 mg $C.l^{-1}$ and from 1.0 to 2.7 mg $C.l^{-1}$ respectively. Both profiles show a rapid increase in DOC at the interface between the oxic seawater and the anoxic brine. At the interface the density changes

within a few meters from 1.025 g.cm^{-3} in the oxic water to 1.21 g.cm^{-3} in the anoxic brine. The interface is for the Tyro Basin at a depth of 3383 dbar (3328 m) and for the Bannock Basin it is at 3330 dbar (3276 m) (Boldrin and Rabitti, 1990). In the Bannock Basin the DOC decreases slightly just above the interface.

In the oxic water column of the Tyro area the POC values gradually decrease from 20 μg C.l^{-1} to 5 μg C.l^{-1} (Fig. 7.1B). The POC content sharply increases from 5 μg C.l^{-1} just above the interface to 152 μg C.l^{-1} at the interface. In the brine the POC values are about 50 μg C.l^{-1}.

Although there are no data for the oxic water column in the Bannock area, we are confident that the values of POC will not deviate significantly from those found in the water column of the Tyro Basin (Fig. 7.2B). For both areas the profiles of other biogeochemically involved constituents such as oxygen, nitrate, silica, phosphate and Ba, are identical (De Lange et al., 1990a). The POC value at the interface of the Bannock Basin is within the range of that of the Tyro Basin, namely 146 μg C.l^{-1} versus 150 μg C.l^{-1}. The POC in the Bannock brine decreases with depth, but there is a large scatter in the data.

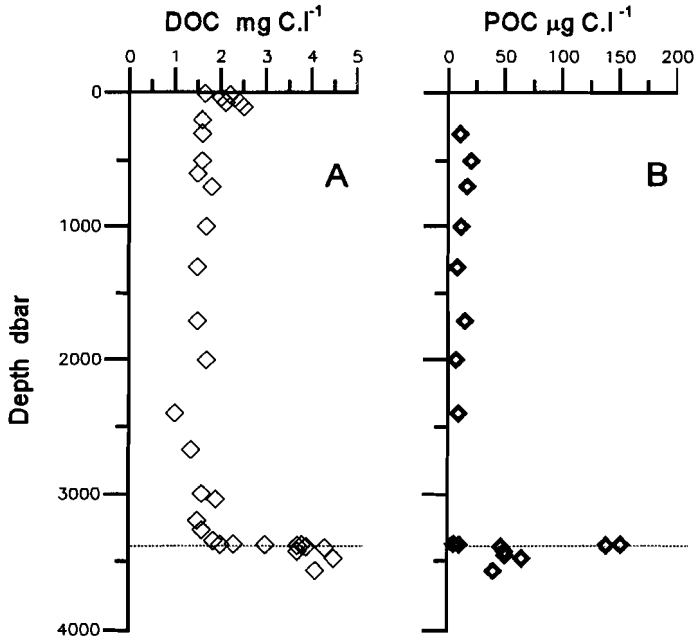

Figure 7.1: DOC and POC data of the water-column of the Tyro Basin
A)DOC expressed in mg C.l^{-1} and B)POC expressed in μg C.l^{-1}; dashed line represents the interface between the oxic seawater (190 μM O_2, density 1.025 g.cm^{-3}) and the underlying anoxic brine (2 mM HS^-, density 1.21 g.cm^{-3})

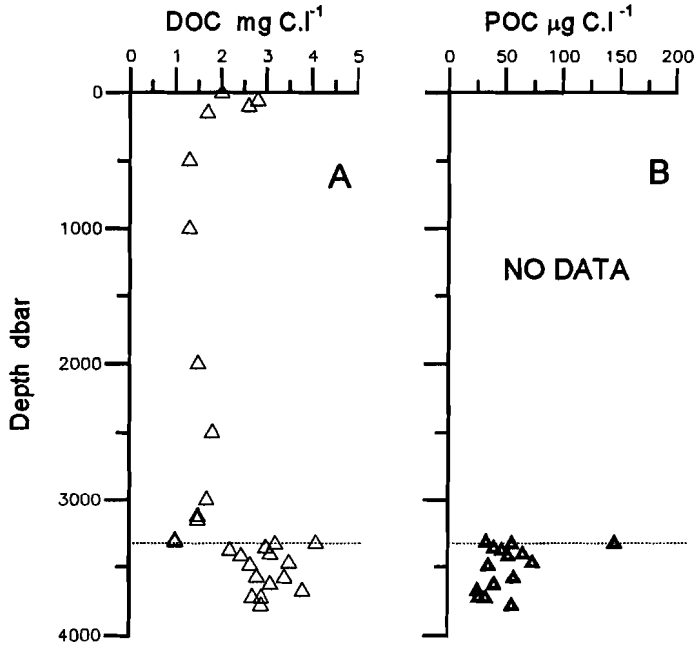

Figure 7.2: DOC and POC data of the water-column of the Bannock Basin
A) DOC expressed in mg $C.l^{-1}$ and **B)** POC expressed in μg $C.l^{-1}$; dashed line represents the interface between the oxic seawater (200 μM O_2, density 1.025 $g.cm^{-3}$) and the underlying anoxic brine (2 mM HS^-, density 1.21 $g.cm^{-3}$)

7.4 Discussion

The DOC values in the oxic water column of the Tyro and the Bannock Basins range within the values reported for other oceanic areas. Starikova (1970) has reported a range of 1.5-2.0 mg $C.l^{-1}$ for the Indian, Pacific and Atlantic Ocean using dry combustion techniques. For the Black Sea values ranging from 2.5 - 3.0 mg $C.l^{-1}$ have been reported (Williams, 1975).

In the western Mediterranean DOC values ranging from 0.8 mg $C.l^{-1}$ to 1.3 mg $C.l^{-1}$ have been measured (Williams, 1975). These data were obtained using peroxydisulphate oxidation. Cauwet (1984) reported that the DOC content decreases from 1-1.5 ppm to 0.2 ppm in the deep water of the western Mediterranean. The data from the eastern

Mediterranean, which are reported here, deviate considerably from those from the western Mediterranean reported by Cauwet (1984). The differences may be due to differences in the analytical technique and equipment used. A relative small difference is observed between the data from this study and those reported by Williams (1975).

Sugimura and Suzuki (1988) have indicated that in the surface waters considerably higher DOC values may be measured, if a newly developed catalytic oxidation step is used in the analysis of DOC. However, with regard to the DOC content of deep waters these authors observed relatively small differences in the results obtained by their analytical technique and by the conventional method (Sugimura and Suzuki, 1988). Suzuki et al.(1988) reported on an intercomparison of different analytical techniques for DOC analyses. They found large differences between the data measured using persulphate oxidation, using the Suzuki method (Sugimura and Suzuki, 1988) and using a commercially available high temperature combustion instrument (Shimadzu TOC500). When used to measure seawater samples, the Suzuki method gave values that were 3.5 times higher than those obtained with the persulphate method. Recently, Suzuki (1993) retracted the results of the DOC measurements published by Sugimura and Suzuki (1988). The Shimadzu instrument gave values that were about twice those measured by persulphate oxidation. This indicates that it is mandatory to use a consistent and adequate measuring technique to interpretate concentrations of DOC in the oceans and seas. Although the persulphate method may miss some of the DOC (Sharp 1973; Gordon and Sutcliffe, 1973; Sugimura and Suzuki, 1988), the values discussed here can be compared for depth profiles with other oceanic data done by the same method.

The DOC profiles of the water column in both basins show a dramatic increase at the interface between seawater and brine. Within the brine the DOC value remains fairly constant. A similar increase in DOC within the brine relative to seawater has been observed in another anoxic hypersaline basin, the Orca Basin (Reid et al., 1977; Sackett et al., 1979). The observed values found in the Orca brine are within the range of the values measured in the Tyro and the Bannock brines.

The small decrease in DOC just above the interface in the Bannock Basin can probably be attributed to the utilization of DOC by bacteria (Cho & Azam, 1988; Pett, 1990). This is confirmed by the fact that gelatinous pellicles are more numerous in the Bannock area than in the Tyro area (Erba et al., 1987; Erba, 1991). It is also possible that sampling resolution causes this difference. However, further research needs to be done to explain why this decrease has been observed in the Bannock Basin and not in the Tyro Basin.

The POC values in the oxic water column of Tyro Basin decrease from about 20 μg C.l^{-1} at 400 m to 5 μg C.l^{-1} at 3315 m. These values are within the range of values observed by Wangersky (1976) in the Pacific and Atlantic Ocean. He found that values in the two oceans were similar at all depths. The POC distribution in the Black Sea shows a similar profile but with considerably higher concentrations: in the oxic waters the concentration decreases with depth from 120 μg C.l^{-1} to 40 μg C.l^{-1} (Radford-Knoery and Cutter, 1988).

The literature shows that in an ocean the maximum POC content occurs in the upper 0-100 m. In the 100-500 m layer it tends to decrease. However, a difference has been observed between stations. Below the 500 m a gradual decline in POC concentrations has been observed, pointing to continuing decomposition and utilization of organic matter. (Romankevich, 1984). The POC data for the Tyro Basin show a gradual decrease in the upper oxic column. In the Mediterranean, values of 44-171 μg C.l^{-1} (average about 80 μg C.l^{-1}) for POC have been observed in the upper part of the water-column (Romankevich, 1984). Using these values I have calculated that 75% of POC has been utilized at 400 m depth, and almost 95% of POC has been utilized just above the interface. Similarly, Bruland et al. (1989) found that during transit from the bottom of the euphotic zone to the deep-sea floor, more than 90% of the sinking particulate organic material degrades (Bruland et al., 1989). Flocculation is known to have only a negligible effect on the POC distribution in the water-column (pers. comm. Eisma).

At the interface there is a sharp increase in POC. The only report on POC in anoxic cold brines has been presented by Reid et al. (1977) and Sackett et al. (1979). They report an increase in POC levels in the

intermediate zone between seawater and brine of up to 140 μg $C.l^{-1}$ for the Orca Basin, whereas within the brine an average POC concentration of 71 μg $C.l^{-1}$ is observed. This is about seven times higher than in the overlying seawater (Sackett et al., 1979). In the Tyro and Bannock Basins an average of 50 μg $C.l^{-1}$ has been measured for POC; this is about ten times higher than the value measured in the overlying seawater. Because of the density difference between the oxic seawater (1.025 $g.cm^{-3}$) and anoxic brine (1.21 $g.cm^{-3}$) an accumulation of POC may occur.

The sharp increase in POC at the interface may be caused not only to accumulation, but also to the production of POC by bacteria. Romankevich (1984) reported that in water basins, where the water mass or bottom sediments are periodically or continuously contaminated with hydrogen sulphide, bacterial chemo-synthesis of organic matter may be significant. In the Orca Basin an increased biomass has been observed at the interface (LaRock et al., 1979). This bacterial community may contribute organics to both DOC and POC (Sackett et al., 1979).

DeDomenico and DeDomenico (1989) have reported the occurrence of a much larger population of bacteria at the interface than in the brine of the Bannock Basin. These bacteria have not yet been identified or quantified. In addition, Luther et al. (1990) report sulphate reduction and sulphide oxidation at the interface. Manganese oxidation and reduction at the interface have been reported by De Lange et al. (1990a,c). The report of the occurrence of gelatinous pellicles of bacterial origin at the interface (Erba et al., 1987; Erba, 1991) also points to the option of bacterial activity and therefore to the production of POC.

7.5 Conclusions

DOC and POC show a similar trend in the water-column of the Tyro and the Bannock Basins. In the oxic layer a slow decrease in DOC and POC with depth is found. At the interface both parameters increase sharply, the POC increases more than the DOC. DOC increases at the interface by a factor of 2 - 2.5 and POC by a factor of 15 - 20.

At the interface the increase in POC could be caused by the accumulation of POC due to a density difference between the seawater and the anoxic brine, and by bacterial production at the interface. The slow turnover rate of the residual, possibly more resistent, particulate organic matter at this depth may cause this extreme increase in DOC content.

The presence of a high POC content at the interface and high DOC content and high nutrient concentrations in the brine all favor the development of a bacterial community at the interface. This is consistent with sulphate reduction, manganese oxidation and reduction processes, and the occurrence of gelatinous pellicels reported by other researchers (Luther et al., 1990; De Lange et al., 1990a,c; Erba, 1991).

Chapter 8: The determination of solid phase sulphur species.[1]

Abstract

The inorganic and organic solid phase sulphur speciation in anoxic hypersaline sediments from the eastern Mediterranean has been identified and quantified. The following sulphur species have been studied: Acid Volatile Sulphur (AVS), pyrite, total zerovalent sulphur (elemental sulphur and low molecular weight non-polar organic sulphur), organic polysulphides and humic sulphur (0.5 N NaOH extractable).

The determination of AVS and pyrite was based respectively on the acidification with 3 M HCl and Cr(II)-reduction of these sulphur components to H_2S. The H_2S was collected in base and the sulphide concentration was measured by polarography. Standard Na_2S and pyrite gave recoveries of 100% ± 4% and 97% ± 12% respectively. A sequential sulphur extraction scheme was used to quantify the amount of zerovalent sulphur, organic polysulphides and humic sulphur. The extracts were analyzed by either HPLC-techniques or ICPES.

Zerovalent sulphur extracted, with a mixture of methanol and toluene, from these sediments consists only of S_8 and not of low molecular weight non-polar organic sulphur since the results of the S_8 and zerovalent sulphur derived thiosulphate measurements gave similar concentrations. Previously, an acetone/freon mixture was used to extract zerovalent sulphur from very small amount of wet sediment (25-35 mg). The zerovalent derived thiosulphate was measured by polarography. Zerovalent sulphur values from the methanol/toluene extraction differed slightly from those obtained by this extraction. The discrepancy between the two extractions could be due to oxygen contamination in the later case.

The humic sulphur was extracted by a NaOH solution. In the NaOH-extract the possible coextracted pyritic sulphur was found to be insignificant compare to the total amount of humic acid sulphur in these anoxic sediments.

8.1 Introduction

In marine sediments the sulphur cycle is dominated by solid phase inorganic iron-sulphur compounds, e.g. FeS and FeS_2 (Luther and Church, 1991). Iron sulphides are generally separated into two "operational" categories: acid volatile sulphides (hereafter referred to as AVS) and pyrite (Berner, 1964). AVS-forms are generally considered to include 'amorphous-FeS', mackinawite, greigite and pyrrhotite (Cornwell and Morse, 1987).

Iron sulphides are found in varying concentrations in marine sediments.

[1]Part of this chapter has been published in Henneke et al. (1991). Mar. Geol., 100: 115-123.

Most studies have focused on pyrite in normal marine sediments (e.g. Luther et al., 1982; Berner, 1984; Raiswell and Berner, 1985; Cutter and Velinsky, 1988). In the last few years, several studies of iron sulphides in recent anoxic marine sediments have been published (Morse and Cornwell, 1987; Boesen and Postma, 1988; Calvert and Karlin, 1991; Middelburg, 1991).

It is possible to identify sedimentary pyrite by means of Scanning Electron Microscope-EDS, X-ray diffraction and microscopic examination. However, for quantitative work pyrite can be extracted by oxidative dissolution and quantified by gravimetry as $BaSO_4$ (Goldhaber et al., 1977). Begheyn et al. (1978) and Lord (1982) have described how the amount of pyrite can be determined on the basis of Fe-liberated by HNO_3 digestion after all other Fe-forms have been removed by selective leaching. Pyrite and AVS can be determined on the basis of the generation of H_2S. For pyrite the sediment is reacted with a chromium reduction method (Zhabina and Volkov, 1978; Howarth and Merkel, 1984; Canfield et al., 1986; Cutter and Oats, 1987). The classic determination technique for AVS is acidification of wet sediment. The H_2S generated can be measured by gas chromatography (Cutter and Oatts, 1987), or by trapping in an appropriate agent. The collected H_2S can be analyzed by iodometric titration (Kolthoff and Sandell, 1952), gravimetrically as Ag_2S or $BaSO_4$, by potentiometric titration (Cornwell and Morse, 1987), or it can be measured as ZnS suspension with the methylene blue method (Cline, 1969; Boesen and Postma, 1988).

Recently Hsieh and Yang (1989) have reported on the use of diffusion methods for the determination of AVS, pyrite and elemental S. Their methods are similar to the above mentioned techniques. However, they do not involve active distillation.

Polarographic methods are more sensitive than iodometry, potentiometry and methylene blue analysis (Luther and Tsamakis, 1989). Polarography has already been used successfully in determining sulphur species in natural waters (Davison and Gabbutt, 1979), seawater (Luther and Tsamakis, 1989), hypersaline brines (Luther et al., 1990) and pore waters (Luther et al., 1985). These polarographic techniques have been applied successfully to recent hypersaline anoxic sediments from the Eastern Mediterranean (Henneke et al., 1991) and salt marshes (Luther et

al., 1991a).

Less is known about the organic sulphur species in recent marine sediments. Recently some reports have been published about diagenetic organic sulphur formation (Francois, 1987a,b; Kohnen et al., 1989; Brassell et al., 1986; Ferdelman et al., 1991). Brassell et al. (1986) identified isoprenoid thiophenes in recent and ancient deep-sea sediments. Kohnen et al. (1989) showed the incorporation of polysulphides in organic matter during early diagenesis. Francois (1987b) published a study on the sulphur enrichment in the humic fraction of marine sediments during early diagenesis. Organic sulphur species have been identified using combined GC-MS or HPLC techniques (Kohnen, 1991) or sequential procedures (Francois, 1987a, Ferdelman et al., 1991; Mossmann et al., 1991).

In this chapter methods used for the determination of inorganic and organic sulphur species in anoxic hypersaline sediments from the eastern Mediterranean will be discussed.

8.2 Iron sulphides by polarographic techniques

The determination of the sulphur species AVS and pyrite in the sediments is based on the reduction of these sulphur compounds to H_2S (Zhabina and Volkov, 1978; Canfield et al., 1986; Cutter and Oatts, 1987). The H_2S is collected in 1 M NaOH and measured by polarographic techniques (Luther et al., 1985). H_2S dissolves in 1 M NaOH to form bisulphide according to the following reaction:

$$H_2S + NaOH \rightarrow HS^- + Na^+ + H_2O \qquad [8.1]$$

Bisulphide can be measured by polarography at a potential of -0.68V. Polarograms of the samples were recorded with a Princeton Applied Research model 364 polarograph and a model RE0073 X-Y recorder with a static mercury drop electrode, model 303. Linear sweep voltammetry (LSV) was used with a potential scan rate of 50 mV/s from 0 to -1.0 V. A standard curve was constructed with Na_2S (anhydrous, Alfa products), dissolved in degassed quarts distilled water.

The recovery of H_2S in 1 M NaOH, previously purged with N_2, was

checked by acidification of standard Na_2S in a reaction vessel similar in design to the one used by Cutter and Oatts (1987). The collection vessel contained 20 ml 1 M NaOH. The system was continuously purged with nitrogen to prevent any contamination by oxygen. Ten ml of 3 M HCl was added to 2 ml Na_2S (concentration 0.5 - 1 mM). After a reaction time of 20 min a recovery of 100% ± 4%, n=4, was obtained.

The acidification of AVS in the sediment was analogous to the acidification of the standard Na_2S. Between 10 mg and 20 mg wet sediment were weighed in a tared aluminium boat and placed in the reaction vessel. The sediments were put into the boats in a glove bag filled with nitrogen to prevent oxidation.

A modification of the method described by Cutter and Oatts (1987) was used to determine the pyrite. Pyrite is reduced to H_2S by oxidation of the ion chromium-II (Zhabina and Volkov, 1978; Luther, 1987). The chromium reduction method has been shown to be specific for inorganic reduced sulphur phases; organic sulphur and sulphate S are not converted into H_2S (Canfield et al., 1986).

Ten mg of dried sediment, which was extracted with acetone to remove elemental sulphur, was placed in a reaction vessel and 20 ml 1 M Cr^{2+} in a 1 M HCl solution (1 mole $CrCl_3$ in 1 M HCl was passed over an amalgamated zinc column to form Cr^{2+}) was added. During the reaction the solution was stirred and flushed with nitrogen. The H_2S was collected in 1 M NaOH. This method was first verified with pure pyrite (Alfa products). Using a reaction time of 60 minutes a recovery of 97% ± 12% (n=6) was obtained.

8.3 Zerovalent sulphur by polarographic techniques

Zerovalent sulphur, which includes elemental sulphur and low molecular weight non-polar organic polysulphides, is determined by measuring thiosulphate formed by the reaction of S(0) with sulphite. The extraction method used to determine total zerovalent sulphur in the sediments is a modification of the reaction with sulphite (Jørgensen et al., 1979; Ferdelman et al., 1991). Between 25 and 35 mg wet sediment was weighed and transferred to a test-tube, which was purged with nitrogen.

Approximately 10 ml of a degassed solution of trichlorotrifluroethane(freon)-acetone (3:1) was added. The test-tube was placed in an ultrasonic cleaner for one hour. After centrifuging, the liquid layer was put into another test-tube. The extraction was repeated with 5 ml freon-acetone. The extracts were put together and the liquid was allowed to evaporate; the precipitate consisted of S_8 and organic S(0) forms. One ml of 0.01 M Na_2SO_3 and 4 ml of 0.1 M $NaClO_4$ were added and the test-tube was capped. The test-tube was placed in an oven at 60 - 70 °C for 12 hours. The sulphite reacted with low molecular weight non-polar organic sulphides and elemental sulphur to form thiosulphate according to reaction [8.2] (Tuller, 1970; Jørgensen et al., 1979):

$$S_8 + 8\ SO_3^{2-} \rightarrow 8\ S_2O_3^{2-} \qquad [8.2]$$

This solution was added to a polarographic cell with 5 ml of 0.1 M $NaClO_4$ and analyzed for thiosulphate at a potential of -0.12 V using linear sweep voltammetry (Luther et al., 1985). A recovery of 97% was obtained by Ferdelman et al. (1991) for elemental sulphur.

8.4 Organic sulphur species

A sequential sulphur extraction scheme was applied to the sediments (Fig. 8.1) to estimate their content of elemental sulphur, organic polysulphides and humic sulphur. This extraction scheme is based on the work of Francois (1987a,b) and Ferdelman et al. (1991). The extractions were done in duplicate and performed under nitrogen. One to two grams wet sediment were subsampled and placed in a polyethylene tube.

In the first step, a 0.5 M NaCl rinse, removes residual pore water sulphate. Ten ml, degassed 0.5 M NaCl solution was added and the tubes were shaken for two hours. NaCl was used instead of distilled water in order to prevent bacterial cells from bursting. After shaking the tubes were centrifuged and the liquid decanted. This procedure was repeated. The second extraction step contains a mixture of methanol and toluene (3:1). This mixture extracts low molecular weight non-polar organic sulphur and elemental sulphur. A methanol/toluene mixture was used

instead of an acetone/freon mixture for environmental reasons. Twenty ml of this mixture, purged with nitrogen, was added and the tubes were shaken for 14 hours. The tubes were centrifuged and the liquid was decanted and collected. This procedure was repeated. The extracts were divided into two parts. One part was measured directly for S_8 by HPLC techniques. From the other part ten ml were subsampled and allowed to evaporate, the residue consists of S_8 and organic S_0 forms. To the residue 5 ml of 0.02 M Na_2SO_3 solution was added and treated in the same way as the samples for the acetone/freon extraction. The formed thiosulphate was measured by HPLC techniques.

The third step uses 1 M HCL, degassed with nitrogen. The acidification of the sample removes AVS and breaks down organic polysulphides (R-S_x-R, $x \geq 3$). Twenty ml 1 M HCl was added to the tube and the sediment/solution mixture was purged for 5 min. with nitrogen to remove all H_2S. After purging the tubes were capped and shaken for 14 hours. The liquid was decanted and collected, after centrifuging the tubes.

The broken organic polysulphides form mainly elemental sulphur which can be extracted with the methanol/toluene mixture. This procedure, similar as step two was done in the fourth step.

The final step consists of the extraction of humic sulphur compounds by 0.5 M NaOH. Twenty ml of the degassed NaOH solution was added to the tubes. The tubes were shaken for 14 hours, after which they were centrifuged and the liquid decanted. The procedure was repeated. The liquid was collected and measured for total sulphur by ICPES (ARL 34000).

Figure 8.1: Sulphur extraction scheme, modified after Francois, 1987a,b) and Ferdelman et al., (1991)

SULPHUR EXTRACTION SCHEME*

SAMPLE

0.5 M NaCl	→	Remove residual porewater sulphate
↓		
Methanol/Toluene	→	LMW non-polar organic sulphur and elemental sulphur
↓		
Acidification 1 M HCl	→	Remove AVS Break down organic polysulphides
↓		
Methanol/Toluene	→	Organic polysulphides
↓		
0.5 M NaOH	→	Humic Sulphur

*All extractions are performed under nitrogen atmosphere.

8.5 HPLC Techniques

Sulphur homocycles can be measured by reversed-phase HPLC (Möckel, 1984a,b). A HPLC-unit from Scientific Science Inc. (SSI) was used in combination with an UV-detector (λ = 254 nm) for the determination of S_8. The eluent was purged through the system with a flow velocity of 1 ml/min, the pressure was about 1200 psi. The samples were injected into a Rheodyne injector #7125 with a 100 μl loop and passed through a C-18 column (Zorbax ODS). A methanol solution was used as the eluent, depending on the percentage of water the retention time of S_8 is 10 minutes using 2% H_2O and 13 minutes when using about 5% H_2O. The eluent was continuously purged with He, to degas the eluent.

A standard was prepared by dissolving powdered elemental sulphur in toluene. Dilutions from this stock solution (26.5 mM S(0)) were prepared in methanol. A standard curve was made ranging from 25 μM to 262 μM S(0). The standard curves gave good reproducibility during the two month period of analysis, and the analytical precision was usually within 1%. The detection limit was improved when methanol was used in the reference cell instead of air. Figure 8.2 shows some standard curves.

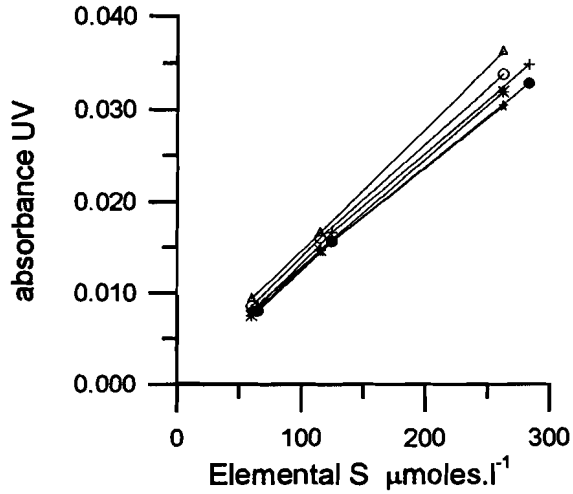

Figure 8.2: Standardcurves for S_6; UV absorbance (λ = 254nm) versus the concentration S in μmoles.l^{-1} (* 19 nov., ° 22 nov., ^ 26 nov., ⋆ 3 dec., 9 dec., + 18 dec. 1990)

In figure 8.3 an example of a chromatogram is given for a standard solution (Fig. 8.3A) and for a first methanol/toluene extract (Fig. 8.3B). Using a 95% methanol solution as an eluent gave a good separation of the toluene peak and the S_8 peak, so there was no need to dilute the samples.In the chromatogram of the second methanol/toluene extract three peaks were observed (Fig. 8.4). One peak corresponds to S_8, whereas the other two peaks are attributed to S_6 and S_7 due to decomposition of organic polysulphides after acidification.

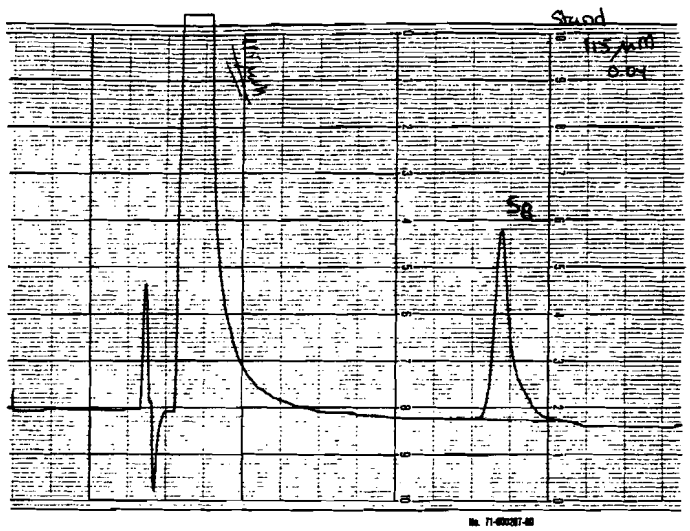

A

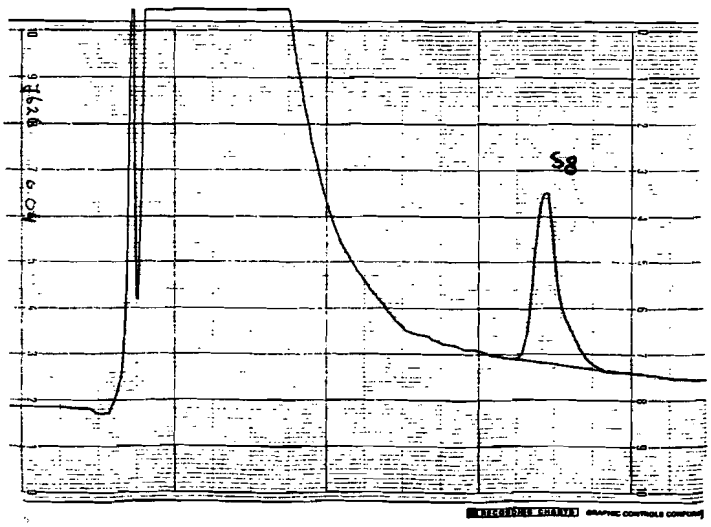

B

Figure 8.3: Chromatogram of S_8; A) standard solution 115 μM, B) first methanol/toluene extract (step 2 of the extraction scheme) of a sample.

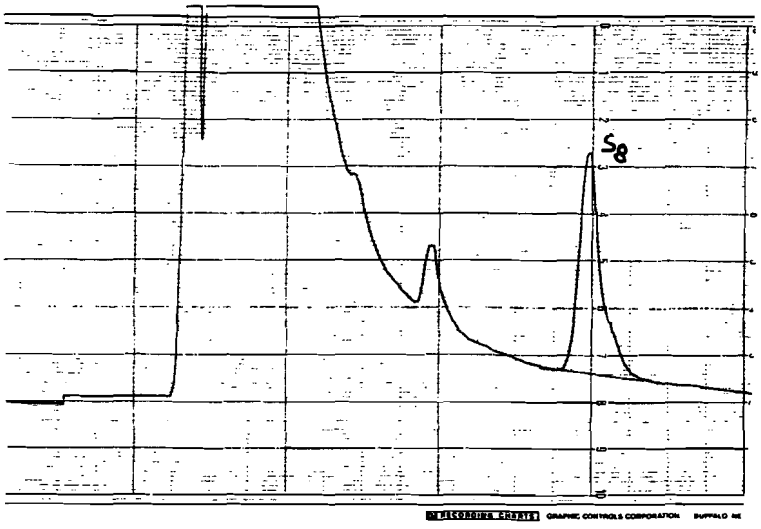

Figure 8.4: Chromatogram of second methanol/toluene extract (step 4 of the extraction scheme) of a sample.

A subsample of the methanol/toluene extract was taken from step two and step four and reacted with sulphite to form thiosulphate (see for preparation above). The formed thiosulphate was measured using HPLC techniques in combination with an electrochemical detector (EG&G, PAR model 400). The electrode consists of a golden disk, amalgamated with mercury. The potential was 0 mV. Thiosulphate is oxidized at the electrode, and negative currents were recorded. The eluent (70% methanol, in 0.1 N NaAC solution pH = 6) was purged through the system with a flow velocity of 1 ml/min, the pressure was about 800 psi. The samples were injected through a 20 μl loop and passed over a BIO-RAD strong anion column. Using these conditions thiosulphate has a retention time of 14 minutes.

8.6 Some remarks on the methods

Zerovalent sulphur: Elemental sulphur and low molecular weight non-polar organic sulphides can be dissolved in a non-polar organic solution such as benzene, toluene and Freon-TF In this study, zerovalent sulphur has been extracted by two different solutions, an acetone/freon mixture (3:1) and a methanol/toluene mixture (3:1). In case of the acetone/freon extraction total zerovalent sulphur has been extracted from very small amounts of wet sediments (25 - 35 mg). The extract was reacted with sulphite to form thiosulphate, which was measured by polarography as described earlier in this chapter. The extraction with a methanol/toluene mixture formed a part of the sequential sulphur extraction scheme (step 2). In this case the extract was divided into two parts. One part was directly measured for the elemental sulphur content as S_8 with HPLC techniques (see below). The other part was reacted with sulphite and the formed thiosulphate was also measured by HPLC. The results of these two extraction "methods" are given in the appendix table 8.1 and 8.2 for the Tyro Basin and the Bannock Basin, respectively. Comparing the data from these tables a few remarks can be made. Firstly, the data from the methanol/toluene extraction show a good correlation ($r > 0.92$) between the values of S(0) as S_8 and S(0) as thiosulphate for sediments from both basins (Fig. 8.5 and 8.6). The slope of this relation is 1.08 for sediments from the Tyro Basin (Fig. 8.5) and for sediments from the Bannock Basin m is 0.99 (Fig. 8.6). This suggests that the zerovalent sulphur extracted by a methanol/toluene only consist of S_8 and does not contain low molecular weight non-polar organic sulphides in these anoxic hypersaline sediments. This is in contrast to sediment from the salt marshes (Ferdelman et al., 1991).

Secondly, the zerovalent sulphur data measured as thiosulphate show higher values for the acetone/freon mixture than for the methanol/toluene extraction in the sediments from the Tyro Basin (table 8.1). In the case of the sediments for the Bannock Basin the data of the acetone/freon extract seem to be in the same range as the first methanol/toluene extract from the sequential sulphur extraction scheme for most of the depths. Both extracts will extract S_8 and low molecular weight non-polar organic sulphur. Oxidation of the wet sediment might be the main factor for the

discrepancy between the two extracts. The amount of extractable S_8 might increase due to oxidation of residual pore water, AVS and organic polysulphides. The data from the acetone/freon mixture are more likely to have been more sensitive for oxygen contamination since very small amounts of wet sediments were used. In chapter 9 data obtained with the methanol/toluene extraction will be discussed.

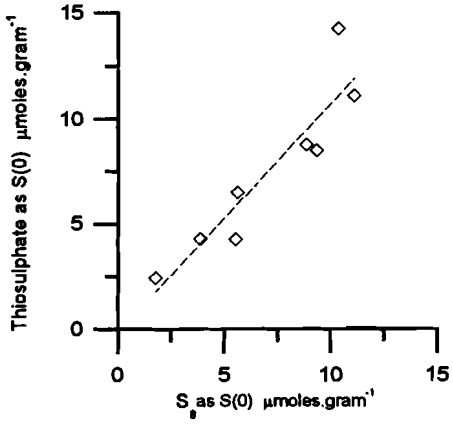

Figure 8.5: Zerovalent sulphur extracted by methanol/toluene mixture (step 2 from the sequential sulphur extraction scheme): data obtained by thiosulphate measurements versus the data obtained by S_8 measurements (HPLC, see text) for sediments of the Tyro Basin, core ABC15.

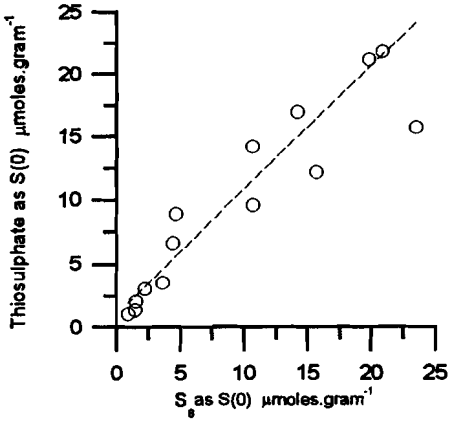

Figure 8.6: Zerovalent sulphur extracted by methanol/toluene mixture (step 2 from the sequential sulphur extraction scheme): data obtained by thiosulphate measurements versus the data obtained by S_8 measurements (HPLC, see text) for sediments of the Bannock Basin, core ABC45.

Organic polysulphides: The second methanol/toluene extraction could not be measured for the thiosulphate method. Due to interference of iron in the extract thiosulphate could not be identified. Thiosulphate is oxidized by iron according to the following reaction:

$$2\ Fe^{3+} + 2\ S_2O_3^{2-} \rightarrow 2\ Fe^{2+} + S_4O_6^{2-} \qquad [8.3]$$

NaOH fraction Francois (1987a) observed that 30-45% of the sulphur in the NaOH-fraction can be attributed to pyritic sulphur. He estimated the amount of pyritic S by the amount of H_2S that was liberated after a $CrCl_2$-treatment on the humic acid fraction.

Samples from this study have been measured, after ten times dilution, by ICPES. Using this method not only S data are obtained but also Fe data. Assuming all iron in the NaOH-fraction is due to extracted pyrite it can be calculated that between 1.1% - 7.3% of the total amount of NaOH extractable S can be due to coextracted pyrite (Appendix: Table 8.3). The average amount is about 4%, this is less than the average standard deviation between duplicate extractions. Based on these observation it can be stated that the amount of sulphur in the NaOH extract represents the humic sulphur fraction.

Appendix chapter 8

Table 8.1: Zerovalent sulphur presented as S(0) μmoles per gram dry weight in sediments from core ABC15, the Tyro Basin.

		Methanol/Toluene		Freon/Acetone
Sample	Depth (cm)	S(0) as S_8 by HPLC	S(0) as thiosulphate by HPLC	S(0) as thiosulphate by polarography
7609	12.0	1.8 ± 0.4	2.46 ± 0.04	13.0 ± 1.0
7614	66.5	9.3 ± 0.6	8.5 ± 1.4	15.9 ± 1.2
7618	127.5	11.1 ± 1.5	11.1 ± 0.2	15.0 ± 0.3
7626	265.5	10.3 ± 2.9	14.25 ± 0.06	n.a.
7630	321.5	8.8 ± 3.7	8.8 ± 2.4	31.8 ± 0.4
7635	413.5	5.6 ± 0.3	6.5 ± 0.5	32.1 ± 5.9
7639	486.0	3.9 ± 1	4.3 ± 0.8	13.4[1)]
7642	529.0	5.5 ± 3.3	4.3 ± 2.0	10.8 ± 2.0

[1)] single measurement
n.a. not analyzed

Table 8.2: Zerovalent sulphur presented as S(0) μmoles per gram dry weight in sediments from core ABC45, the Bannock Basin

		Methanol/Toluene		Freon/Acetone
Sample	Depth (cm)	S(0) as S_8 by HPLC	S(0) as thiosulphate by HPLC	S(0) as thiosulphate by polarography
7743	7.0	3.6 ± 2.2	3.6 ± 2.3	11.6 ± 1.8
7745	26.0	15.63[1)]	12.2 ± 0.7	n.a.
7746	42.0	1.5 ± 0.1	2.1 ± 0.3	n.a.
7747	51.5	4.4 ± 1.3	6.6 ± 1.8	n.a.
7748	66.5	1.4 ± 1.1	1.4 ± 1.0	n.a.
7750	107.5	0.9 ± 0.6	1.1 ± 0.5	n.a.
7751	127.5	20.9 ± 2.1	21.8 ± 3.4	7.3[1)]
7756	207.0	14.2 ± 0.4	17.0 ± 1.9	9.5 ± 3.3
7758	253.0	4.6 ± 0.9	8.9 ± 1.0	13.2 ± 2.3
7768	449.5	2.2 ± 0.9	3.1 ± 1.1	4.7 ± 1.0
7771	504.5	10.7 ± 3.6	9.6 ± 0.7	13.8 ± 2.9
7777	631.0	19.8 ± 2.4	21.2 ± 0.8	n.a.
7783	752.0	10.7 ± 0.6	14.2 ± 0.6	21.7 ± 0.3
7786	810.5	23.4 ± 8.8	15.7 ± 2.4	7.5 ± 2.1

[1)] single measurement
n.a. not analyzed

Table 8.3: Possible contribution of pyritic sulphur based on iron concentration in the NaOH-fraction. Concentrations are given per gram wet sediment.

SAMPLE	Fe μmoles	S pyritic μmoles	S NaOH μmoles	% S pyritic
7609	0.81	1.62	36.9	4.4
7614	0.63	1.26	40.7	3.1
7618	1.26	2.52	68.0	3.7
7626	1.23	2.46	56.0	4.4
7630	1.44	2.87	54.8	5.2
7635	0.73	1.46	55.0	2.7
7639	1.46	2.91	49.6	5.9
7642	1.37	2.75	68.9	4.0
7743	0.24	0.48	18.0	2.7
7745	0.48	0.96	36.6	2.6
7746	0.49	0.98	31.8	3.1
7747	1.61	3.22	79.3	4.1
7748	0.36	0.72	9.8	7.3
7750	0.21	0.42	36.6	1.1
7751	0.98	1.95	52.9	3.7
7756	0.30	0.60	27.2	2.2
7758	1.03	2.06	41.2	5.0
7768	0.55	1.10	80.8	1.7
7771	0.75	1.50	70.5	2.1
7777	0.73	1.46	34.4	4.2
7783	0.59	1.71	25.0	6.8
7786	0.68	1.35	48.4	2.8

Chapter 9: Sulphur speciation in anoxic hypersaline sediments from the Eastern Mediterranean[1]

Abstract

The anoxic hypersaline Tyro and Bannock Basins are among the most sulphidic bodies of water in the marine environment (H_2S > 2mM). The sulphur cycle in these basins has been studied.

Elamental sulphur, Acid Volatile Sulphur (AVS), organic polysulphides, humic sulphur (0.5 M NaOH extractable) and pyritic sulphur have been found in the sediments from these basins. Pyritic sulphur appears to be the main phase of inorganic reduced sulphur (50 - 80 % of the total sulphur pool), and is at the same level (about 250 μmoles per gram dry weight) in cores recovered from the two areas. Remarkably, humic sulphur has been found to account for 17 to 28 % of the total sulphur pool in the Tyro Basin, and for 10 - 43 % in the Bannock Basin. Sulphur isotope data show negative $\delta^{34}S$ values for both pyritic sulphur ($\delta^{34}S$: -16 ‰ to -40 ‰) and humic sulphur ($\delta^{34}S$: -16‰ to -30‰). This suggests that both pyritic and humic sulphur originate from microbially produced H_2S.

In neither basin is there a significant correlation between pyritic sulphur and organic carbon, suggesting syngenetic pyrite formation. Additionally, the degree of pyritization in these sediments (DOP is 0.62) indicates that pyrite formation is limited by the reactivity of iron. Humic sulphur correlates reasonable with the pyritic sulphur distribution and seems to be related with gelatinous pellicles (bacterial mats at the interface between oxic seawater and brine). Both pyritic and humic sulphur are thought to be formed at the interface of oxic seawater and brine. The presence of a bacterial mat and a high H_2S content in the brines seem to favour such conditions. Although these basins differ in their major element chemistry, their reduced sulphur species chemistry appears to be similar.

9.1 Introduction

Decomposition of organic matter by sulphate reducing bacteria leads to the formation of hydrogen sulphide (e.g. Berner, 1964,1980; Goldhaber and Kaplan, 1974, 1975; Jørgensen, 1982) and an increase of other metabolites (equation 9.1):

$$C_{106}H_{263}O_{110}N_{16}P + 53SO_4^{2-} \rightarrow 39CO_2 + 67HCO_3^- + 16NH_4^+ + HPO_4^{2-} + 53HS^- + 39H_2O \quad [9.1]$$

Such pore water chemistry has been observed in various marine environments, such as, in near-shore organic-rich sediments at the FOAM-site (Goldhaber et al., 1977), coastal sediments (Howarth and Jørgensen,

[1] Part of this chapter has been published as Henneke et al. (1991). Mar. Geol., 100: 115-123.

1984; Lin and Morse, 1991), in upwelling zones (Gieskes et al., 1984; Mossmann et al., 1991) and salt marshes (Luther et al., 1982; Howarth and Merkel, 1984; Oenema, 1990). In anoxic basins sulphate reduction can take place within the water column. The Black Sea is the largest known basin in which sulphate reduction is observed within the water column (Degens and Ross,1974; Murray, 1991). Other anoxic basins are known in the Baltic Sea (Boesen and Postma, 1988), Framvaren Fjord (Skei, 1983) and Cariaco Trench (Hastings and Emerson, 1988). Sulphate reduction in the water column can also take place in extreme saline environment, examples are the Dead Sea (Shatkey and Magaritz, 1987), Solar Lake (Jørgensen and Cohen, 1977), the Orca Basin (Ishizuka et al., 1985b; Presley and Stearns, 1985) and the Tyro and Bannock Basins (Luther et al., 1990).

Part of the hydrogen sulphide may react with iron (Berner, 1984) or organic matter (Kohnen et al., 1989) (Fig. 9.1). The distribution and interaction of inorganic sulphur species like pyrite, Acid Volatile Sulphur (AVS) and zerovalent sulphur have received much attention (e.g. Luther et al., 1982, Berner, 1984; King et al., 1985; Morse and Cornwell, 1987; Cutter and Velinsky, 1988; Boesen and Postma, 1988; Middelburg, 1991; Fossing, 1990, Ferdelman et al., 1991).

Recently some reports have been published about diagenetic organic sulphur formation (Francois, 1987a,b; Kohnen et al, 1989; Mossmann et al., 1990; Ferdelman et al., 1991). In nearshore sediments the organically bound sulphur content makes up only a few percent of the total sulphur content (Berner and Westrich, 1985; Francois, 1987a,b). However, in salt marsh sediments with high sulphate reduction rates up to 60% of the sulphur was present in the organic fraction (Ferdelman et al., 1991). Mossman et al. (1990) observed uptake of sulphide in kerogen after most of the reactive iron-minerals were converted to pyrite. The incorporation of sulphur in organic matter generally takes place in sediments which are iron-poor and/or have a high production rate of H_2S.

The anoxic hypersaline Tyro and Bannock Basins are among the most sulphidic bodies of water in the marine environment (Luther et al., 1990). Sediments in the Mediterranean are relatively iron-poor. In the anoxic hypersaline basins from the eastern Mediterranean pyritic sulphur and organic sulphur have been observed. In this chapter their distribution will

be discussed and an attempt will be made to describe the mechanism of pyrite and organic sulphur formation. Parameters such as C/S/Fe relationships, degree of pyritization and sulphur isotopes give avenues to evolve this mechanism.

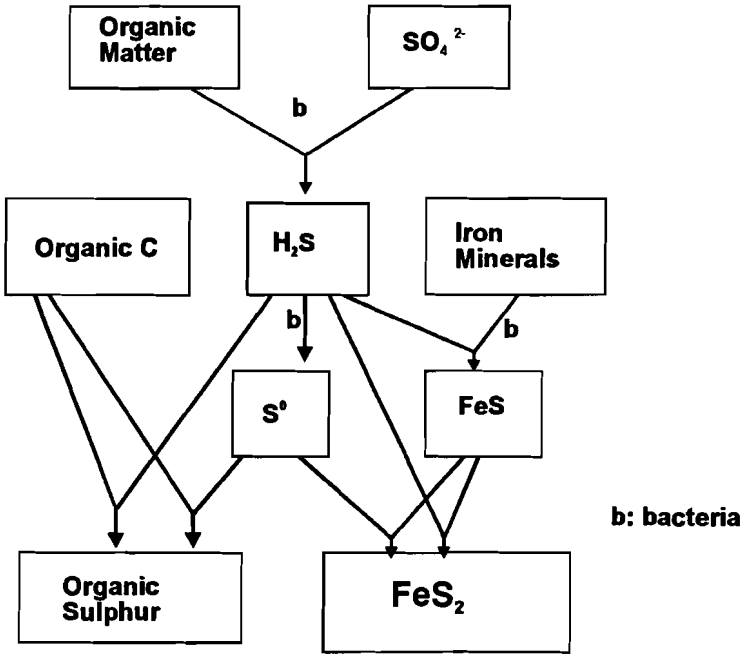

Figure 9.1: Sulphur diagenesis in anoxic marine sediments

9.2 Material and methods

Sediments

Gravity cores ABC15 and ABC45 have been sampled to study their inorganic and organic sulphur speciation. Core ABC15 was taken from the Tyro Basin and core ABC45 from the Bannock Basin, during the ABC-expedition in 1987 with the R.V. Tyro. Both cores contain anoxic sediments.

Sample processing has been described in detail by De Lange (1992). Sediment-samples were squeezed with modified Reeburgh-type squeezers in a glove box flushed with high-purity nitrogen. The squeezed sediment was sub-sampled for the remaining water content and for further

analyses. One part of the sediment samples was stored under nitrogen in air-tight glass bottles at 4°C.

After the removal of carbonate carbon with 1 M HCl organic carbon was determined by combustion of organic carbon in an oxygen atmosphere and measuring the CO_2 content by pressure. Based on duplicate analyses the precision of the organic carbon analyses is 3.5%. Dried sediment (250 mg) was completely dissolved with an acid mixture of $HF/HNO_3/HClO_4$. After evaporation the residue was taken up in 1 M HCl (50 ml), this solution was analyzed for total sulphur by ICPES (ARL 34000). Analytical precision was obtained by replicate analyses of an international standard and an in-house standard.

The determination of the sulphur species in the sediments has been be discussed in chapter 8. An outline of the methods is shown in table 9.1. The amount of reactive iron was determined in the acid fraction of the sequential sulphur extraction scheme (chapter 8) and measured by ICPES.

Table 9.1: Analytical methods applied for inorganic and organic sulphur speciation in anoxic hypersaline sediments from the eastern Mediterranean.

wet sediment sample A			
↓			
0.5 M NaCl	→	remove residual pore water sulphate	
↓			
Methanol/Toluene	→	elemental sulphur	
		LMW non-polar organic sulphur	→ HPLC
1 M HCl	→	remove AVS and breakdown organic polysulphides	
↓			
Methanol/Toluene	→	organic polysulphides	→ HPLC
↓			
0.5 M NaOH	→	humic sulphur	→ ICPES
wet sediment sample B			
↓			
3 M HCl	→	AVS	→ Polarography
dry sediment sample C			
↓			
Acetone	→	remove elemental sulphur	
↓			
1 M $CrCl_3$	→	pyritic sulphur	→ Polarography

Sulphur isotopes of the pyritic and the humic sulphur fraction were determined with a Finnegan MAT 251 (Göttingen, Germany). Samples were measured as SO_2 gas after oxidation of the Ag_2S with V_2O_5. Pyritic sulphur was converted into H_2S with a Cr(II) reduction method (Zhabina and Volkov, 1978) and collected in Cd-acetate. The formed CdS was converted to Ag_2S by addition of $AgNO_3$. To the 0.5 M NaOH extract, which contained humic-S, $BaCl_2$ was added. Prior to this the samples were acidified with concentrated HNO_3 for the converging of humic sulphur to SO_4^{2-}. The formed $BaSO_4$ was converted with a KIBA reagent (Sasaki et al., 1979) to H_2S and treated similar as the pyritic sulphur samples. Small amounts of pyritic and humic sulphur were directly collected as Ag_2S on quartz-wool, which had been soaked in $AgNO_3$, after their conversion to H_2S.

Interface

A special designed Interface Sampler (IS-II) was used for detailed sampling of the interface between oxic seawater and anoxic brine. The IS-II, designed at Utrecht University, consisted of a coated aluminium rack with 15 evenly spaced 2 litre teflon bottles. These bottles could be closed simultaneously upon an electronic signal. With the IS-II 15 samples were collected within a vertical interval of 3 m across the sharp interface. Samples from the interface in the Bannock Basin were taken during a Mast expedition with the R.V. Tyro, october 1991.

On deck sub-sampling was done with acid-cleaned syringes, equipped with a three-way stopcock. During sampling nitrogen was flushed into the bottles to avoid oxygen contamination. Total sulphur and Mn were measured by ICPES (ARL 34000) after 10 to 100 times dilution, obtaining a concentration for Na equal to one-tenth of that of normal seawater. Sulphide was measured by polarographic techniques (Luther et al., 1985) using square-wave voltammetry. An aliquot of 25 μl to 200 μl seawater was added to a polarographic cell, which contained 10 ml of a 0.1 M NaOH solution.

For total zerovalent sulphur an aliquot of 100 to 300 ml was filtered through a 0.2 μm polycarbonate filter. All samples were filtered in a glove

bag. The filters were put on a polyethylene bottle. To the filter 1 ml of 0.1 M Na_2SO_3 and 9 ml $NaClO_4$ was added. The bottles were put in an oven at 60°C for at least four hours. The sulphite reacts with the zerovalent sulphur and forms thiosulphate. Thiosulphate was measured by polarography using square wave voltammetry (SWV) (Luther et al., 1991b) using an EG&G Princeton Applied Research model 384B-4 with a Model 303 static dropping mercury electrode.

On board ship samples for stable isotope determination were prepared as follows. About 50 ml seawater was put into a glass bottle. In one bottle sulphide was removed by adding 1 ml of 3 M HCl. In the other bottle sulphide was fixed with Zn-acetate. All handling was done within a glove bag filled with nitrogen. Back home in the acidified bottle the sulphate was precipitated as $BaSO_4$ by adding 10 - 15 ml of 0.1 M $BaCl_2$. The formed $BaSO_4$ was converted to H_2S with KIBA reagent and further prepared for analyses as described above. For sulphide, the ZnS precipitate was collected in a reaction vessel similar as the ones used for AVS determinations. The reaction vessel was kept anoxic by flushing with nitrogen. Ten ml of 3 M HCl was added to the vessel. The liberated H_2S was collected on quartz-wool which had been soaked with $AgNO_3$. Samples were measured as SO_2 gas with a Finnegan MAT 251 (Göttingen). The $\delta^{34}S$ values are reported versus Canyon Diablo standard. Most values are based on single measurements, a few duplicates were done. These duplicates gave a standard deviation of 1‰.

9.3 Results

The sulphur speciation data from samples of core ABC15 and core ABC45 are given in table 9.2 and 9.3 in the appendix, respectively. All data are based on duplicate or triplicate extractions, except those for total sulphur. Figures 9.2 and 9.3 show the distribution of the sulphur species with depth in the sediments of the Tyro and the Bannock Basins respectively.

The amount of AVS measured is the cumulative of the monosulphides and the soluble H_2S that remains from residual pore-water. The contribution of H_2S to the total amount of AVS is less than 1 μmole per

gram dry weight and therefore its contribution can be neglected. Although there are large error-bars, the changes in concentration with depth in each core are significant (Fig. 9.2B and 9.3B). The lower precision of the AVS analyses is mainly due to sample inhomogeneity. In most cases it was possible to measure the pyrite with a relative precision of better than 5%.

In the Tyro Basin (ABC15) the pyritic sulphur value ranges from 150 to 300 μmoles per gram dry weight (Fig. 9.2C). AVS ranges from 5 to 20 μmoles per gram dry weight (Fig. 9.2B). Below a depth of about 100 cm the pyritic sulphur content in the Bannock Basin (ABC45) is fairly constant, about 250 μmoles per gram dry weight (Fig. 9.3C). In the top of this core the pyritic sulphur content seems to increase from 80 to 250 μmoles per gram dry weight, interfered by an enrichment at 50 cm of 350 μmoles S per gram dry weight (Fig. 9.3C). AVS ranges from 5 to 25 μmoles per gram dry weight (Fig. 9.3B).

In the Tyro Basin the amount of S_8 increases in the upper 125 cm (Fig. 9.2A), a maximum of 11 μmoles S per gram dry weight. After this maximum the S_8 concentration slowly decreases till about 5 μmoles per gram dry weight. The sediments from the Bannock Basin show more variation in the S_8 concentration (Fig. 9.3A). In the Bannock Basin higher S_8 values are measured than in the Tyro Basin.

Figures 9.2A and 9.3A show the organic polysulphides concentrations versus depth for core ABC15 and ABC45, respectively. In core ABC15 the concentration of the organic polysulphides increases with depth in the upper three meter. The value is constant, approximately 40 μmoles per gram dry weight, over an interval of about 150 cm (from 265.5 till 413.5 cm), after which it decreases significantly to 3 μmoles per gram dry weight. The maximum amount of organic polysulphides is significantly higher than the amount of S_8, namely 40 μmoles versus 11 μmoles per gram dry weight. In contrast, the profile of organic polysulphides in the Bannock Basin shows a similar pattern as that of the S_8 profile (Fig. 9.3A). In addition, the concentration of organic polysulphides are in the same range as those of the S_8.

In core ABC15 the humic sulphur is about 50 μmoles per gram dry weight in the upper meter, whereas it is higher below this depth, with a maximum value of approximately 100 μmoles per gram dry weight at 127 cm (Fig. 9.2D). The humic sulphur content in the sediments from core

ABC45 are highly variable in the upper meter, ranging from 25 to 140 μmoles per gram dry weight (Fig. 9.3D). This variability continues downcore.

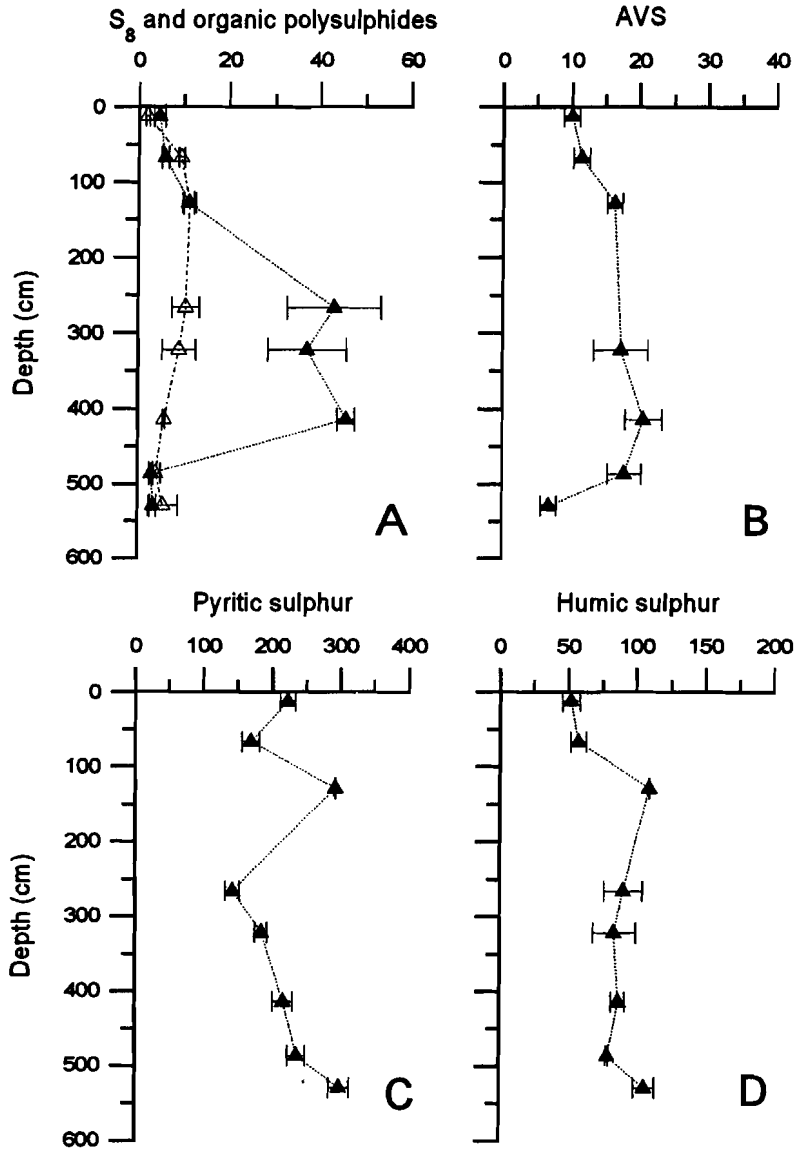

Figure 9.2: Sulphur speciation versus depth in sediments from the Tyro Basin, ABC15. All species are given as μmoles per gram dry weight. A) elemental sulphur (open triangles) and organic polysulphides (filled triangles), B) Acid Volatile Sulphur, C) Pyritic sulphur and D) Humic sulphur.

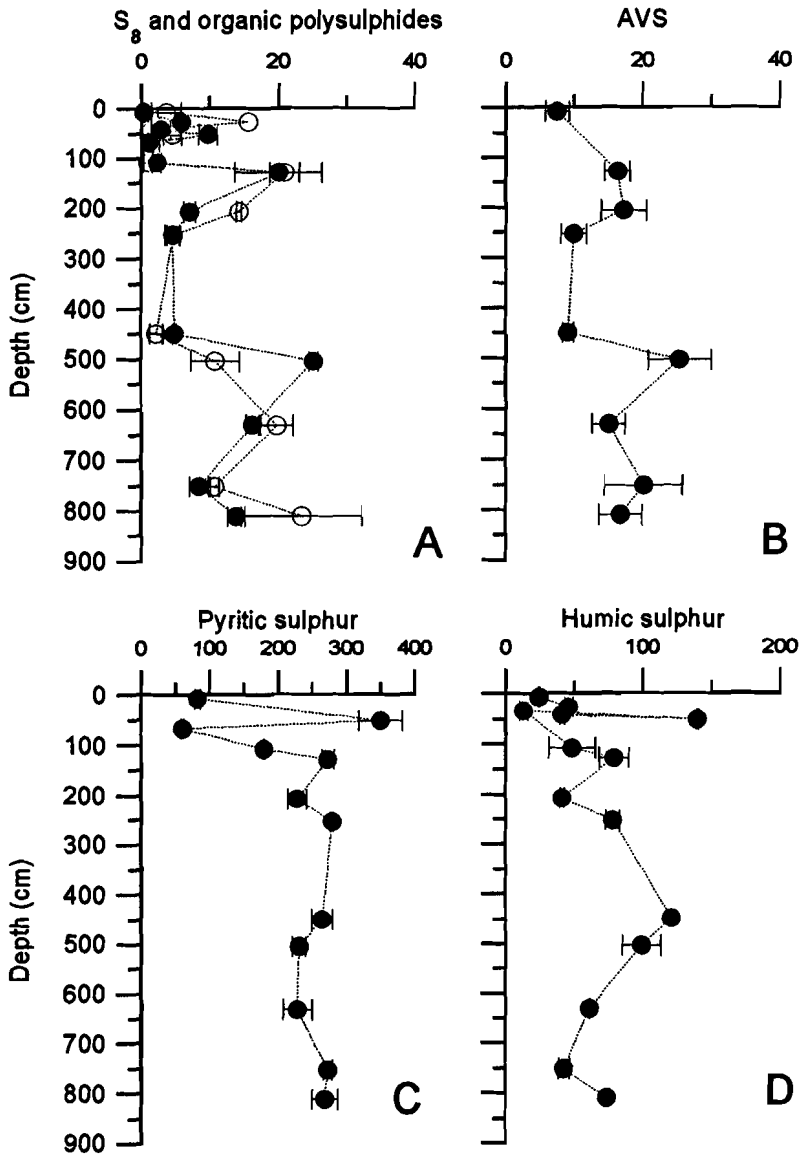

Figure 9.3: Sulphur speciation versus depth in sediments from the Bannock Basin, ABC45. All species are given as μmoles per gram dry weight. A) elemental sulphur (open circles) and organic polysulphides (filled circles), B) Acid Volatile Sulphur, C) Pyritic sulphur and D) Humic sulphur.

9.4 Discussion

9.4.1 Sulphur speciation and the total amount of S

In the sediments from the Tyro and Bannock Basins, the inorganic reduced sulphur phases (S_8, AVS and FeS_2) are higher in concentration than the organic reduced phases (organic polysulphides and humic sulphur) (Fig. 9.4). Pyrite is the main inorganic reduced sulphur species in the sediments from these two anoxic hypersaline basins, whereas humic sulphur is the most abundant organic reduced sulphur phase. The sum of the inorganic and organic sulphur species is in reasonable agreement with the total amount of sulphur (Fig. 9.4) and there is no apparent difference in total reduced sulphur content for both basins.

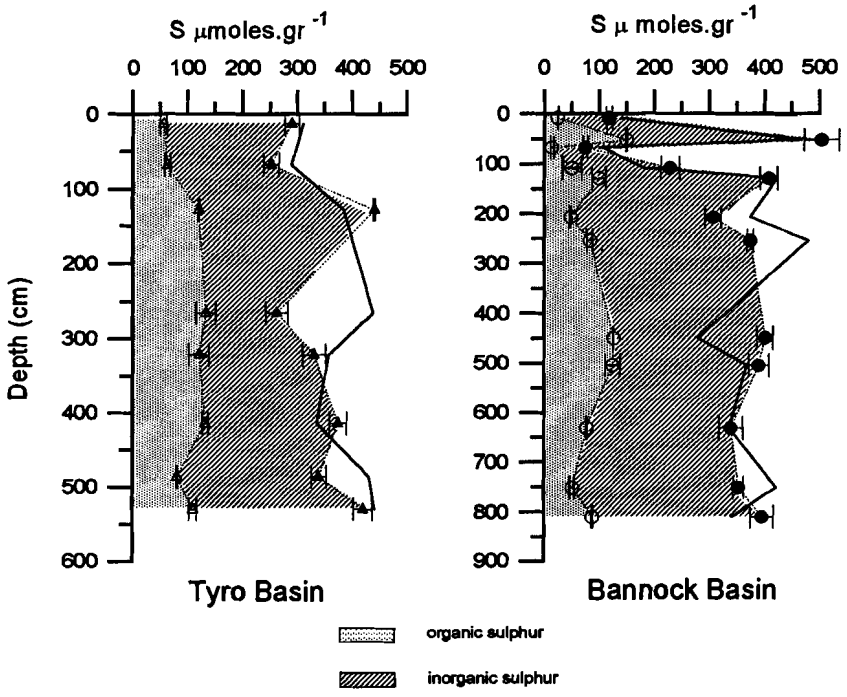

Figure 9.4: The sum of organic sulphur (organic polysulphides and humic sulphur) and the sum of inorganic sulphur (S_8, AVS and pyritic sulphur). Solid line represents the total amount of sulphur measured by ICPES.

9.4.2 Pyrite formation

The formation of pyrite has been summarized by various researchers (e.g. Berner 1970, 1984; Goldhaber and Kaplan, 1974,1975), and include the decomposition of organic matter by sulphate reducing bacteria, followed by the reaction of hydrogen sulphide with iron minerals to form ironsulphides and subsequently the reaction with elemental or zerovalent sulphur to pyrite (Fig. 9.1). The amount of pyrite formed in a sediment may be limited by: (1) the concentration of dissolved sulphide, (2) the amount of reactive iron, (3) the transformation of ironsulphides to pyrite, (4) S_8 or zerovalent sulphur and (5) organic matter.

In normal marine sediments pyrite formation is limited by organic matter and the H_2S produced from the decomposition of this organic matter (Berner, 1984). Under such conditions there is a significant positive correlation between pyritic sulphur and organic C and the best linear fit extends through zero.

In anoxic environments, H_2S is present above the sediment-water interface as well as within the sediments. Pyrite can form from sedimenting detrital iron minerals prior to burial both in the water-column and at the sediment-water interface (syngenetic pyrite) (Raiswell and Berner, 1985). As a result of the omnipresence of H_2S, organic carbon is not needed for pyrite formation at any given location (Raiswell and Berner, 1985).

Sediments of the Tyro and Bannock Basin indicate that there is no relation (Fig. 9.5A) between pyritic sulphur and organic carbon. The sediments of both basins are enriched in pyritic sulphur relative to organic carbon in comparison with normal marine sediments. This is consistent with the observation that generally an enrichment of pyritic sulphur relative to organic carbon is observed in anoxic environments in comparison with normal marine sediments (Leventhal, 1983; Berner, 1984; Raiswelll and Berner, 1985).

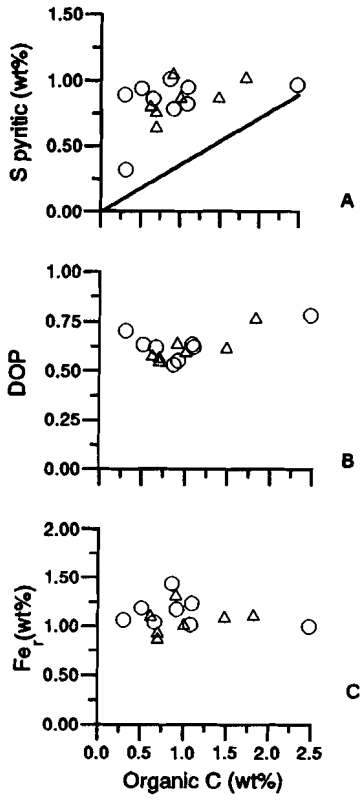

Figure 9.5: Organic carbon-pyritic sulphur-iron relationships in the sediments from the Tyro (open triangles) and Bannock (open circles) basins. A) Pyritic sulphur versus organic carbon, dashed line represents the S/C in normal marine sediments, B) DOP versus organic carbon and C) Fe_r (pyritic iron and HCl leached iron) versus organic carbon.

It is generally thought that pyrite is formed by the reaction of iron-monosulphides with elemental sulphur (Berner, 1970) or polysulphides (Rickard, 1975; Luther, 1991).

$$FeS + S^0 \rightarrow FeS_2 \qquad [9.2]$$

A complete transformation of AVS into pyrite is expected in presence of elemental sulphur on a time scale of years (Berner et al., 1979).

In the anoxic hypersaline sediments from the Tyro and Bannock Basins AVS and elemental sulphur were observed down to the maximum depth of recovery (Fig 9.2 and 9.3). The presence of AVS and S_8 at great depth in the sediment cores from the Tyro and Bannock Basins may be due to 1) a slow rate of pyrite formation with in the sediments or 2) to the incomplete transformation of AVS into pyrite.

9.4.3 Degree of pyritization

The iron which may react with H_2S (reactive iron) is mainly non-silicate bound iron, including amorphous iron (oxyhydr)oxides, some crystalline ironoxides and iron-monosulphides (Canfield, 1989). Recently, Canfield et al., (1992) have reported measurable but low reactivities of ironsilicates towards sulphide. Berner (1970) proposed that the amount of iron, reactive towards H_2S, can be determined by extracting iron with concentrated (12M) hot HCl for one minute. With this measurement for reactive iron the Degree of Pyritization (DOP) can be calculated using the following equation (Berner, 1970):

$$DOP = \frac{Pyritic\ iron}{Pyritic\ iron\ +\ Reactive\ iron} \qquad [9.3]$$

Although this parameter is widely used, no consensus exists on the concentration of the HCl and the time used to extract the reactive iron. A comparison between different methods used for reactive iron determinations is given by Leventhal and Taylor (1990). They suggested an extraction of 1 M HCl, shaken for 24 h although 12 h gave identical results[2], for reactve iron determination. For practical reasons, the amount of reactive iron in this study has been determined by an extraction of 1 M HCl shaken for 14 h.

When there is a significant amount of AVS present in the sediments the DOP parameter underestimates the amount of iron which has reacted with H_2S (Boesen and Postma, 1988). The Degree of Sulphidization (DOS) is therefore a better parameter:

$$DOS = \frac{Pyritic\ iron\ +\ AVS\text{-}iron}{Pyritic\ iron\ +\ reactive\ iron} \qquad [9.4]$$

[2]Morse showed that 12 hours shaken gave already similar results as Berner, 1970(comment in Leventhal and Taylor, 90)

The DOP values for the sediment of the Tyro and Bannock Basins are about 0.62 (Fig. 9.6). Part of the sulphidized iron is AVS therefore the DOS values are slightly higher, around 0.70.

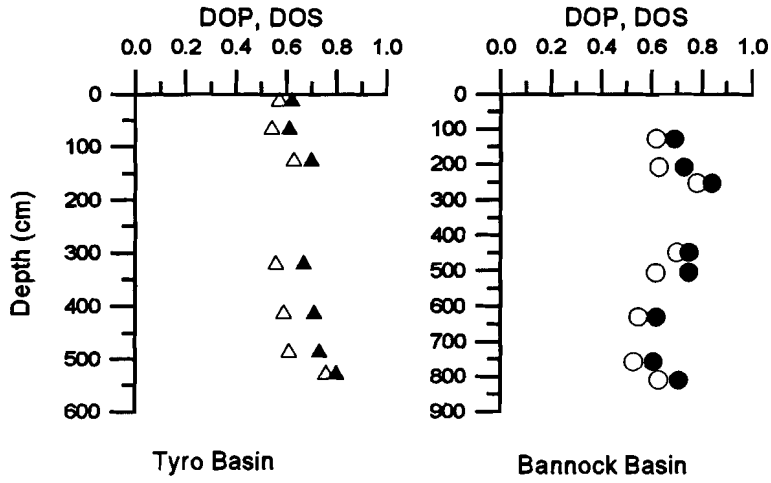

Figure 9.6: DOP (open) and DOS (filled) versus depth in the sediments.

Raiswell et al. (1988) showed that the DOP parameter can be used to distinguish normal marine sediments from anoxic sediments in case of ancient marine sediments. They observed that the DOP values for the anoxic sediments are between 0.55 and 0.93, whereas the normal marine sediments had DOP values less than 0.42. The observed DOP and DOS values in the sediments from the anoxic hypersaline Tyro and Bannock Basins are in good agreement with the findings for ancient anoxic marine sediments.

An average DOS value of 0.70 in the sediments from the Tyro and Bannock Basins (Fig. 9.6) suggests that there is still iron available to react with hydrogen sulphide. A possible overestimation of the amount of reactive iron due to the dissolution of iron-aluminium-silicates may be a reason. Studies of reactive iron estimation of recent sediments when extracted with increasing acid concentrations showed that iron-aluminium-silicates were coextracted (unpublished results, Henneke and Middelburg). These iron-aluminium-silicates may be reactive towards H_2S as has been reported by Canfield et al. (1992). However, they showed that the reaction rate is very slow. Iron containing clay minerals, such as smectite,

have a low crystallinity in the anoxic sediments from the Bannock Basin (Tomadin and Landuzzi, 1991). These "amorphous" silicates could have been partially extracted using the 1 M HCl procedure. Therefore the DOP value may have been slightly underestimated with respect to the overestimated amount of reactive iron available. Based upon the average Al/Fe ratio in the sediments and the Al content in the HCl fraction, the amount of Fe derived from silicates is estimated to be 20 - 30% of the total amount of Fe extracted with HCl. Subtracting the amount of Fe related to silicates from the total amount of reactive Fe will increase the DOP and DOS with approximately 0.06. This indicates that there is still iron available as (oxyhydr)oxides.

Canfield et al. (1992) argued that DOP values only give information on the potentially reactive iron and nothing on the actual reactivity of the iron (Canfield et al.,1992). The DOP values in the anoxic hypersaline sediments from the Tyro and Bannock Basins still suggest that iron is available to react with H_2S. However, the values for DOP and DOS are constant with depth (Fig. 9.6) and hydrogen sulphide is building up within the pore waters (for ABC15 > 2 mM and for ABC45 about 0.5 mM). These observations suggest that pyrite formation in these sediments is limited by the reactivity of iron.

9.4.4 Organic carbon-pyritic sulphur-iron relationships

The formation of pyrite is controlled by the decomposition of organic matter by sulphate reducing bacteria and the reaction of the formed hydrogen sulphide with iron minerals. Based upon the relationships between organic carbon, pyritic sulphur and reactive iron Raiswell and Berner (1985) distinguished three scenarios for pyrite formation in anoxic environments. Their findings are summarized in figure 9.7.

The organic carbon-pyritic sulphur-reactive iron relationships for the anoxic hypersaline sediments from the Tyro and Bannock Basins are shown in figure 9.5. There are no relations observed between pyritic sulphur and organic carbon. The DOP values and reactive iron (pyritic iron and HCl leached iron) are both independent of the amount of organic carbon. Additionally, at low carbon content high pyritic values are observed. These observations correspond to the scenario in which the

formation of pyrite is mainly syngenetic and limited by iron. The decoupling of iron and carbon suggests that the fluxes of iron and carbon to the sediments are different.

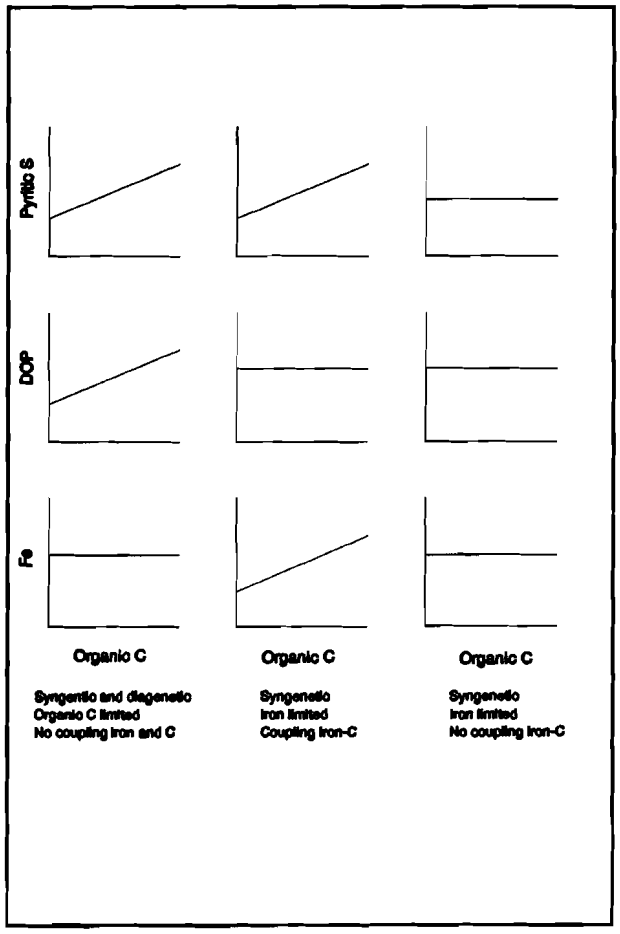

Figure 9.7: Organic carbon-pyritic sulphur-iron relationships as defined by Raiswell and Berner, 1985.

9.4.5 Organic reduced sulphur

Organically bound sulphur makes up between 12 to 40% of the total amount of sulphur in these anoxic hypersaline basins (Fig. 9.4). The humic sulphur compounds are the major organic sulphur species. Organically bound sulphur is formed by an abiotic reaction of reduced sulphur species with organic matter (Nissenbaum and Kaplan, 1972; Francois 1987b; Sinninghe Damsté et al., 1989). As possible reactants hydrogen sulphide, polysulphides, elemental sulphur and thiosulphate (Nissenbaum and Kaplan, 1972; Luther et al., 1986; Vairavamurthy and Mopper, 1987; Kohnen et al., 1989) have been mentioned.

The increase of organic polysulphides and the humic sulphur within the zone of sulphate reduction suggests that those compounds are diagenetic reaction products between organic matter and inorganic reduced sulphur. Organic polysulphides in the Tyro Basin strongly increase with depth up to 40 μmoles per gram dry weight till about 450 cm (Fig. 9.2A). At this depth the amount of organic polysulphides drops to 3 μmoles per gram dry weight. In the Bannock Basin there is no clear pattern observed, the concentration is mostly at 10 μmoles per gram dry weight and never exceeds the amount of 25 μmoles per gram dry weight (Fig. 9.3A). Organic polysulphides are known to be unstable under strongly reducing conditions (Boulegue, 1982) and will degrade to tri- and/or di-sulphides during prograde diagenesis (Kohnen, 1991). The profile observed in the Tyro Basin (Fig. 9.2A) can be explained as being the result of formation of organic polysulphides and their degradation at depth. The decrease in organic polysulphides is accompanied with a decrease in AVS and a small increase in pyrite, which may suggest the conversion of the degradation products of organic polysulphides into pyrite. For the Bannock Basin this is not so straight forward.

Nissenbaum and Kaplan (1972) reported that the S/C ratio (mole based) for humic substances in anoxic sediments is much higher (up to 0.037) than those observed in marine plankton (0.004 - 0.011). The S/C of humic substances in various anoxic sediments is given in table 9.4:

Table 9.4: S/C ratios of humic substances in various anoxic marine sediments, ratios are given on mole basis.

Location	S/C ratio	References
Jervis Inlet, British Columbia	0.009 - 0.015	Francois, 1987b
Salt Marsh, Delaware	0.018	Ferdelman et al., 1991
Peru Margin	0.056 - 0.112	Mossmann et al., 1991
Bannock Basin	0.038 - 0.204	this study
Tyro Basin	0.062 - 0.162	this study

The S/C ratio of the humic compounds in the sediments from the Tyro and Bannock Basins are higher than those reported by Francois (1987b) and Ferdelman et al., (1991). Such a high sulphur content of organic matter was also observed in sediments from the Peru Margin (Mossmann et al., 1991).

The incorporation of sulphur in organic matter takes place during the early stages of diagenesis (Nissenbaum and Kaplan , 1972; Francois, 1987b; Mossmann et al., 1991; Ferdelman et al., 1991). It has been demonstrated that reactive iron controls the organically bound sulphur, because the reaction of organic matter with reduced sulphur species is slower than the reaction of these sulphur species with detrital iron minerals. So, organically bound sulphur will be formed after reactive iron oxides have been converted to iron monosulphides and pyrite (Mossmann et al., 1990). However, in the anoxic hypersaline sediments from the Tyro and Bannock Basins the profile of humic sulphur correlates reasonable with that of pyrite (Figs. 9.2 and 9.3). Additionally, there is no prograde formation of humic sulphur with depth observed. Organic carbon- pyritic sulphur and reactive iron relationships (Fig. 9.5) suggest that the formation of pyrite is mainly syngenetic and limited by iron. The humic sulphur compounds seem to correlate with an enrichment of gelatinous pellicles in the sediments. Gelatinous pellicles are bacterial mats formed at the interface between oxic seawater and brine (Erba, 1991). Therefore, it is suggested that humic sulphur is also formed syngenetic.

9.4.6 Sulphur isotopes

The sulphur atom has four stable isotopes: ^{32}S (95.02%), ^{33}S (0.75%), ^{34}S (4.21%) and ^{36}S (0.02%). Normal seawater has an isotopic composition of $\delta^{34}S$ = + 20 ‰. During sulphate reduction of organic matter the stable isotope distribution of sulphur is modified. The produced hydrogen sulphide contains more ^{32}S than the sulphate, enriching the latter in ^{34}S. Accordingly, the hydrogen sulphide will have a negative $\delta^{34}S$ value. A fractionation of 60 ‰, giving a $\delta^{34}S$ for H_2S of -40‰, has been observed in marine sediments (e.g. Hartmann and Nielsen, 1969; Kaplan and Rittenberg, 1964). During prograde diagenesis the sulphate component will become "heavier" (a higher $\delta^{34}S$). Subsequently the isotope of the H_2S produced will also become "heavier" and the $\delta^{34}S$ will become less negative (Hartmann and Nielsen, 1969; Goldhaber and Kaplan, 1980).

The sulphate concentration of the anoxic hypersaline bottom waters in the Tyro and Bannock Basins is determined by a mixture of normal marine seawater and evaporitic source. The isotopic composition of the Messinian evaporite is about the same as that of normal seawater (De Lange et al., 1990b). The isotopic composition of sulphate in the Tyro Brine is $\delta^{34}S$ = + 26 ‰ (De Lange et al., 1990a,b) and in the Bannock Brine $\delta^{34}S$ = + 21 ‰ (Fig. 9.8). Both basins contain sulphidic bottom water (Luther et al., 1990), indicating that sulphate reduction takes place. A fractionation of more than 50‰ is observed in the Bannock brine, where the isotopic composition of the H_2S in the Bannock brine is about -30 ‰. Unfortunately, there are no isotopic data available for H_2S in the Tyro brine. A fractionation of more than 50 ‰ would give a bacterial fractionation factor α of 1.050 according to the relation Δ ($\delta^{34}S_{SO4}$-$\delta^{34}S_{H2S}$) = (α-1)1000. However, laboratory studies predict α = 1.000 - 1.025 (Goldhaber and Kaplan, 1980). The high fractionation between $\delta^{34}S$-sulphate and $\delta^{34}S$-H_2S and their constant profile across the interface (Fig. 9.8) indicate an open sulphate reduction system in the Bannock brine, due to a high amount of sulphate in this brine.

Rayleigh distillation is also observed within the pore waters. The increase of the $\delta^{34}S$ and the decrease of the sulphate concentration with depth indicate that continuing sulphate reduction has taken place within

these anoxic hypersaline sediments (Fig. 9.9). The bacterial isotope fractionation factor α can be obtained from a Raleigh plot. The logarithm of the isotope ratio is plotted against the logarithm of the sulphate concentration. In case of a closed system and steady state the slope of this plot is equal to $(1-1/\alpha)$ (Goldhaber and Kaplan, 1980). The Raleigh plots for cores ABC15 and ABC45 are shown in figure 9.10. A fractionation factor α of 1.014 is found for core ABC15 and α is 1.005 for core ABC45. These values are in the range of laboratory studies. However, as shown in chapter 5, sulphate reduction in core ABC45 is only of importance in the upper 150 cm. The α for this deth interval is estimated to be 1.025.

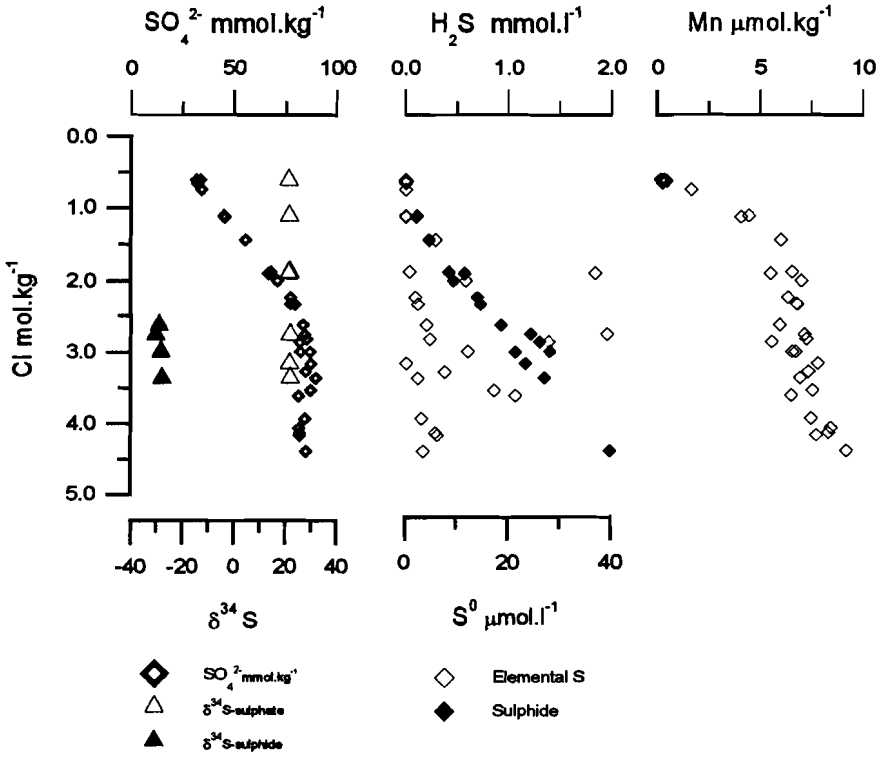

Figure 9.8: Interface between oxic seawater and brine in the Bannock Basin. A) Sulphate concentration versus the Cl concentration (semi-closed diamond); $\delta^{34}S$ of sulphate (open triangle) and $\delta^{34}S$ of sulphide (closed triangle). B) H_2S (closed diamonds) and zerovalent sulphur (open diamonds) versus Cl. C) dissolved Mn versus Cl.

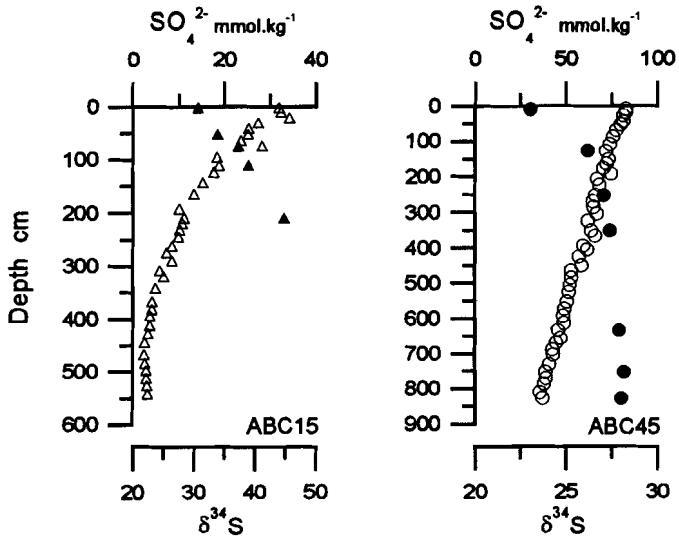

Figure 9.9: SO_4^{2-} (mmoles.kg^{-1}) in pore waters versus depth (ABC15, open triangle; ABC45, open circle) and $\delta^{34}S$ of the pore water sulphate (‰) versus depth (ABC15, filled triangle; ABC45, filled circle).

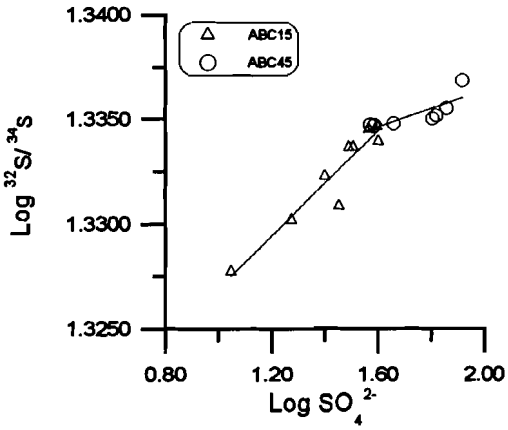

Figure 9.10: Raleigh plot for ABC15 (open triangle) and ABC45 (open circle). The Log [SO_4^{2-}] versus the Log [$^{32}S/^{34}S$] of the pore water SO_4^{2-}

When hydrogen sulphide reacts with iron minerals or organic matter there is hardly any fractionation (Frey et al., 1984). The $\delta^{34}S$ for the pyritic sulphur and the humic sulphur are shown in figure 9.11. The range of the $\delta^{34}S$ values lies between -19‰ and -39‰ for the pyritic sulphur, whereas for the humic sulphur this range is from -15‰ to -29‰. The $\delta^{34}S$ values of the humic sulphur are between 1‰ and 13‰ heavier than the pyritic sulphur. This is concordant with the observation that H_2S reacts faster with iron minerals than with organic matter (Mossmann et al., 1990). Therefore the lighter, earlier produced, sulphide will be incorporated in pyritic sulphur, whereas the more heavy sulphide will be incorporated into organic matter.

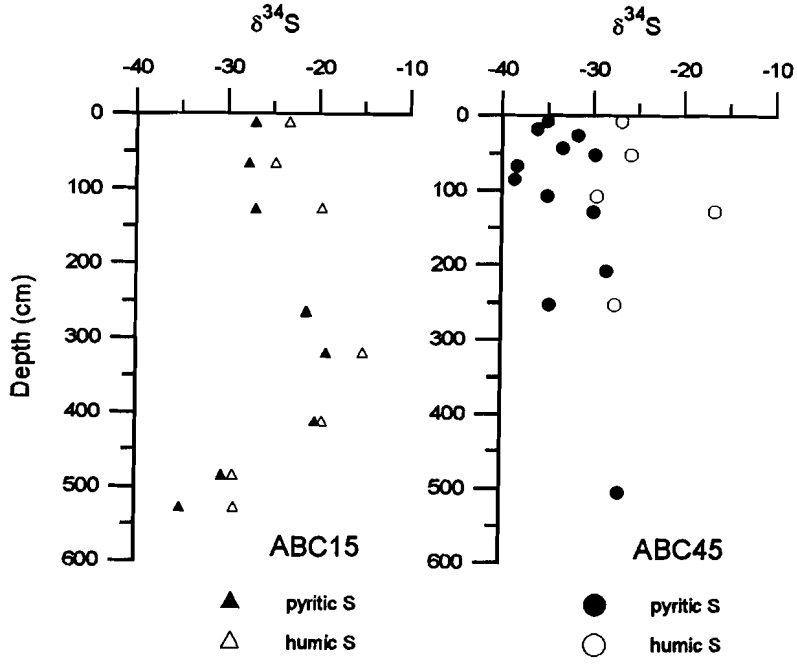

Figure 9.11: $\delta^{34}S$ of pyritic sulphur (filled) and $\delta^{34}S$ humic sulphur (open) versus depth in the sediments.

9.5 A scenario for syngenetic pyrite and humic sulphur formation

Pyritic and humic sulphur are the end products of the sulphur cycle in anoxic hypersaline sediments from the eastern Mediterranean. Their distribution in relative magnitude and in $\delta^{34}S$ is almost identically. The observation of high pyritic sulphur at low organic carbon and the organic carbon-pyritic sulphur and reactive iron relationsships show in figure 9.5 suggest the formation of syngenetic pyrite.

At the interface between oxic seawater and the anoxic brine in both basins higher amounts of dissolved and particulate organic carbon have been observed (chapter 7; Henneke and De Lange, 1990). Additionally, gelatinous pellicles have been found at these interfaces (Erba, 1991). The presence of sulphate reducing bacteria in these mats (Erba, 1991), is indicative of sulphate reduction occurring at the interface.

Due to the large density difference between the oxic seawater and the brine pelagic fall out is captured at the interface (Erba, 1991). Within the brines there is an abundancy of H_2S present which can react with detrital iron to form monosulphides and subsequently pyrite. To form pyrite the monosulphides must react with zerovalent sulphur. This zerovalent sulphur may be S_8 (Berner, 1970) or polysulphides (Rickard, 1975; Luther, 1991). In the Bannock Basin zerovalent sulphur was found to be enriched at the interface; values up to 40 $\mu mol.l^{-1}$ (Fig. 9.8) were found. Manganese oxides are the likely oxidants that may oxidize the H_2S to elemental sulphur (Burdige and Nealson, 1986; Aller and Rude, 1988). An increase of dissolved Mn is observed at the interface in the Bannock Basin (De Lange, 1989; De Lange et al., 1990a,c; Schijf, 1992). Data obtained from the IS-II for dissolved Mn are shown in figure 9.8. Van der Sloot et al. (1990) and Saager et al. (1993) found a particulate Mn maximum near the seawater-brine interface in the Tyro Basin.

According to these observations pyrite formation at the interface is likely to occur. This is supported by a relatively constant and highly negative $\delta^{34}S$ for pyritic sulphur. Assuming a closed system, a biological fractionation factor α of 1.014 and 1.022 was found in the sediments from the Tyro and Bannock Basins, respectively. This fractionation factor can not produce the highly negative $\delta^{34}S$ values as found for pyritic sulphur. However an open system, as observed in the Bannock brine, can

produce such negative $\delta^{34}S$ values.

Because of the omnipresence of H_2S in the brines, incorporation into organic matter may also take place at the interface. High bacterial activity has been recorded at the interfaces (DeDomenico and DeDomenico, 1989). This newly formed organic matter, including gelatinous pellicles, may incorporated sulphide. As reported, humic sulphur seems to be closely related to these gelatinous pellicles. Unfortunuately, the mechanism involved in the formation of humic sulphur still remains unsolved.

Turbiditic deposition transports pyritic sulphur and humic sulphur compounds to the sediments in the Tyro and Bannock Basins. The Tyro Basin has a more turbiditic regime than the Bannock Basin (Erba, 1991). These turbidites also provide also extra iron minerals which can be converted to pyrite within these sediments. The isotopic data of pyritic sulphur in the Tyro Basin show a slight increase. This increase is related to an increase of the $\delta^{34}S$ of the pore water sulphate, which is indicative for progressive diagenesis.

9.6 A comparison with the Orca Basin

The conditions of sediment deposition in the Tyro and Bannock Basins can be contrasted with those in the Orca Basin. The Orca Basin is a small, deep-water depression in the northern Gulf of Mexico. The bottom-water in this basin is anoxic and hypersaline (Shokes et al., 1977). For the Orca Basin a high content of dissolved iron in the brine has been reported (Trefry et al., 1984). Dissolved sulphide concentrations have been reported to be low (less than 1 μM, Trefry et al., 1984). Data from the Orca Basin sediments show a direct covariance between carbon and sulphur, with a positive intercept at the S-axis (Sheu and Presley, 1986; Sheu, 1987). Sheu and Presley (1986) conclude that carbon is the limiting factor for sulphate reduction, since dissolved sulphate and reactive iron are abundant at all levels of the sediment column in the Orca Basin. An increased biomass was observed at the interface (LaRock et al., 1979). However no bacterial mats have been recorded. Iron monosulphides are reported to be the major sulphur species in the anoxic hypersaline

sediments from the Orca Basin (Sheu, 1990). By contrast, in the Tyro and Bannock brines H_2S is observed at a concentration of > 2 mM (Luther et al., 1990) and dissolved iron is very low (Saager et al., 1993). Pyritic and organic sulphur are the major sulphur species in these basins.

9.7 Conclusions

Pyritic and humic sulphur are the major end-products of the sulphur diagenesis in anoxic hypersaline sediments from the eastern Mediterranean. The $\delta^{34}S$ for pyrite lies between -19‰ and 39‰, for the humic sulphur this range is from -15‰ to -29‰. The sediments from the Tyro and Bannock Basins show no relation between the amount of pyritic sulphur and the organic carbon content. In both basins the sediments are enriched in pyritic sulphur relative to organic carbon in comparison with normal marine sediments. This is consistent with the observations generally found in anoxic environments (Leventhal, 1983; Raiswell and Berner, 1985).

The DOP values, in both basins approximately 0.62, indicate that there is still iron available to react with hydrogen sulphide. However, the DOP values are essentially constant with depth and hydrogen sulphide is build up with in the pore waters. Pyrite formation is limited by the reactivity of iron and not by the availability of iron as had been argued by Canfield et al. (1992).

Humic sulphur makes up to 40% of the total amount of sulphur found in these anoxic hypersaline sediments. The humic compounds are formed by the interaction between reduced sulphur species and organic matter. The profile of humic sulphur correlates reasonable with that of pyrite. Additionally, they seem to be related with the gelatinous pellicles observed at the interfaces.

Because of the omnipresence of H_2S organic sulphur compounds can be formed at an almost equal timescale as the interaction of iron minerals with H_2S. The presence of a bacterial mat and a high H_2S content in the brines favour pyritic and organic sulphur formation at the interface of the Tyro and Bannock Basins. Turbiditic deposition transports organic sulphur compounds and pyrite to the sediments in these basins. Additional pyritic

and humic sulphur is formed diagenetically within the anoxic hypersaline sediments. Although these basins differ in their major element chemistry, their reduced sulphur chemistry appears to be similar.

Appendix chapter 9

Table 9.2: Sulphur speciation in anoxic hypersaline sediments from the Tyro Basin, ABC15. All species are given in μmoles S per gram dry weight.

Sample	Depth (cm)	S_8	Organic polysulphides	Humic Sulphur	AVS	Pyritic Sulphur
7609	12.0	1.6 ± 0.5	4.5 ± 1.3	51.5 ± 6.4	10.0 ± 1.2	222 ± 11.0
7614	66.5	9.3 ± 0.6	5.8 ± 0.7	57.1 ± 5.6	11.4 ± 1.2	168 ± 12.4
7618	127.5	11.1 ± 1.5	11.0 ± 1.1	109 ± 0.01	16.3 ± 1.2	292 ± 1.0
7626	265.5	10.3 ± 2.9	42.9 ± 10.3	90 ± 14	n.a.	158 ± 8.0
7630	321.5	8.8 ± 3.7	37.0 ± 8.6	83.6 ± 16	17.2 ± 4.0	184 ± 8.6
7635	413.5	5.6 ± 0.3	45.5 ± 1.9	86.6 ± 5.0	20.6 ± 2.7	216 ± 14.4
7639	486.0	3.9 ± 1.0	2.8 ± 0.4	78.7 ± 1.0	17.8 ± 2.5	236 ± 13.2
7642	529.0	5.5 ± 3.3	3.3 ± 0.7	106 ± 7.5	6.7 ± 1.1	298 ± 14.8

n.a. not analyzed

Table 9.3: Sulphur speciation in anoxic hypersaline sediments from the Bannock Basin, ABC45. All species are given in μmoles S per gram dry weight.

Sample	Depth (cm)	S_8	Organic polysulphides	Humic Sulphur	AVS	Pyritic Sulphur
7743	7.0	3.6 ± 2.2	0.24 ± 0.16	24.2 ± 0.3	7.5 ± 1.7	82 ± 4
7745	26.0	n.a.	5.9 ± 0.2	45.9 ± 3.1	n.a.	n.a.
7746	42.0	1.5 ± 0.1	2.8 ± 1.4	41.2 ± 1.6	n.a.	n.a.
7747	51.5	4.4 ± 1.3	9.7 ± 1.4	140 ± 1.0	n.a.	356 ±16
7748	66.5	1.4 ± 1.1	1.0 ± 0.03	13.0 ± 3.2	n.a.	56 ± 1
7750	107.5	0.9 ± 0.6	2.2 ± 0.6	48 ± 17	n.a.	179 ± 1
7751	127.5	20.9 ± 2.1	20.0 ± 6.4	79 ± 11	16.3 ± 1.8	272 ± 9
7756	207.0	14.2 ± 0.4	6.9 ± 0.9	40.6 ± 1.5	17.2 ± 3.3	228 ± 14
7758	253.0	4.6 ± 0.9	4.5 ± 1.2	77.9 ± 5.1	9.9 ± 1.9	278 ± 2
7768	449.5	2.2 ± 0.9	4.8 ± 0.2	121[1)]	9.1 ± 0.8	264 ± 15
7771	504.5	10.7 ± 3.6	25.1 ± 0.7	99 ± 14	25.3 ± 4.7	230 ± 10
7777	631.0	19.8 ± 2.4	16.2 ± 0.9	60.8 ± 0.1	15.0 ± 2.4	228 ± 21
7783	752.0	10.7 ± 0.6	8.4 ± 1.4	42.2 ± 4.2	20.0 ± 5.7	272 ± 6
7786	810.5	23.4 ± 8.8	13.9 ± 1.3	73.6[1)]	16.7 ± 3.1	268 ± 19

n.a. not analyzed
[1)] single measurement

Appendix A: Diffusion Coefficients

Calculation of the diffusion coefficients after Li and Gregory (1974).

The $D_j°$, the tracer and self-diffusion coefficient of ions at infinite dilution is linear with temperature T. The temperature of Mediterranean bottom-water is 13°C. The $D_j°$ of several ions at 13°C have been calculated from the $D_j°$ data of Li and Gregory (1974). The calculated $D_j°$ are listed in table A-I.

Table A-I: Tracer and self-diffusion coefficients of ions at infinite solution, at 13°C (Calculated according to Li and Gregory, 1974)

Cation	$D_j°$ (10^{-6} cm^2/sec)	Anion	$D_j°$ (10^{-6} cm^2/sec)
Na^+	9.90	Cl^-	15.2
K^+	14.8	HCO_3^-	8.72
Mg^{2+}	5.28	CO_3^{2-}	6.85
Ca^{2+}	5.90	SO_4^{2-}	7.82
Sr^{2+}	5.87	HPO_4^{2-}	5.42
Ba^{2+}	6.27	$H_2PO_4^-$	6.18
NH_4^+	14.86		

The tracer and self-diffusion coefficients of ions in seawater D_j can be predicted from the viscosity of seawater

$$D_j = D_j^o \left(\frac{\eta^o}{\eta}\right) \qquad \text{A-1}$$

The viscosity η is depended of temperature, pressure and density ρ.

$\eta^o/\eta_{\text{sea water (35)}} = 0.92$ at 25°C and 0.95 at 0°C

The influence on the amount of salt in solution can be estimate from the relation between η°/η and salinity given in the Handbook of Chemistry and Physics (CRC Press, 66th edition). The η_o/η for seawater at 20°C is 0.997 en for brine water 0.94.

The effect of temperature and density on the D_j is relative small, respectively 3% and 6%. Also the pressure effect has been show to be at most 8% (Li and Gregory, 1984). The D_j is brine water is at most 8% smaller than D_j°, therefore no corrections have been made for viscosity.

To calculate the diffusion coefficient for interstitial solution in sediment the following equation is used.

$$D_{j,sed} = \frac{D_j}{\theta^2} \qquad \text{A-2}$$

The tortuosity θ of the sediment depnds on the geometry of the sediment and is difficult to measure directly. The tortuosity can be calculated as follow (ullman and Aller, 1982/3): $\theta^2 = F * \phi$
So equation A-2 becomes

$$D_{j,sed} = \frac{D_j}{\phi * F} \qquad \text{A-3}$$

F = formation factor or resistivity, which can be estimated from Ullman and Aller (1983).

$$F = \phi^{-n} \qquad \text{A-4}$$

n = 2 for sediments with a porosity $\phi \leq 0.7$
n = 2.5 - 3 for sediments with a porosity ϕ = 0.7 - 0.9.

Recently, Iversen and Jφrgensen (1993) postulated a new empirical relationship to estimate $D_{j,sed}$

$$D_{j,sed} = \frac{D_j}{1 + n(1-\phi)} \qquad \text{A-5}$$

At a porosity above 0.7 they found no difference in the estimated diffusion coefficients for sulphate. For clay-silt sediments a value of n=3 seemed to be the best choice. Applying A-5 to the sulphate diffusion coefficients for the anoxic hypersaline sediments from the eastern Mediterranean this will give a $D_{j,sed}$ value 25% lower than the ones given in table A-2.

Table A-2: Calculated diffusion coefficients for interstitial solutions in sediments. $D_{j,sed}$ is given in $cm^2.y^{-1}$ calculated according to equation A-3

	ABC15 ABC45 *)	ABC17	ABC23
porosity φ	0.63 ± 0.03	0.87 ± 0.06	0.71 ± 0.11
n	2	3	2.5
Ion	$D_{j,sed}$	$D_{j,sed}$	$D_{j,sed}$
Na^+	197	229	187
Cl^-	302	352	287
K^+	294	342	279
Ca^{2+}	117	137	111
Mg^{2+}	105	123	100
Sr^{2+}	117	136	111
Ba^{2+}	125	145	118
SO_4^{2-}	156	180	148
NH_4^+	296	344	281
HCO_3^-	173	202	165
CO_3^{2-}	136	158	129
HPO_4^{2-}	108	125	102
$H_2PO_4^{2-}$	123	143	117

*)From core ABC45 no porosity data are available. The porosity is assumed to be similar to that in as core ABC15, since their lithology is comparable. The standard deviation of the porosity in core ABC23 will give an error of less than 15% for all diffusion coefficients.

Cross-coupling terms

The diffusive flux is driven by the gradient of the concentration $\delta C_i/\delta x$ and the electrical potential $\delta E/\delta x$ (McDuff and Ellis, 1979):

$$J_i = -U_i \{RT(\frac{\delta C_i}{\delta x}) + Z_i C_i F(\frac{\delta E}{\delta x})\} \qquad \text{A-6}$$

R = gasconstant
F = Faraday's constant
T = absolute temperature
Z = charge of the ion
U = ionic mobility of ion i ($cm^2.mol.J^{-1}.sec^{-1}$)

This equation can be applied to an isothermal solution under the assumption that the gradient of concentration is identical to the gradient of the chemical potential, meaning that $\delta\gamma_i/\delta x = 0$, where γ_i is the activity of i.

U is the ionic mobility of i at infinite solution and can be calculated from the following equation (Ben-Yaakov, 1972):

$$U_i = \frac{\lambda_i^\circ}{|Z_i| * F^2} \qquad \text{A-7}$$

λ = equivalence conductance (Handbook of Chemistry and Physics; CRC Press, 66th edition)

Electroneutrality is required so $\Sigma Z_i J_i = 0$ A-8

Also the diffusion coefficient is an empirical constant defined by Fick's First Law:

$$D_i = \frac{-J_i}{(\delta C_i / \delta x)} \qquad \text{A-9}$$

Combining equations 6, 8 and 9 gives the following equation

$$D_i = U_i RT\left[1 - Z_i C_i \frac{\sum Z_j U_j \frac{\delta C_i / \delta x}{\delta C_j / \delta x}}{\sum Z_j^2 U_j C_j}\right] \qquad \text{A-10}$$

The diffusion coefficient is composed of a leading term equal to the tracer diffusion coefficient ($U_i RT$) and a correction term arising from cross-coupling of the ionic fluxes. McDuff and Ellis (1979) showed that for pore waters of geochemical interest the cross-coupling term are very small and that the magnitude of the cross-coupling term is concentration dependent. The cross-coupling terms for diffusion coefficients in the pore waters of the anoxic hypersaline sediments in the eastern Mediterranean have been calculated. The outcomes indicate that they can be neglected in cores ABC15, ABC33 and ABC45. In cores ABC17 and ABC23 a large gradient in Cl and Na with depth is observed, resulting in a cross-coupling term for Mg^{2+}, Sr^{2+}, SO_4^{2-}, Na^+, Cl^- and HCO_3^-. An example of the calculation of the cross-coupling term is given in table A-3, the cross-coupling terms for the pore waters of ABC17 and ABC23 are given in table A-4.

Table A-3: Calculation of cross-coupling terms in pore waters of core ABC17, Poseidon Basin (after McDuff and Ellis, 1979).

j	Z_j	C_j^*	U_j	A_{Mg}	A_{Na}	B_j
				$Z_jU_j(\Delta C_j/\Delta C_{Mg})$	$Z_jU_j(\Delta C_j/\Delta C_{Na})$	$Z_j^2U_jC_j$
Cl	-1	1116	8.2	401	-8.45	9151
Na	+1	1068	5.38	-255	5.38	5746
K	+1	11	7.89	0	0	87
Mg	+2	53	2.85	5.7	-0.12	600
Ca	+2	14	3.19	0	0	172
Sr	+2	0.12	3.19	-0.008	0.0002	1.5
SO_4	-2	33	4.3	0	0	568
HCO_3	-1	10	4.79	3.4	-0.07	48
				154.7	-3.26	16326

*) average concentration in the pore waters over total depth
$D_j = D_j^0 (1 - Z_jC_jA_j/B)$

Table A-4: Cross-coupling term for the ions Na^+, Cl^-, Mg^{2+}, Ca^{2+}, Sr^{2+}, SO_4^{2-} and HCO_3^- in the Poseidon and Kretheus Basins

	Poseidon D_j ($^*D_j^0$)	Kretheus D_j ($^*D_j^0$)
Cl^-	0.78	0.84
Na^+	1.21	1.18
Mg^{2+}	0.006	0.64
Ca^{2+}	no cross-coupling	0.40
Sr^{2+}	2.92	2.68
SO_4^{2-}	no cross-coupling	1.50
HCO_3^-	0.87	0.82

For most ions the cross coupling term is of minor importance for the estimated $D_{j,sed}$. The uncertianties in the estimated $D_{j,sed}$ values are largely due to the unknowence of the totuosity of the sediment and its relation with the porosity.

Appendix B: Thermodynamic equilibrium calculations, the PHRQPITZ model

A computer program for geochemical calculations in brines has been used to estimate the ion-activity products of Ca,Mg-carbonates, Ca-sulphates and halite (PHRQPITZ, Plummer et al., 1988). This model is based on the Pitzer equations and can therefore be applied to solutions with high ionic strength.

The model program PHRQPITZ has two options for scaling the individual ion activity coefficients. The first option is based on the work of Harvie et al. (1984). The other option is that the activity coefficients are scaled according to the MacInnes (1919) convention. In this case the activity coefficient of Cl is equal to the mean activity of KCl in a KCl solution of equivalent ionic strength. The choice of the activity-coefficient scale to be used is important when a measured pH is introduced in the geochemical solutions. Measured pH is not likely to be on the same activity-coefficient as the aqueous model because there are uncertainties in the measured pH in brines such as the influence of the liquid-junction potentials (Westcott, 1978; Plummer et al., 1988). The choice of scaling is particularly sensitive in case of the carbonate system. The differences in the calculated saturation index (Log IAP/K) between unscaled and scaled (MacInnes) activity coefficients largely depends on the ionic strength of the solution. At an ionic strength equal to 6.3 (Tyro brine) the difference between unscaled and scaled saturation indices is at most 0.50. The saturation indices for carbonates presented here are based on the unscaled individual-ion activity coefficients.

The PHRQPITZ program calculates the solubility products at a pressure of 1 atm. The sediment cores are taken from a depth between 3000 and 3500 meter. A water-depth of 3500 m. corresponds to a pressure of 350 to 400 bar. It is known that the pressure will increase the solubility product. A pressure of about 400 bar. will give a solubility product that is about two times the solubility product at 1 bar. (Stumm and Morgan, 1981; Millero, 1983). The uncertainties in the scaling of the individual-ion activity coefficients, the pressure effect and solid solution formation gives rise to problems in defining whether or not a solution is saturated with respect to a specific mineral. The uncertainty due to the choice of scaling is marked by an area enclosed by two solid lines in the figures.

References

Aghib, F.S, Bernoulli, D. and Weissert, H., 1991. Hardground formation in the Bannock Basin, eastern Mediterranean. Mar. Geol., 100: 103-113.

Aller, R.C. and Mackin, J. E., 1984. Preservation of reactive organic matter in marine sediments. Earth and Planetary Science Lett., 70: 260-266.

Aller, R.C. and Rude, P.D., 1988. Complete oxidation of solid phase sulfides by manganese and bacteria in anoxic marine sediments. Geochim. Cosmochim., Acta, 52: 751-765.

Alperin, M.J., 1989. The carbon cycle in an anoxic marine sediment: concentrations, rates, isotope ratios, and diagenetic models. PhD. Thesis, University of Alaska, USA, 241 pp.

Baker, P.A. and Kastner, M. 1981. Constraints on the formation of sedimentary dolomite. Science, 213: 214-216.

Baker, P.A., Gieskes, J.M. and Elderfield, H., 1982. Diagenesis of carbonates in deep-sea sediments - evidence from Sr/Ca ratios and interstitial dissolved Sr^{2+} data. J. Sed. Petrol., 52: 71-82.

Baker, P.A. and Burns, S.J., 1985. Occurrence and formation of dolomite in organic-rich continental margine sediments. The Amer. Assoc. Petrol. Geol. Bull., 69: 1917-1930.

Begheyn, L.Th., Van Breemen, N. and Veldhorst, E.J., 1978. Analysis of sulfur compounds in acid sulfate soils and other recent marine soils. Comm. Soil Sci. Plant Anal., 9: 873-882.

Bender, M.L. and Heggie, D.T., 1984. Fate of organic carbon reaching the deep sea floor: a status report. Geochim. Cosmochim. Acta, 48: 977-986.

Berger, W.H., Smetacek, V.S., and Wefer, G., 1989. Ocean productivity and paleoproductivity - an overview. In: W.H. Berger, V.S. Smetacek and G.Wefer (Eds), productivity of the ocean: Present and Past. John Wiley & Sons limited. pp. 1-34.

Berner, R.A., 1964. An idealized model of dissolved sulfate distribution in recent sediments. Geochim. Cosmochim. Acta, 28: 1497-1503.

Berner, R.A. 1970. Sedimentary pyrite formation. Am. J. of Science, 268: 1-23.

Berner, R.A., Scott, M.R. and Thomlinson, C., 1970. Carbonate alkalinity in the pore waters of anoxic marine sediments. Limnol. Oceanogr., 15: 544-549.

Berner, R.A., 1977. Stoichiometric models for nutrient regeneration in anoxic sediments. Limnol. Oceanogr., 22: 781-786.

Berner, R.A., 1978. Sulphate reduction and the rate of deposition of marine sediments. Earth Planet. Science Lett., 37: 492-498.

Berner, R.A., Baldwin, T. and Holdren, Jr., G.r., 1979. Authigenic iron sulfides as paleosalinity indicators. J. of Sed. Petrology., 49: 1345-1350.

Berner, R.A., 1980. Early Diagenesis. A theoretical approach. Princeton University Press, 241 p.

Berner, R.A., 1984. Sedimentary pyrite formation: An update. Geochim. Cosmochim. Acta, 47: 605-615

Berner, R.A. and Westrich, J.T., 1985. Bioturbation and the early diagenesis of carbon and sulfur. Amer. J. Science, 285: 193-206.
Bishop, J.K.B., 1988. The barite-opal-organic carbon association in oceanic particulate matter. Nature, 332: 341-343.
Boesen, C. and D. Postma, 1988. Pyrite formation in anoxic environments of the Baltic. Amer. J. Sci., 288: 575-603.
Boldrin, A. and Rabitti, S., 1990. Hydrography of the brines in the Bannock and Tyro anoxic basins (eastern Mediterranean). Mar. Chem., 31: 21-33.
Boudreau, B.P. and Canfield, D.E., 1993. A comparison of closed- and open-system models for porewater pH and calcite-saturation state. Geochim. Cosmochim Acta, 57: 317-334.
Boulegue, J. Lord, C.J. and Church, T.M., 1982. Sulfur speciation and associated trace metals (Fe,Cu) in the pore waters of Great marsh, Delaware. Geochim. Cosmochim. Acta, 46: 453-464.
Brassell, S.C., C.A. Lewis, J.W. de Leeuw, F. de Lange and J.S. Sinninghe Damsté, 1986. Isoprenoid thiophenes: novel products of sediment diagenesis? Nature, 320: 160-162.
Bruland, K.W., Bienfang, P.K., Bishop, J.K.B., Eglinton, G., Ittekot, V.A.W., Lampitt, R., Sarnthein, M., Thiede, J., Walsh, J.J. and Wefer, G., 1989. Group report: Flux to the seafloor. In: W.H. Berger, V.S. Smetacek and G. Wefer (Eds), Productivity of the ocean: Present and Past. John Wiley & Sons limited. p.193-215.
Brumsack, H.J., 1986. The inorganic geochemistry of Cretaceous black shales (DSDP Leg 41) in comparison to modern upwelling sediments from the Gulf of California. *From:* Eds. Summerhayes C.P. and Shackleton, N.J., *North Atlantic Paleoceanography*, Geological Society Special Publication 21: 447-462.
Brumsack, H.J. and Gieskes, J.M., 1983. Interstitial water trace-metal chemistry of laminated sediments from the Gulf of California, Mexico. Mar. Chem., 14: 89-106.
Burdige, D.J. and Nealson, K.H., 1986. Chemical and microbiological studies of sulfide mediated manganese reduction. Geomicrobiology J., 4: 361-387.
Calvert, S.E., 1983. Geochemistry of pleistocene sapropels and associated sediments from the eastern Mediterranean. Oceanol. Acta, 6: 255-267.
Calvert, S.E. and Karlin, R.E., 1991. Relationships between sulphur, organic carbon, and iron in the modern sediments of the Black Sea. Geochim. Cosmochim. Acta, 55: 2483-2490.
Camerlenghi, A., 1990. Anoxic basins of the eastern Mediterranean: geolocial framework. Mar. Chem., 31: 1-19.
Canfield, D.E., Raiswell, R., Westrich, J.T., Reaves, C.M. and Berner, R.A., 1986. The use of chromium reduction in the analysis of reduced inorganic sulfur in sediments and shales. Chem. Geol.,54: 149-155.
Canfield, D.E., 1989. Reactive iron in marine sediments. Geochim. Cosmochim. Acta, 53: 619-632.
Canfield, D.E., 1991. Sulfate reduction in deep-sea sediments. Am. J. Science, 291: 177-188.

Canfield, D.E., Raiswell, R. and Bottrell, S., 1992. The reactivity of sedimentary iron minerals toward sulfide. Am. J. of Science, 292: 659-683.

Capone, D.G. and Kiene, R.P., 1988. Comparison of microbial dynamics in marine and freshwater sediments: contrasts in anaerobic carbon catabolism. Limnol. Oceanogr., 33: 725-749.

Cauwet, G., 1984. Automatic determination of dissolved organic carbon in seawater in the sub-ppm range. Mar. Chem., 14: 297-306.

Cho, B.C. and Azam, F., 1988. Major role of bacteria in biogeochemical fluxes in the ocean's interior. Nature, 332: 441-443.

Church, Th.M. and Wolgemuth, K., 1972. Marine barite saturation. Earth Planet. Science Lett., 15: 35-44.

Cita, M.B., De Lange, G.J., and Olausson, E., 1991. Anoxic basins and sapropel deposition in the eastern Mediterranean: past and present. Special Issue Marine Geology, 100.

Cline, J.D., 1969. Spectrophotometric determination of hydrogen sulfide in natural waters. Limnol. Oceonogr., 14: 454-458.

Compton, J.S., 1988. Degree of supersaturation and precipitation of organic dolomite. Geology, 16: 318-321.

Cornwell, J.C. and Morse, J.W., 1987. The characterization of iron sulfide minerals in anoxic marine sediments. Mar. Chem, 22: 193-206.

Cutter, G.A. and Oatts, Th.J., 1987. Determination of dissolved sulfide and sedimentary sulfur speciation using gas chromatography photoionization detection. Anal. Chem.,59: 717-721.

Cutter, G.A. and D.J. Velinsky, 1988. Sulfur diagenesis in a coastal salt marsh. Mar. Chem., 23: 311-327.

Davison, W. and Gabbutt, C.D., 1979. Polarographic methods for measuring uncomplexed sulphide ions in natural waters. J. Electroanal. Chem., 99: 311-320

De Lange, G.J. and ten Haven, H.L., 1983. Recent sapropel formation in the eastern Mediterranean. Nature, 305: 797-798.

De Lange, G.J., 1986. Chemical composition of interstitial water in cores from the Nares abyssal plain (Western North Atlantic). Oceanologica Acta, 9: 159-168.

De Lange, G.J., Middelburg, J.J., Van der Weijden, C.H., Catalano, G., Luther, III, G.W., Hydes, D.J., Woittiez, J.R.W. and Klinkhammer, G.P., 1990a. Composition of anoxic hypersaline brines in the Tyro and Bannock Basins, eastern Mediterranean. Mar. Chem., 31: 63-88.

De Lange, G.J., Boelrijk, N.A.I.M., Catalano, G., Corselli, C., Klinikhammer, G.P., Middelburg, J.J., Müller, D.W., Ullman, W.J., Van Gaans, P. and Woittiez, 1990b. Sulphate-related equilibria in the hypersaline brines of the Tyro and Bannock Basins, eastern Mediterranean. Mar. Chem., 31: 89-112.

De Lange, G.J., Catalano, G., Klinkhammer, G.P. and Luther, III, G.W., 1990c. The interface between oxic seawater and the anoxic Bannock brine; its sharpness and the consequences for the redox-related cycling of Mn and Ba. Mar. Chem., 31: 205-217.

De Lange, G.J., 1992. Shipboard routine and pressure-filtration system for pore-water extraction from suboxic sediments. mar. Geol., 109: 77-81.

DeDomenico, E. and DeDomenico, M., 1989. Bannock Basin: first approach to water microbiology. In: M.B. Cita, A. Camerlenghi and C. Corselli (Eds.), Anoxic Basins of the Eastern Mediterranean. Results of the third conference, Bergamo (Italy), December 14 - 16 1988. Università degli studi di Milano, Supplemento n.72 pp.100-101.

Degens, E.T., 1969. Biogeochemistry of stable carbon isotopes. *In* Organic Geochemistry (Eglinton, E. and Murphy, M.T.J., Eds.), Springer-Verlag, Berlin, pp: 304-325.

Degens, E.T. and Ross, D.A. (Eds.), 1974. The Black Sea-geology, chemistry and biology. American Association of Petroleum Geologists, Tulsa, OK, 633 pp.

DeHairs, F., Lambert, C.E., Chesselet, R. and Risler, N., 1987. The biological production of marine suspended barite and the barium cycle in the western Mediterranean sea. Biogeochemistry, 4: 119-139.

Devol, A.H. and Ahmed, S.I., 1981. Are high rates of sulphate reduction associated with anaerobic oxidation of methane? Nature, 291: 407-408.

Devol, A.H., Anderson, J.J., Kuivila, K. and Murray, J.W., 1984. A model for coupled sulfate reduction and methane oxidation in the sediments of Saanich Inlet. Geochim. Cosmochim. Acta, 48: 993-1004.

Duursma, E.K., 1961. Dissolved organic carbon, nitrogen and phosphorus in the sea. Neth. J. Sea Res., 1: 1-148.

Duursma, E.K., 1965. The dissolved organic constituents of seawater. In: J.P. Riley and G. Skirrow (Eds.), Chemical Oceonography, Vol 1. Academic Press, London, pp.433-475.

Dymond, J., Suess, E. and Lyle, M., 1992. Barium in deep-sea sediment: a geochemical proxy for paleoproductivity. Paleoceanography, 7: 163-181.

Ehrhardt, M., 1977. Organic substances in seawater. Mar.Chem.,5: 307-316.

Elderfield, H., 1981. Metal organic associations in interstitial waters of Narragansett bay sediments. Am. J. Sci., 281: 1184-1196.

Elderfield, H., McCaffrey, R.J., Luedtke, N., Bender, M. and Truesdale, V.W., 1981. Chemical diagenesis in Narraganesett Bay sediments. Am. J. Science, 281: 1024-1055.

Erba, E., Rondondi, G., Parisi, E., ten Haven, H.L., Nip, M. and de Leeuw, J.W., 1987. Gelatinous pellicles in deep anoxic hypersaline basins from the Eastern Mediterranean. Mar. Geol., 75: 165-184.

Erba, E., 1991. Deep mid-water bacterial mats from anoxic basins of the Eastern Mediteranean. Mar. Geol., 100: 83-101.

Falkner, K.K, Klinkhammer, G.P., Bowers, T.S., Todd, J.F., Lewis, B.L., Landing, W.M. and Edmond, J.M., 1993. The behavior of barium in anoxic marine waters. Geochim. Cosmochim. Acta, 57: 537-554.

Ferdelman, T.G., Church, Th.M. and Luther III, G.W., 1991. Sulfur enrichment of humic substances in a Delaware salt marsh sediment core. Geochim. Cosmochim. Acta, 55: 979-988.

Fossing, H., 1990. Sulfate reduction in shelf sediments in the upwelling region off Central Peru. Continental Shelf Res., 10: 355-367.

Francois, R., 1987a. A study of the extraction conditions of sedimentary humic acids to estimate their true in situ sulphur content. Limnol. Oceano., 32: 964-972.

Francois, R., 1987b. A study of sulphur enrichment in the humic fraction of marine sediments during early diagenesis. Geochim, Cosmochim. Acta, 51: 17-27.

Fredericks, A.D. and Sackett, W.M., 1970. Organic carbon in the Gulf of Mexico. J. of Geophys. Res., 75: 2199-2206.

Frey, B., Gest, H. and Hayes, J.M., 1984. Isotope effects associated with anaerobic oxidation of sulfide by the purple photosynthetic bacterium, *Chromatium vinosum*. Microbio. Lett., 22: 283-287.

Froelich, P.N., Klinkhammer, G.P., Bender, M.L., Luedtke, N.A., Heath, G.R., Cullen, D., Dauphin, P., Hammond, D., Hartman, B. and Maynard, V., 1979. Early oxidation of organic matter in pelagic sediments of the eastern equatorial Atlantic: suboxic diagenesis. Geochim. Cosmochim. Acta, 43: 1075-1090.

Froelich, P.N., Bender, M.L., Luedtke, N.A., Heath, G.R. and DeVries, T., 1982. The marine phosphorus cycle. Am. J. Science, 282: 474-511.

Gaillard J.F., Pauwels, H. and Michard, G., 1989. Chemical diagenesis in coastal marine sediments. Oceanologica Acta, 12: 175-187.

Gaskell, S.J., Morris, R.J., Eglinton, G. and Calvert, S.E., 1975. The geochemistry of a recent marine sediment off north-west Africa - an assesment of source of input and early diagenesis. Deep Sea Res. 22A: 777-789.

Gieskes, J.M., 1975. Chemistry of interstitial waters of marine sediments. Ann. Rev. Earth. Planet. Sci., 3: 433-453.

Gieskes, J.M., Johnston, K., Boehm, M. and Nohara, M., 1984. Interstitial water studies, Deep Sea Drilling Project, Leg 75. *In* Hay, W.W., Sibuet, J.-C., et al., *Init. Repts. DSDP*,75: 959-963. Washington (U.S. Govt. Printing Office).

Goldhaber, M.B., and Kaplan, I.R., 1974. The Sulfur Cycle. In *The Sea* (ed. E.D. Goldberg), vol. 5: 569-655. J. Wiley & Sons.

Goldhaber, M.B., and Kaplan, I.R., 1975. Controls and consequences of sulfate reduction rates in recent sedimnets. Soil Science, 119: 42-55.

Goldhaber, M.B., Aller, R.C., Cochran, J.K., Rosenfeld, J.K., Martens, C.S. and Berner, R.A., 1977. Sulfate reduction, diffusion, and bioturbation in Long Island Sound sediments: report of the FOAM group. Am. J. Science, 277: 193-237.

Goldhaber, M.B. and Kaplan, I.R., 1980. Mechanisms of sulfur incorporation and isotope fractionation during early diagenesis in sediments of the Gulf of California. Mar. Chem., 9: 95-143.

Gordon Jr., D.C. and Sutcliffe Jr., W.H., 1973. A new dry combustion method for the simultaneous determination of total organic carbon and nitrogen in seawater. Mar. Chem., 1: 231-244.

Hartmann, M. and Nielsen, H.N., 1969. δ^{34}S-Werte in rezenten Meeressedimenten und ihre Deutung am Beispiel einiger Sedimentprofile aus der westlichen Ostsee. Geologische Rundschau, 58: 621-655.

Hastings, D. and Emerson, S., 1988. Sulfate reduction in the presence of low oxygen levels in the water column of the Cariaco Trench. Limnol. Oceanogr. 33: 391-396.

Harvie, C.E., Møller, N. and Weare, J.H., 1984. The prediction of mineral solubilities in natural waters: The Na-K-Mg-Ca-H-Cl-SO_4-OH-HCO_3-CO_3-CO_2-H_2O system to high ionic strenghts at 25°C. Geochim. Cosmochim. Acta, 48: 723-751.

Heggie, D., Maris, C., Hudson, A., Dymond, J., Beach, R. and Cullen, J., 1987. Organic carbon oxidation and preservation in NW atlantic continental margin sediments. Geology and geochemistry of Abyssal Plains. Geological Society Special Publication, 31: 215-236.

Henneke, E. and de Lange, G.J., 1990. The distribution of DOC and POC in the water column and brines of the Tyro and Bannock Basins. Mar. Chem., 31: 113-122.

Henneke, E., Luther III, G.W. and de Lange, G.J., 1991. Determination of inorganic sulphur speciation with polarographic techniques: some preliminary results for recent hypersaline anoxic sediments. Mar. Geol., 100: 115-123.

Howarth, R.W. and Jørgensen, 1984. Formation of ^{35}S-labelled elemental sulfur and pyrite in coastal marine sediments (Limfjorden and Kysing Fjord, Denmark) during short-term $^{35}SO_4^{2-}$ reduction measuremnts. Geochim. Cosmochim. Acta, 48: 1807-1818.

Howarth, R.W. and Merkel, S., 1984. Pyrite formation and the measurement of sulfate reduction in salt marsh sediments. Limnol. Oceanogr., 29: 598-609.

Hsieh, Y.P., and Yang, C.H., 1989. Diffusion methods for the determination of reduced inorganic sulfur species in sediments. Limnol. Oceanogr., 34: 1126-1130.

Ishizuka, T., Ittekot, V., Degens, E.T. and Kawahata, H., 1985a. Preliminary data on dissolved organic carbon and sugar in interstitial water from the Missippi fan and Orca and Pigmy Basins, Deep Sea Drilling Project, Leg 96. *In* Bouma et al., *Init. Reports DSDP*, 96: 729-732. Washington (U.S. Govt. Printing Office).

Ishizuka, T., Kawahata, H. and Aoki, S., 1985b. Interstitial water geochemistry and clay mineralogy of the Missippi fan and Orca and Pigmy Basins, Deep Sea Drilling Project, Leg 96. *In* Bouma et al., *Init. Reports DSDP*, 96: 711-728. Washington (U.S. Govt. Printing Office)

Iversen, N. and Jørgensen, B.B., 1993. Diffusion coefficients of sulfate and methane in marine sediments: Influence of porosity. Geochim. Cosmochim. Acta, 57: 571-578.

Jongsma, D., Fortuin, A.R., Huson, W., Troelstra, S.R., Klaver, G.T., Peters, J.M., van Harten, D., de Lange G.J. and ten Haven, H.L., 1983. Discovery of an anoxic basin within the Strabo Trench, Eastern Mediterranean. Nature, 305: 795-797.

Jørgensen, B.B., 1978. A comparison of methods for the quantification of bacterial sulfate reduction in coastal marine sediments. Geomicrobiol., 1: 49-64.

Jørgensen, B.B., J.G. Kuenen and Y. Cohen, 1979. Microbial transformations of sulfur compounds in a stratified lake (Solar Lake, Sinai). Limnol. Oceanogr., 24: 799-822.

Jørgensen, B.B., 1982. Mineralization of organic matter in the sea bed - the role of sulphate reduction. Nature, 296: 643-645.

Kaplan, I.R. and Rittenberg, S.C., 1964. Microbiological fractionation of sulfur isotopes. J. Gen. Microbiol., 34: 195-212.

Kastner, M., Keene, J.B. and Gieskes, J.M., 1977. Diagenesis of siliceous oozes - I. Chemical controls on the rate of opal-A to opal-CT transformation - an experimental study. Geochim. Cosmochim. Acta, 41: 1041-1059.

Kastner, M., Elderfield, H., Martin, J.B., Suess, E., Kvenholden, K.A. and Garrison, R.E., 1990. Diagenesis and interstitial water chemistry at the Peruvian continental margin- major constituents and strontium isotopes. *In* Suess, E., Von Huene, R., et al., *Proc.of ODP, Scientific Results*, 112: 413-440.

King, G.M., B.L. Howes and W.H. Dacey, 1985. Short-term endproducts of sulfate reduction in a salt marsh: Formation of acid volatile sulfides, elemental sulfur, and pyrite. Geochim. Cosmochim. Acta, 49: 1561-1566.

Klinkhammer, G.P. and Lambert, C.E., 1989. Preservation of organic matter during salinity excursions. Nature, 339: 271-274.

Kohnen, M.E.L, J.S. Sinninghe Damsté, H.L. ten Haven and J.W. de Leeuw, 1989. Early incorporation of polysulphides in sedimentary organic matter. Nature, 341: 640-641.

Kohnen, M.E.L., 1991. Sulphurised Lipids in sedimens: The key to reconstruct palaeobiochemicals and their origin. PhD.-thesis, Technical University of Delft, The Netherlands, 248 p.

Kolthoff, I.M. and Sandell, E.B., 1952. Textbook of Quantative Inorganic Analysis. MacMillan, New York, 159 pp.

Krom, M.D. and Sholkovitz, E.R., 1977. Nature and reactions of dissolved organic matter in the interstitial waters of marine sediments. Geochim. Cosmochim. Acta, 41: 1565-1574.

Krom, M.D. and Berner, R.A., 1980. Adsorption of phosphate in anoxic marine sediments. Limnol. Oceanogr., 25: 797-806.

Krom, M.D. and Westrich, J.T., 1980. Dissolved organic matter in the pore waters of recent marine sediments; a review. Biogéochimie de la matière organique à l'interface eau-sédiment marin, 293: 103-111. Colloques Internationaux du C.N.R.S.

Krom, M.D., Kress, N. and Brenner, S., 1991. Phosphorus limitation of primary productivity in the eastern Mediterranean Sea. Limnol. Oceanogr., 36: 424-432.

LaRock, P.A., Lauer, R.D., Schwarz, J.R., Watanabe, K.K., and Wiesenburg, D.A., 1979. Microbial biomass and activity distribution in an anoxic hypersaline basin. Applied and Environmental Microbiology, 37: 466-470.

Leventhal, J.S., 1983. An interpretation of carbon and sulfur relationships in Black Sea sediments as indicators of environment deposition. Geochim. Cosmochim. Acta, 47: 133-137.

Leventhal, J. and Taylor, C., 1990. Comparison of methods to determine degree of pyritization. Geochim. Cosmochim. Acta, 54: 2621-2625.
Li, Y-H. and Gregory, S., 1974. Diffusion of ions in sea water and in deep-sea sediments. Geochim. Cosmochim. Acta, 38: 703-714.
Lin, S. and Morse, J.W., 1991. Sulfate reduction and iron sulfide mineral formation in Gulf of Mexico anoxic sediments. Am. J. Science, 291: 55-89.
Lord III, C.J., 1982. A selective and precise method for pyrite determination in sedimentary materials. J. Sediments Petrol., 52: 664-666.
Luther III, G.W., Giblin, A., Howarth, R.W. and Ryans, R.A., 1982. Pyrite and oxidized iron mineral phases formed from pyrite oxidation in salt marsh and estuarine sediments. Geochim. Cosmochim. Acta, 46: 2665-2669.
Luther III, G.W., Giblin, A.E. and Varsolona, R., 1985. Polarographic analysis of sulfur species in marine porewaters. Limnol. Oceanogr., 30: 727-736.
Luther, III, G.W., Church, Th.M., Scudlark, J.R. and Cosman, M., 1986. Inorganic and organic sulfur cycling in salt-marsh pore waters. Science, 232: 746-749.
Luther III, G.W., 1987. Pyrite oxidation and reduction: Molecular orbital theory considerations. Geochim. Cosmochim Acta, 47: 133-137.
Luther III, G.W. and Tsamakis, E., 1989. On the from of dissolved sulfide in the oxic water column of the ocean. Mar. Chem., 27: 165-177.
Luther III, G.W., G. Catalano, G.J. de Lange and J.R.W. Woittiez, 1990. Reduced Sulfur in the Hypersaline Anoxic Basins of the Mediterranean Sea. Mar. Chem., 31: 137-152.
Luther III, G.W., 1991. Pyrite synthesis via polysulfide compounds. Geochim. Cosmochim. Acta, 55: 2839-2849.
Luther III, G.W. and Church,T.M., 1992. An overview of the environmental chemistry of sulphur in wetland systems. *In* "Sulphur Cycling on the Continents" (eds. Howarth, R.W., Stewart, J.W.B. and Ivanov, M.V.), John Wiley and Sons, New York, pp. 125-144.
Luther III, G.W., Ferdelman, T.G., Kostka, J.E., Tsamakis, E.J. and Church, Th. M., 1991a. Temporal and spatial variability of reduced sulfur species (FeS_2, $S_2O_3^{2-}$) and porewater parameters in salt marsh sediments. Biogeochemistry 14: 57-88.
Luther III, G.W., Church, T.M. and Powell, D., 1991b. Sulfur speciation and sulfide oxidation in the water column of the Black Sea. Deep-Sea Res., vol. 38, suppl. 2, pp.: S1121-S1137.
Lyons, Wm.B., Gaudette, H. and Hewitt, A. D., 1979. Dissolved organic matter in pore water of carbonate sediments from Bermuda. Geochim. Cosmochim. Acta, 43: 433-437.
Lyons, Wm.B., Gaudette, H.E. and Gustafson H.C., 1982. Dissolved organic carbon in pore waters from a hypersaline environment. Org. Geochem., 3: 133-135.
MacInnes, D.A., 1919. The activities of the ions of strong electrolytes. J. Am. Chem. Soc., 41: 1086-1092.

Manheim, F.T. and Chan, K.M., 1974. Interstitial water of Black Sea sediments: new data and review. *In* Degens, E.T. and Ross, D.A.(eds.) The Black Sea - geology, chemistry and biology. Am. Ass. Petroleum Geologists, Memoir 20.

Martens, C.S., Berner, R.A. and Rosenfeld, J.K., 1978. Interstitial water chemistry of anoxic Long Island Sound sediments. 2. Nutrient regeneration and phosphate removal. Limnol. Oceanogr. 23: 605-617.

Martens, C.S. and Klump, J.V., 1984. Biogeochemical cycle in an organic-rich marine basin. 4. An organic carbon budget for sediments dominated by sulphate reduction and methanogenesis. Geochim. Cosmochim. Acta, 48: 1987-2004.

McDuff, R.E. and Ellis, R.A., 1979. Determining diffusion coefficients in marine sediments: a laboratory study of the validity of resistivity techniques. Am. J. Science, 279: 666-675.

Menzel, D.W. and Vaccaro, R.F., 1964. The measurement of dissolved organic and particulate carbon in seawater. Limnol. Oceanogr., 9: 138-142.

Michard, G., Church, Th.M. and Bernat, M., 1974. The pore water chemistry of recent sediments in the western Mediterranean Basin. J. Geophysical Res., 79: 817-824.

Middelburg, J.J. and de Lange, G.J., 1989. The isolation of Kau Bay during the last glaciation: direct evidence from interstitial water chlorinity. Neth. J. Sea Res.,: 615-622.

Middelburg, J.J., 1990. Early diagenesis and authigenic mineral formation in anoxic sediments of Kau Bay, Indonesia. Mededelingen van de Faculteit Aardwetenschappen der Rijksuniversiteit te Utrecht. Geologica Ultraiectina, No. 71, 177 p.

Middelburg, J.J., De Lange, G.J. and Kreulen R., 1990. Dolomite formation in anoxic sediments of Kau Bay, Indonesia. Geology, 18: 399-402.

Middelburg, J.J., 1991. Organic carbon, sulphur and iron in recent semi-euxinic sediments of Kau Bay, Indonesia. Geochim. Cosmochim. Acta, 55: 815-828.

Millero, F.J., 1983. Influence of pressure on chemical porcesses in the sea. *In* Chemical Oceaongraphy, vol. 8 (Riley, J.P. and Chester, R., eds.): 1-88.

Möckel, H.J., 1984a. Retention of sulphur and sulphur organics in reversed-phase liquid chromatography. J. Chromatogr., 317: 589-614.

Möckel, H.J., 1984b. The retention of sulphur homocycles in reversed-phase HPLC. Anal. Chem., 318: 327-334.

Morrow, D.W., 1982. Diagenesis 1. Dolomite - Part 1: The chemistry of dolomitization and dolomite precipitation. Geoscience Can., 9: 5-13.

Morse, J.W. and Cornwell, J.C., 1987. Analysis and distribution of iron sulfide minerals in recent anoxic marine sediments. Mar. Chem., 22: 55-69.

Morse, J.W. and Mackenzie, F.T., 1990. Geochemistry of sedimentary carbonates. Developements in Sedimentology 48, Elsevier.

Mossmann, J.-R., Aplin, A.C., Curtis, Ch.D. and Coleman, M.L., 1990. Sulfur geochemistry at sites 680 and 686 on the Peru Margin. *In* Suess, E., von Huene, R., et al. (Eds), *Proc. ODP, Sci. Results*, 112: 455-464. College Station, TX (Ocean Drilling Program).

Mossmann, J.R., Aplin, A.C., Curtis, Ch.D. and Coleman, M.L., 1991. Geochemistry of inorganic and organic sulphur in organic-rich sediments from the Peru Margin. Geochim. Cosmochim. Acta, 55: 3581-3595.

Murray, J.W., 1991. (Editor) Black Sea, Oceanography. Results from the 1988 Black Sea Expedition. Deep-Sea Research, vol. 38, Suppl. Issue No. 2A, 1266 p.

Nissenbaum, A. and I.R. Kaplan, 1972. Chemical and isotopic evidence for the in situ origin of marine humic substances. Limnol. Oceanogr., 17: 570-582.

Nissenbaum, A., Baedecker, M.J. and Kaplan, I.R., 1972. Studies on dissolved organic matter from interstitial water of a reducing marine fjord. *In* Advances in Organic Geochemistry, 1971, H.R. von Gaertner and H. Wehner (eds.), Pergamon Press, Oxford, p: 427-440.

Oenema, O., 1990. Pyrite accumulation in salt marshes in the Eastern Scheldt, southwest Netherlands. Biogeochemistry, 9: 75-98.

Orem, W.H., Hatcher, P.G. and Spiker, E.C., 1986. Dissolved organic matter in anoxic pore waters from Mangrove Lake, Bermuda. Geochim. Cosmochim. Acta, 50: 609-618.

Pett, R.J., 1990. Utilization of water column dissolved organic carbon by a coastal marine benthic community. submitted to Limnol. Oceanogr.

Plummer, L.N., Parkhurst, D.L., Fleming, G.W. and Dunkle, S.A., 1988. A computer program incorporating Pitzer's equations for calculation of geochemical reactions in brines. U.S. Geological Survey, Water Resources Investigations Report 88-4153.

Presley, B.J. and Stearns, S., 1985. Interstitial water chemistry, Deep Sea Drilling Project, Leg 96. *In* Bouma et al., *Init. Reports. DSDP*, 96: 697-709. Washington (U.S. Govt. Printing Office).

Pruysers, P.A., De Lange, G.J. and Middelburg, J.J., 1991. Geochemistry of eastern Mediterranean sediments: Primary sediment composition and diagenetic alterations. Mar. Geol., 100: 137-154.

Radford-Knoery, J. and Cutter, G.A., 1988. Particulate nitrogen and carbon in the Black Sea. EOS, 69: 1240.

Raiswell, R. and Berner, R.A., 1985. Pyrite formation in euxinic and semi-euxinic sediments. Am. J. Science, 285: 710-724.

Raiswell, R., Buckley, F., Berner, R.A. and Anderson, T.F., 1988. Degree of pyritization of iron as a paleoenvironmental indicator of bottom-water oxygenation. J. of Sed. Petrology, 58: 812-819.

Reid,D.F., Brooks, J.M., Bernard, B.B. and Sackett, W.M., 1977. Chemical and isotopic analyses of the Orca Basin and east Flower Garden brines. EOS, 56: 1175.

Rickard, D.T., 1975. Kinetics and mechanisms of pyrite formation at low temperatures. Am. J. of Science, 275: 636-652.

Romankevich, E.A., 1984. Geochemistry of organic matter in the ocean, Springer Verlag. pp.1-104.

Rosenfeld, J.K., 1979. Ammonium adsorption in nearshore anoxic sediments. Limnol. Oceanogr., 24: 356-364.
Rowe, G.T. and Howarth, R., 1985. Early diagenesis of organic matter in sediments off the coast of Peru. Deep-sea Research, 32: 43-55.
Saager, P.M., Schijf, J. and De Baar, H.J.W., 1993. Trace-metal distributions in seawater and anoxic brines in the eastern Mediterranean Sea. Geochim. Cosmochim. Acta, 57: 1419-1432.
Sackett, W.M., Brooks, J.M., Bernard, B.B., Schwab, C.R., Chung, H. and Parker, R.A., 1979. A carbon inventory for Orca Basin brines and sediments. Earth Planet. Sci. Lett., 44: 73-81.
Sasaki, A., Arikawa, Y. and Folinsbee, R.E., 1979. Kiba reagent method of sulfur extraction applied to isotopic work. Bull. Geol. Surv. Japan, 30: 241-245.
Schijf, J., 1992. Aqueous geochemistry of the rare earth elements in marine anoxic basins. Mededelingen van de Faculteit Aardwetenschappen der Rijksuniversiteit te Utrecht. Geologica Ultraiectina, No. 85, 256 p.
Scientific staff of Cruise Bannock 1984-12, 1985. Gypsum precipitation from cold brines in an anoxic basin in the eastern Mediterranean. Nature, 314: 152-154.
Sharp, J.H., 1973. Total organic carbon in seawater - comparison of measurements using persulfate oxidation and high temperature combustion. Mar. Chem., 1: 211-229.
Shatkay, M. and Magaritz, M., 1987. Dolomitization and sulfate reduction in the mixing zone between brine and meteoric water in the newly exposed shores of the Dead Sea. Geochim. Cosmochim. Acta, 51: 1135-1141.
Sheu, Der-Duen, 1987. Sulfur and organic carbon contents in sediment cores from the Tyro and Orca Basins. Mar. Geol., 75: 157-164.
Sheu, Der-Duen, 1990. The anoxic Orca Basin (Gulf of Mexico): Geochemistry of brines and sediments. Reviews in Aquatic Sciences, 2: 491-507.
Sheu, Der-Duen and Presley, B.J., 1986. Variations of calcium carbonate, organic carbon and iron sulfides in anoxic sediments from the Orca Basin, Gulf of Mexico. Mar. Geol., 70: 103-118.
Shokes, R.F., Trabant, P.K., Presley, B.J. and Reid, D.F., 1977. Anoxic, hypersaline basin in the northern Gulf of Mexico. Science, 196: 1443-1446.
Sinninghe Damsté, J.S., I.C. Rijpstra, A.C. Kock-van Dalen, J.W. de Leeuw and P.A. Schenck, 1989. Quenching of labile functionalized lipids by inorganic sulphur species: Evidence for the formation of sedimentary organic sulphur compounds at the early stages of diagenesis. Geochim. Cosmochim Acta, 53: 1343-1355.
Skei, J., 1983. Geochemical and sedimentological considerarions of a permanently anoxic fjord - Framvaren, South Norway. Sed. Geology, 36: 131-145.
Starikova, N.D., 1970. Vertical distribution patterns of issolved organic carbon in seawater and interstitial solutions. Oceanology, 10: 796-807.
Stumm, W. and Morgan, J.J., 1981. Aquatic chemistry: an introduction emphasizing chemical equilibria in natural waters. Wiley, 2nd Ed.

Suess, E., 1979. Mineral phases in anoxic sediments by microbial decomposition of organic matter. Geochim. Cosmochim. Acta, 43: 339-352.

Suess, E., Von Huene, R. and Leg 112 Shipboard Scientists, 1988. Ocean Drilling Program Leg 112, Peru continental margin: Part 2, Sedimentary history and diagenesis in a coastal upwelling environment. Geology, 16: 939-943.

Sugimara, Y. and Suzuki, Y., 1988. A high-temperature catalytic oxidation method for the determination of non-volatile dissolved organic carbon in seawater by direct injection of a liquid sample. Mar. Chem., 24: 105-131.

Suzuki, Y., Sharp, J.H. and Munday, W.L., 1988. Intercomparison of dissolved organic carbon analyses in estuarine and coastal waters of the North Atlantic Ocean, EOS 69: 1134.

Suzuki, Y., 1993. On the measurement of DOC and DON in seawater. Mar. Chem., 41: 287-288.

Swallow, J.C. and Crease, J., 1965. Hot salty water at the bottom of the Red Sea. Nature, 205: 165-166.

Ten Haven, H.L, De Lange, G.J. and McDuff, R.E., 1987a. Interstitial water studies of Late Quaternary eastern Mediterranean sediments with emphasis on early diagenetic reactions and evaporitic salt influences. Mar. Geol., 75: 119-136.

Ten Haven, H.L., Baas, M., De Leeuw, J.W., Maassen, J.M. and Schenck, P.A., 1987b. Organic geochemical characteristrics of sediments from the anoxic brine-filled Tyro Basin (eastern Mediterranean). Org. Geochem., 11: 605-611.

Toggweiler, J.R., 1989. Is downward DOM flux important in carbon transport? In: W.H.Berger,V.S. Smetacek and G.Wefer (Eds), Productivity of the ocean: Present and Past. John Wiley & Sons limited. pp.65-83.

Tomadin, L. and Landuzzi, V., 1991. Origin and differentiation of clay minerals in pelagic sediments and sapropels of the Bannock Basin (Eastern Mediterranean). Mar. Geol., 100: 35-43.

Toth, D.J. and Lerman, A., 1977. Organic matter reactivity and sedimentation rates in the ocean. Am J. Science, 277: 465-485.

Trefry, J.H., Presley, B.J., Keeney-Kennicutt, W.L. and Trocine, P., 1984. Distribution and chemistry of manganese, iron and suspended particulates in Orca Basin. Geo-Mar. Lett., 4:125-130.

Tuller, W.N., 1970. Elemental sulfur. In: The analytical chemistry of sulfur and its compounds (ed. J.H. Karcher), pp. 1-18. Wiley Interscience.

Vairavamurthy, A. and Mopper, K., 1987 Geochemical formation of organosulphur compounds (thiols) by addition of H_2S to sedimentary organic matter. Nature, 329: 623-625.

Van Der Sloot, H.A, Hoede, D., Hamburg, G., Woittiez, J.R.W. and Van Der Weijden, C.H., 1990. Trace elements in suspended matter from the anoxic hypersaline Tyro and Bannock Basins. Mar. Chem., 31: 171-186.

Van Der Weijden, C.H., Luther, III, G.W. and Bregant, D., 1990. Anoxic brines of the Mediterranean Sea (geology and hydrography; major, minor and trace element chemistry; speciation and stable isotopes). Special Issue Marine Chemstry, 31.

Van Hinte, J.E., Cita, M.B. and Van Der Weijden, C.H., 1987. Extant and ancient anoxic basin conditions in the eastern Mediterranean. Special Issue Marine Geology, 75.

Van Os, B.J.H., Middelburg, J.J. and De Lange, G.J., 1991. Possible diagenetic mobilization of barium in sapropelic sediment from the eastern Mediterranean. Mar. Geol., 100: 125-136.

Van Os, B.J.H., 1993. Primary and diagenetic signals in Mediterranean sapropels and North Atlantic turbidities: origin and fate of trace metals and paleo-proxies. Mededelingen van de Faculteit Aardwetenschappen der Rijksuniversiteit te Utrecht. Geologica Ultraiectina, No. 109

Von Breymann, M.T., Emeis, K-C. and Camerlenghi, A., 1990. Geochemistry of sediments from the Peru upwelling area: results from sites 680, 682, 685 and 688. *In* Suess, E., Von Huene, R., et al. *Proc. ODP, Sci. Results,* 112: 491-503.

Walls, R.A., Ragland, P.C. and Crisp, E.L., 1977. Experimental and natural early diagenetic mobility of Sr and Mg in biogenic carbonates. Geochim. Cosmochim. Acta, 41: 1731-1737.

Wangersky, P.J., 1976. Particulate organic carbon in the Atlantic and Pacific oceans. Deep-Sea Res., 23: 457-465.

Westcott, C.C., 1978. pH Measurements. New York, Academic Press.

Westrich, J.T. and Berner, R.A., 1984. The role of sedimentary organic matter in bacterial sulfate reduction: The G model tested. Limnol. Oceanogr., 29: 236-249.

Williams, P.J.LeB., 1975. Biological and chemical aspects of dissolved organic matter in seawater. In: J.P. Riley and G. Skirrow (Eds), Chemical Oceonography, Vol 2. Academic Press, London, pp.301-363.

Williams, P.M., Oeschger, H. and Kinney, P., 1969. Natural radiocarbon activity of dissolved organic carbon in the North-east Pacific Ocean. Nature, 224: 256-258.

Wilson, R.F., 1961. Measurements of organic-carbon in seawater. Limnol.Oceanogr., 6: 254-261.

Zhabina, N.N. and Volkov, I.I., 1978. A method of determination of various sulphur compounds in sea sediments and rocks. In: W.E. Krumbein (Editor), Environmental Biogeochmeistry and Geomicrobiology. Vol. 3, Methods, Metals and Assessment. Ann Arbor Science, Ann Arbor, Mich., pp. 735-746.

Curriculum vitae

De auteur van dit proefschrift werd geboren op 7 december 1962 te Vlaardingen. Na het behalen van het VWO-diploma begon zij in 1984 aan de studie Geologie. Tijdens haar doctoraal studie bij de vakgroep Mariene Geochemie maakte zij kennis met de fascinerende anoxische hypersaline Tyro en Bannock Bekkens in de Middellandse Zee. Na deelname aan de expeditie Anoxic Basins Cruise in 1987 met de R.V. Tyro raakte zij in de ban van de mariene geochemie. Zij was dan ook zeer verheugd toen haar werd aangeboden om na haar afstuderen een promotie-onderzoek te doen naar de geochemische karakteristieken en diagenetische processen in de sedimenten uit de Tyro en Bannock Bekkens. Op 1 april 1989 werd zij aangesteld als onderzoeker in opleiding ten behoeve van dit onderzoek bij de vakgroep Mariene Geochemie van het Instituut voor Aardwetenschappen, Universiteit Utrecht. Op vrijdag 10 september zal zij dit proefschrift verdedigen en naar verwachting bij Prof. Dr. C.H. van der Weijden promoveren.